Properties of High Field
Superconductors Containing Localized Magnetic Moments

by **Øystein H. Fischer**

Département de Physique de la Matière Condensée, Université de Genève

(17. VI. 71)

Contents

Abstract. The problem of paramagnetic impurities in high field superconductors is analyzed. Special emphasis is put on the effects that appear when the impurity spins align in an external field or due to interactions. The impurities then produces an exchange field on the conduction electron spins which in some cases may counteract the effect of the external field on the conduction electron spins. In such cases the critical field of the dilute alloy may rise above the value of the pure system and the phase boundary $H_{c_2}(T)$ will have an anomalous shape. This effect is discussed theoretically in detail and experimental results on the system $Mo_{1-x}M_xGa_4$ (M = Nb, Ru, Mn, Fe, Co) are presented.

1. Introduction

Since the first measurements of Matthias et al [1] and the theory of Abrikosov and Gorkov [2] it is well known that magnetic impurities in superconductors have very drastic effects on the superconducting properties. One may distinguish two different effects of the magnetic impurities: (a) the scattering of the Cooper pairs on the impurities (2nd order effect), (b) the effect of the exchange field (1st order effect). The last effect may become predominant in cases where the spins of the impurities are aligned, due to interaction between them, or due to an external field.

If one goes to a well-ordered dense ferromagnet at $T = 0$, the second order processes, i.e. the scattering on the magnetic ions will be absent and at first sight we are left only with the mean exchange field. As first shown by Clogston [3] and Chandrasekhar [4] a simple BCS superconductor in an exchange field H_J will make a first order transition to the normal state when $\chi_{pauli} H_J/2$, the gain in free energy of the normal electron gas, becomes equal to $\Delta^2 N(0)/2$, the condensation energy of the superconducting state (Δ is the energy gap and $N(0)$ the density of states at the fermi level). This gives a first order transition at $H = H_{p0}$ (the Clogston limit)

$$H_{p0} = \sqrt{2}\,\frac{\Delta}{g\,\mu_B} = 18.4\,T_{c0} \quad \text{(kGauss)} . \tag{1}$$

The exchange fields in dense ferromagnets, exceed easily this value by an order of magnitude, thus giving a very simple explanation why so far no dense ferromagnetic superconductor has been found.

In an antiferromagnet, on the contrary, the mean exchange field is zero, and we expect that antiferromagnetism and superconductivity can coexist. This was demonstrated by Baltensperger and Strässler [5] who showed that a well-ordered antiferromagnet can coexist with superconductivity in the 'spin wave region' i.e. $T_c \ll \theta_c$ (θ_c = magnetic transition point). They also showed that the indirect interaction via virtual spinwaves between two conduction electrons is repulsive, but generally weaker than the attractive electron phonon interaction.

The high exchange field in a ferromagnet can, however, in certain cases be compensated by an external magnetic field, allowing the ferromagnet to become superconducting in a region of high magnetic fields. This was first suggested by Jaccarino and Peter [6]. They considered, as Baltensperger and Strässler, a system of localized magnetic ions and a gas of conduction electrons including the attractive electron-phonon-electron interaction, leading to superconductivity. They pointed out that such a compensation should be possible of the mean value of the polarization of the

conduction electrons points opposite to the total magnetic moment of the magnetic ions. In this case the range of superconductivity will be determined by the equation

$$\frac{1}{2} \chi_n (H - H_J)^2 \leqslant \frac{1}{2} N(0) \, \Delta^2$$

i. e.

$$H_J - H_{p0} \leqslant H \leqslant H_J + H_{p0} \, . \tag{2}$$

This is illustrated in Figure 1.
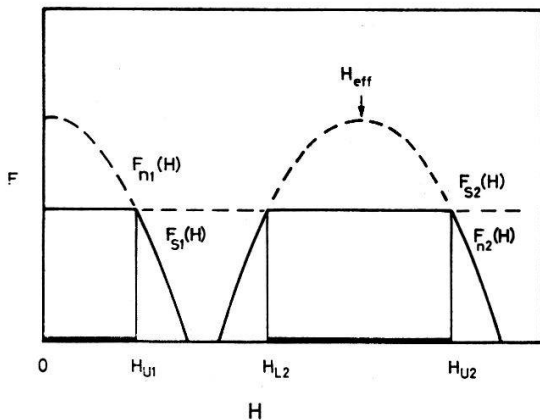
Figure 1
Free energy of the normal state $F_{n1}(H)$ and the superconducting state $F_{s1}(H)$ for a non magnetic metal and the same quantities $(F_{n2}(H), F_{s2}(H))$ for a magnetic superconductor with an exchange field H_{eff} pointing opposite to the external field, neglecting orbital effects H_{u1}, H_{L2}, H_{u2} are the corresponding paramagnetic critical fields.

However, for this to be true, the orbital effects of the external field must be negligible. More recent measurements of critical fields in high field superconductors show that one in those cases mostly has $H_{c_2}^*(0) \approx H_{p0}$, where $H_{c_2}^*(T)$ is the critical field due to purely orbital effects. In such cases the possibility of superconductivity may already be destroyed when H fulfills the condition (2). One question that arises is therefore, how to increase $H_{c_2}^*$. One might think that it should be possible to compensate the orbital effect of the magnetic field by an effective internal field, in the same way as one may compensate the effect of the external field on the spins by an internal exchange field. This problem was analyzed by Avenhaus et al. [7]. They found that the internal field that acts like an external field, and thus might compensate the latter is $4 \pi M$ where M is the mean magnetization of the ferromagnet. The reason is essentially that to compensate the orbital part one needs long range interactions and the only long-range interaction in a ferromagnet is the dipolar magnetic field of the ions [8].

Apart from the difficulties due to the orbital effects of the magnetic field, there is a practical difficulty in observing the effect of Jaccarino-Peter. Since we do not know any ordered dense ferromagnetic superconductor, we have to start with a ferromagnet that we can only hope will become superconducting when the magnetic interactions are removed. This makes of course a systematic search for this effect very difficult.

However, the compensation effect itself may be more easily observed in a superconductor with magnetic impurities, if the critical field is high enough so that the magnetic ions are aligned at $H = H_{c_2}$ at the temperatures available. Schwartz and Gruenberg [9] suggested that one might in such cases observe as one increases the

external magnetic field (at a certain temperature lower that T_c), first a superconducting region, than a normal region and than a superconducting region again, the latter one being determined essentially by condition (2). This second region can again only be observed of $H_{c_2}^*(0) \gg H_{p0}$, a condition not realized in the superconductors we know today. Parks [10] reported the failure of an attempt to find this effect in $La_{3-x}Ce_xIn$. However, in this system one has certainly $H_{c_2}^*(0) < H_{p0}$ and the second domain predicted by Schwartz and Gruenberg will not appear.

We want to point out that even in cases where $H_{c_2}^*(0) < H_{p0}$ it is possible to observe the compensation effect of Jaccarino-Peter by looking at the behaviour of the critical field as a function of concentration (c) of magnetic impurities. The basic idea is the following:

As shown by Fulde and Maki [11], the orbital critical field $H_{c_2}^*(0)$ (neglecting the Clogston limit) decreases linearly with concentration c. We may write

$$H_{c_2}^*(c, T = 0) = H_{c_2}^*(c = 0, T = 0) \left(1 - \frac{c}{c_{crit}}\right), \tag{3}$$

where c_{crit} is the concentration where the superconductivity is destroyed in absence of an external field. On the other hand, the mean exchange field H_J (for aligned spins) increase linearly with concentration.

$$H_J = \frac{c J_c \langle S_z \rangle}{g \mu_B}. \tag{4}$$

J_0 is the mean value of the exchange interaction, S is the spin of the magnetic impurity. Obviously these two fields must meet, and at a certain concentration c' we will have $|H_J| = H_{c_2}^*(0\ c')$. If the sign of H_J is opposite to H (external field) at $H = H_{c_2}^*(0\ c')$ we will have $H_J + H_{c_2}^*(0\ c') = 0$ and there will be no effect on the conduction electron spins. This means however that the real critical field H_{c_2} will be equal to $H_{c_2}^*$ at that concentration. To both sides of c' we will have $H_{c_2} < H_{c_2}^*$ since than there will be a field acting on the conduction electron spins. The quantity $H_{c_2}(c, 0)/H_{c_2}^*(c, 0)$ plotted as a function of concentration should therefore show a maximum at c' in the case of compensation. On the contrary, if H_J and H have the same sign we expect $H_{c_2}(c, c)/H_{c_2}^*(c, 0)$ to decrease monotonously. This is illustrated in Figure 2.

To discuss this effect quantitatively we need an expression for the critical field of a high field superconductor with magnetic impurities. The problem without magnetic impurities has been discussed by many authors [12]–[17] but it is only the work of Werthamer et al. [17] (WHH) which permits a quantitative comparison with experiment, and most recent work on high field superconductors has been compared with this theory. For that reason we shall derive the critical field of a superconductor with magnetic impurities in the WHH-formalism. This is done in chapter 2, where we also discuss the case of a thin film with magnetic impurities. Since the calculation follows very closely the one of WHH, we only give its main features. The more detailed calculations are partly given in Appendix A–D. The final result when specialized to the dirty limit, gives an expression which is analogous to the one obtained by Fulde and Maki [11] but in disagreement with the expression obtained by Bennemann et al. [18]. In chapter 3 we discuss the obtained equations with emphasis on the compensation effect.
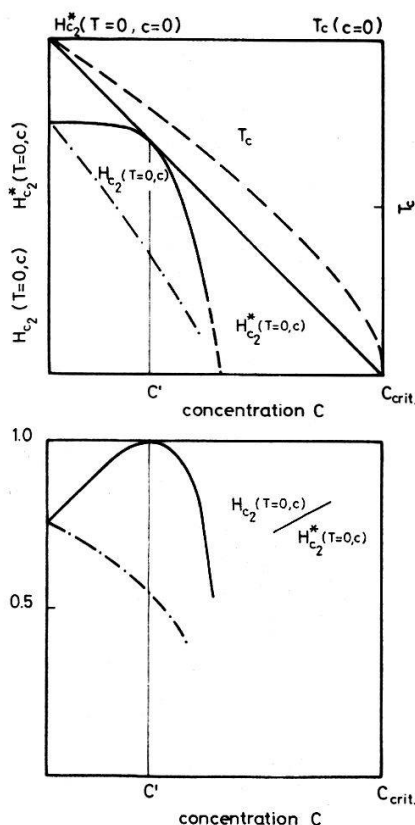
Figure 2
Schematic description of the concentration dependence of the critical field $H_{c_2}(T = 0)$ for a superconductor with magnetic impurities. In the case of a compensation of the paramagnetic effect, the reduced quantity $H_{c_2}^*$ will show a maximum at the concentration c' where $H_J(c') = H_{c_2}^*(c')$. In the second case this reduced quantity should decrease monotonously.

One obvious result from chapter 3 is that to observe this compensation effect one needs very high critical fields. To reach these fields experimentally, we constructed a pulsed field apparatus, described in chapter 4. In chapter 5 we discuss the experimental results on the systems $Mo_{1-x}M_xGa_4$ (M = Nb, Ru, Mn, Fe, Co). Only Mn as impurity showed a well-developed magnetic moment and in that case we were also able to demonstrate the compensation effect.

In chapter 6, finally, we discuss in view of the results obtained in chapters 2–5 the possibility of observing the effect of Jaccarino-Peter in more dense systems.

2. Calculation of the critical Field

As shown by WHH [17], to get a realistic description of the critical field it is necessary to take into account both the orbital and paramagnetic effect of the external field as well as non-magnetic and spin-orbit scatterings. The effect of the non-magnetic scatterings is essentially to reduce the effective coherence length and thus decrease the effect of the orbital part of the magnetic field, whereas the spin-orbit interaction increases the susceptibility of the superconducting gas, thus increasing the paramagnetic limit H_p discussed in the introduction. In addition this we have to take into account the presence of magnetic impurities. We shall, however, not take into account the dynamics of the spins, due to eventual interactions between the ions, since we are mainly concerned with a demonstration of the compensation of the exchange field. Furthermore, due to a recent paper by Keller and Benda [19], the spin dynamics has very little effect on the superconductivity in the limits we are concerned with.

We take as Hamiltonian:

$$\mathscr{H} = \int d^3r \, \psi^+(r) \left[-\frac{1}{2m} (\nabla - i \, e \, A)^2 - g \, \mu_B (\boldsymbol{\sigma} \, H) \right] \psi(r)$$

$$+ \int d^3r \, d^3r' \, \psi^+(r) \left(V_a(r, r') + V_b(r, r') \right) \psi(r') \tag{5}$$

$$+ \frac{g}{2} \int d^3r \, \psi^+(r) \, \psi^+(r) \, \psi(r) \, \psi(r) \, .$$

H is the external field, A is the vector potential, $\psi^+(r)$, $\psi(r)$ are the field operators. V_a is the potential due to non-magnetic impurities, V_b is the potential due to magnetic impurities.

$$V_a(r, r') = \sum_i \left[V_{a1}(r - R_i) \, \delta(r - r') + V_{a2} \left(\frac{r + r'}{2} - R_i, r - r' \right) \right], \tag{6a}$$

$$V_b(r, r') = \sum_j \left[V_{b1}(r - R_j) \, \delta(r - r') + V_{b2} \left(\frac{r + r'}{2} - R_j, r - r' \right) \right.$$

$$\left. + \frac{1}{N} J(r - R_j) \, (\boldsymbol{S} \cdot \boldsymbol{\sigma}) \, \delta(r - r') \right]. \tag{6b}$$

V_{a1} and V_{b1} are non-magnetic potentials, V_{a2} and V_{b2} are spin-orbit potentials and $J(r - R_j)$ is the exchange interaction between the localized ions with spin $\boldsymbol{S}$ and the conduction electrons with spin $\boldsymbol{\sigma}$. N is the number of atoms in our system. R_i, R_j are the positions of the non-magnetic and magnetic ions, respectively. Throughout this and the next chapter we work with units $\hbar = c = k_B = 1$.

To distinguish from the beginning between the mean exchange field and the scattering effect of the magnetic ions, we subtract the mean value J_0 from $J(r - R_j)$ in $V_b(r \, r')$. We then write for the exchange potential

$$\frac{1}{N} \sum_j \left(J(r - R_j) - J_0 \right) (\boldsymbol{S} \cdot \boldsymbol{\sigma}) \, .$$

The subtracted term is added to the term proportional to $(\boldsymbol{H} \, \boldsymbol{\sigma})$. After taking the average of the impurity spins this gives us the mean exchange field, defined by equation (4).

The Hamiltonian (5) gives us the following Gorkov equations

$$\left(i \, \omega_n + \frac{1}{2m} (\nabla - i \, e \, A)^2 + g \, \mu_B \left((H + H_J) \cdot \boldsymbol{\sigma} \right) + \mu \right) \widehat{G}_\omega(r, r')$$

$$- \int \left(\widehat{V}_a(r, r_1) + \widehat{V}_b(r, r_1) \right) \widehat{G}_\omega(r_1, r') \, d^3r_1 \tag{7a}$$

$$+ \widehat{\varDelta}(r) \, \widehat{F}_\omega^+(r, r') = \delta(r - r') \, ,$$

$$\left(i\,\omega_n - \frac{1}{2\,m}\,(\nabla + i\,e\,A)^2 - g\,\mu_B\big((H + H_J)\cdot\sigma\big) - \mu \right) \widehat{F}_\omega{}^+(r, r')$$

$$+ \int \big(\widehat{V}_a^t(r_1, r) + \widehat{V}_b^t(r_1, r)\big)\,\widehat{F}_\omega{}^+(r_1, r')\,d^3r_1 \tag{7b}$$

$$+ \widehat{\Delta}^*(r)\,\widehat{G}_\omega(r, r') = 0 \,,$$

where as usual $\omega_n = \pi\,T(2\,n + 1)$ and $\widehat{A}\cdot\widehat{B}$ denotes the spin matrix product. Furthermore

$$V_{\alpha\beta}^t = V_{\beta\alpha}\,, \quad \alpha,\,\beta = \text{spinindices}.$$

The order parameter $\Delta(r)$ is determined by

$$\widehat{\Delta}(r) = |\,g\,|\,T\sum_\omega \widehat{F}_\omega(r, r)\,. \tag{8}$$

To calculate the second order transition between the superconducting and the normal state we have to find $\widehat{F}_\omega(r, r)$ from equations (7), insert it into equation (8) and take the limit $\Delta \to 0$. Now, as first shown by Gorkov [20], by inverting the equations (7), $\widehat{F}_\omega$ may be expanded in terms of $\Delta(r)$ and $\widehat{G}_\omega^n(r, r')$, where $\widehat{G}_\omega^n(r, r')$ is the normal state Green function determined by equation (7a) with $\Delta(r) = 0$. The term in lowest order in $\Delta(r)$ is (see Appendix A):

$$\widehat{F}_\omega(r, r') = \int \widehat{G}_{-\omega}^n(s, r)\,\widehat{\Delta}(s)\,\widehat{G}_\omega^n(s, r')\,d^3s\,. \tag{9}$$

Using symmetry relations one can show that $\widehat{F}$, $\widehat{G}$, $\widehat{\Delta}$ may be written in the explicit form

$$\widehat{F}_\omega = \begin{pmatrix} 0 & -F_{\omega+} \\ F_{\omega-} & 0 \end{pmatrix}, \quad \widehat{G}_\omega = \begin{pmatrix} G_{\omega+} & 0 \\ 0 & G_{\omega-} \end{pmatrix}, \quad \widehat{\Delta} = \Delta \begin{pmatrix} 0 & 1 \\ -1 & 0 \end{pmatrix}.$$

By multiplying equation (9) by $i\,\sigma_y$ and taking the trace (tr) of equation (8) in spin space we get:

$$\Delta(r) = \frac{1}{2}\,|\,g\,|\,T\sum_\omega \int \text{tr}\,\big(\widehat{G}_{-\omega-\sigma}^n(s, r)\,\widehat{G}_{\omega\sigma}^n(s, r)\big)\,\Delta(s)\,d^3s\,. \tag{10}$$

Finally we have to average over the positions of impurities and the orientation of their spins. This is done in the usual approximation by assuming that $\Delta(s)$ varies slowly in space compared to $\widehat{G}_\omega^n(r, s)$. We then get:

$$\Delta(r) = \frac{1}{2}\,|\,g\,|\,T\sum_\omega \int \text{tr}\,\big(\langle\widehat{G}_{-\omega-\sigma}^n(s, r)\,, \quad \widehat{G}_{\omega\sigma}^n(s, r)\rangle_{R_i R_j S_j}\big)\,\Delta(s)\,d^3s\,. \tag{11}$$

By a standard transformation (see Appendix B), introducing the BCS cutoff equation (11) may be written:

$$\ln\left(\frac{T_{c0}}{T_c}\right)\Delta(r) = \sum_n \int d^3r' \left[\frac{\delta(r - r')}{|\,2\,n + 1\,|} - \frac{1}{2}\,\text{tr}\,\widehat{S}_\omega(r, r') \right]\Delta(r^i) \tag{12}$$

we have here introduced the WHH-Kernel [17]

$$\widehat{S}_\omega(r, r') = \frac{T}{N(0)} \langle \widehat{G}^n_{-\omega-\sigma}(r', r) \, \widehat{G}^n_{\omega\sigma}(r', r) \rangle_{R_i, R_j, S_j} \,. \tag{13}$$

$N(0)$ is the density of states at the Fermi surface. It is now useful to introduce the Kernel $S^0_\omega(r, r')$

$$\widehat{S}^0_\omega(r, r') = \frac{T}{N(0)} \langle \widehat{G}^n_{-\omega-\sigma}(r', r) \rangle_{R_i R_j S_j} \langle \widehat{G}^n_{\omega\sigma}(r', r) \rangle_{R_i R_j S_j} \,. \tag{14}$$

As shown by Abrikosov and Gorkov [2] $\widehat{S}_\omega(r, r')$ can be calculated in terms of $\widehat{S}^0_\omega(r, r')$ by summing the 'chain diagrams'. This gives an integral equation for $\widehat{S}_\omega(r, r')$ which in the WHH notation becomes

$$\widehat{S}_\omega(r, r') = \widehat{S}^0_\omega(r, r') + \int d^3r_1 \, S^0_\omega(r, r_1) \frac{N(0)}{T(\delta^3(0))^2} \int d^3r_2 \tag{15}$$

$$\times \, [\langle \widehat{V}_a(r_1, r_2) \, \widehat{S}_\omega(r_1, r') \, \widehat{V}_a(r_2, r_1) \rangle_{R_i R_j S_j} + \langle \widehat{V}_b(r_1, r_2) \, \widehat{S}_\omega(r_1, r') \, \widehat{V}_b(r_2, r_1) \rangle_{R_i R_j S_j}] \,.$$

$\tilde{V}$ is defined as:

$$\widehat{V}_\sigma(r, r') = V_{-\sigma}(r', r) \,.$$

This form is introduced when we make the transformation with $i\,\sigma_y$ since

$$(2\,i\,\sigma_y)^{-1} \, \boldsymbol{\sigma}^t (2\,i\,\sigma_y) = -\,\boldsymbol{\sigma} \,.$$

Thus V^t_σ is transformed into $\boldsymbol{V}_\sigma$.

Equation (15) is valid if the spin-orbit scatterings are infrequent compared to non-magnetic scatterings. (For a discussion of this point, see WHH [15]).

We now note that equation (12) is an eigenvalue equation for $\widehat{S}_\omega(r, r')$ with $\varDelta(r)$ as eigenfunction. From equation (15) one finds that if $\varDelta(r)$ is an eigenfunction of $\widehat{S}^0_\omega(r, r')$ it is also an eigenfunction of $\widehat{S}_\omega(r, r')$. Thus if one knows the eigenvalue s^0_ω of $\widehat{S}^0_\omega(r, r')$ equation (15) turns into an algebraic equation for the eigenvalue s_ω of $\widehat{S}_\omega(r, r')$. We thus have to study the equation

$$s^0_\omega \, \varphi(r) = \int S^0_\omega(r, r') \, \varphi(r') \, d^3r' \,. \tag{16}$$

Introducing the explicit expressions for the Green function $\langle \widehat{G}^n_\omega(r, r') \rangle_{R_i R_j S}$ [21] we get:

$$s^0_\omega \, \varphi(r) = \frac{T}{2\,v_F} \int \frac{d^3r'}{|r - r'|^2} \exp\left\{\left[-\,i\,2\,g\,\mu_B\,\boldsymbol{\sigma}(\boldsymbol{H} + \boldsymbol{H}_J)\,s\,g\,n\,\omega + 2\,|\,\omega\,| + \frac{1}{\tau}\right]\right.$$

$$\left. \times \frac{|\,r - r'\,|}{v_F} + 2\,i\,e\int\limits_{r'}^{r} \boldsymbol{A}(s)\,d\boldsymbol{s}\right\} \varphi(r') \,. \tag{17}$$

The lifetime τ is given by a sum of contributions of the different potentials defined in equations (6a–b). The different scattering times are defined more precisely in Appendix C. Note here that if the mean free path, $l = v_F \tau$ is short compared with the dimensions of the sample, the only part in $S_\omega(r, r')$ that depends on the shape of the sample is the integral over $A(s)$ in the exponent in $S_\omega^0(r, r')$. Thus any difference in the behaviour of the critical field of, for instance a thin film and a bulk sample must come from that integral.

As shown by Helfand and Werthamer [16] equation (17) gives:

$$s_\omega^0 = \frac{T}{2\, v_F (2\, e\, H)^{1/2}} \int \frac{d^3\varrho}{\varrho^2}\, e^{-(\varrho/\alpha_\omega)}\, e^{(1/4)\varrho_\perp \langle (\nabla - 2ieA)_\perp^2 \rangle / 2eH}, \tag{18}$$

where $\varrho_\perp$ and $(\nabla - 2\, i\, e\, A)_\perp$ are the components perpendicular to the field H. The parameter α_ω is defined as

$$\alpha_\omega = \frac{v_F\, (2\, e\, H)^{1/2}}{2\,|\omega| + \dfrac{1}{\tau} + 2\, i\, g\, \mu_B\, \boldsymbol{\sigma}(H + H_J)\, sgn\, \omega}. \tag{19}$$

The mean value over $(\nabla - 2\, i\, e\, A)_\perp^2$ is to be taken with the lowest eigenfunction [23] $\varphi_0(r)$ of $S_\omega^0(r, r')$, which is also an eigenfunction of $(\nabla - 2\, i\, e\, A)^2$. Our problem is thus equivalent to the problem of one electron in a magnetic field. For the bulksystem we may therefore immediately write

$$\langle (\nabla - 2\, i\, e\, A)_\perp^2 \rangle = -\, 2\, e\, H. \tag{20}$$

For a thin film the boundary conditions make the problem difficult to solve in general, however if d (the film thickness) is smaller than $\xi \approx \sqrt{\xi_0\, l}$ we may take $\Delta(r)$ constant over the film, provided that we use the London gauge [22], $(\nabla \cdot A) = 0$. We then have:

$$\langle (\nabla - 2\, i\, e\, A)_\perp^2 \rangle = -\, 4\, e^2\, \langle A^2 \rangle$$

$$= -\frac{4\, e^2}{d} \int_{-d/2}^{+d/2} H^2\, x^2\, dx = -\frac{1}{3}\, e^2\, H^2\, d^2. \tag{21}$$

Now, inserting equation (20) and equation (21) in equation (18) and introducing the Fourier transform of $(1/\varrho^2)\, e^{-\varrho/\alpha_\omega}$ we finally get

Bulk: $$s_\omega^0 = \frac{2\, \pi\, T}{v_F (2\, e\, H)^{1/2}}\, J(\alpha_\omega). \tag{22}$$

Thin films: $$s_\omega^0 = \frac{2\, \pi\, \sqrt{3}\, T}{v_F\, e\, H\, d}\, J(\beta_\omega). \tag{23}$$

Where

$$J(x) = 2 \int_0^\infty dq\, \tan^{-1}(x\, q)\, e^{-q^2}. \tag{24}$$

α_ω is defined by equation (19). β_ω is defined by

$$\beta_\omega = \frac{\dfrac{v_F\, e\, H\, d}{\sqrt{3}}}{2\,|\,\omega\,| + \dfrac{1}{\tau} + 2\,i\,g\,\mu_B\,\boldsymbol{\sigma}(H + H_J)\,s\,g\,n\,\omega}. \tag{25}$$

By making use of equation (16), equation (15) becomes an equation for the eigenvalue s_ω of $S_\omega(r, r')$. This equation is solved in Appendix C. One finds

$$\frac{1}{2}\operatorname{tr} s_\omega = \left(\frac{1}{\operatorname{Re}\left\{ \dfrac{1}{\dfrac{1}{s_\omega^0} - \lambda + \lambda_{s0}} \right\}} - \lambda_{s0} + \lambda_m \right)^{-1}, \tag{26}$$

where s_ω^0 is now defined with $g(\boldsymbol{\sigma}\,H) = H$ in α_ω (or β_ω). Re means that the real part is to be taken.

The parameters λ, λ_m, λ_{s0}, are defined as

$$\lambda = \frac{1}{2\,\pi\,T_{c0}\,\tau} \qquad \text{'non-magnetic' scattering parameter},$$

$$\lambda_{s0} = \frac{2}{3\,\pi\,T_{c0}\,\tau_{s0}} \qquad \text{generalized spin-orbit scattering parameter}, \tag{26b}$$

$$\lambda_m = \frac{1}{\pi\,T_{c0}\,\tau_s} \qquad \text{exchange scattering parameter}.$$

The different scattering times are defined in Appendix C. Inserting equation (26) in equation (12) we finally get the equation for the phase transition $s - n$:

$$\mathrm{n}\left(\frac{T_{c0}}{T}\right) = \sum_n \left\{ \frac{1}{|\,2\,n + 1\,|} - \left[\frac{1}{\operatorname{Re}\left(\dfrac{1}{\dfrac{1}{s_\omega^0} - \lambda + \lambda_{s0}} \right)} - \lambda_{s0} + \lambda_m \right]^{-1} \right\}. \tag{27}$$

This equation is valid for all mean free paths for the bulk case, the only restriction being that spin-orbit scattering is infrequent in comparison with non-magnetic scattering i.e. $\lambda \gg \lambda_{s0}$.

The cases of a pure superconductor with magnetic impurities, e.g. *La*-Ce or *La*-Gd should be analyzed with this formula rather than the dirty limit formula normally used [11].

For the case of a thin film we have already assumed $d < \sqrt{l\,\xi_0}$ and $l < d$, thus a dirty thin film. However, as shown by de Gennes and Tinkham [24] the result will also be valid for $d < l$ if we replace $l = v_F\,\tau$ by $d \cdot (9/16)$.

The equation [27] simplifies considerably in the dirty limit. As shown in Appendix D we then get:

$$\ln\left(\frac{1}{t}\right) = \sum_{n=-\infty}^{+\infty} \left\{ \frac{1}{|2n+1|} - \frac{1}{|2n+1| + \dfrac{h^\nu + \lambda_m}{t} + \dfrac{\alpha^2(h+h_J)^2}{|2n+1| + \dfrac{h^\nu + \lambda_{s0}}{t}}} \right\}. \quad (28)$$

Here we have written: $t = T/T_{c0}$ and:
for Bulk samples:

$$\nu = 1\,,$$

$$h = \frac{v_F^2\, e\, \tau}{3\,\pi\, T_{c0}}\, H \quad \text{'reduced field'}\,, \quad (29)$$

$$\alpha = \frac{3}{2\,m\, v_F^2\, \tau} \quad \text{Maki parameter[1])}\,. \quad (30)$$

For thin films:

$$\nu = 2\,,$$

$$h = \frac{e\, d\, v_F}{3}\left(\frac{\tau}{2\,\pi\, T_{c0}}\right)^{1/2} H \quad \text{'reduced field'}\,, \quad (31)$$

$$\alpha = \frac{3}{m\, v_F\, d}\, \lambda^{1/2} \quad \text{Maki parameter[1]) for thin films}\,. \quad (32)$$

Equation (28) can now be written in terms of diagamma functions ψ. In Appendix E we have collected a few properties of that function, and we show that equation (28) may be written:

$$\ln\frac{1}{t} = \left(\frac{1}{2} + \frac{i(\lambda_{s0} - \lambda_m)}{4\,\gamma}\right) \psi\left(\frac{1}{2} + \frac{h^\nu + \lambda_m + \dfrac{1}{2}(\lambda_{s0} - \lambda_m) + i\,\gamma}{2t}\right)$$

$$+ \left(\frac{1}{2} - \frac{i(\lambda_{s0} - \lambda_m)}{4\,\gamma}\right) \psi\left(\frac{1}{2} + \frac{h^\nu + \lambda_m + \dfrac{1}{2}(\lambda_{s0} - \lambda_m) - i\,\gamma}{2t}\right) \quad (33)$$

$$- \psi\left(\frac{1}{2}\right),$$

where

$$\gamma = \left(\alpha^2(h+h_J)^2 - \frac{1}{4}(\lambda_{s0} - \lambda_m)^2\right)^{1/2}.$$

---

[1]) Do not confuse the Maki parameter α with the functions α_ω and β_ω defined in equations (19) and (25).

2

This result is analogous to the result of Fulde and Maki [11], if one neglects the effect of the external field on the conduction electron spins. Bennemann et al. [18] give a similar expression for the critical field. However these authors give a third term in γ^2, which comes from the cross term between the non-magnetic and the exchange potential. Such terms are indeed present in the one particle Greens function but drop out in the caculation of the transition $n - s$.

The critical field calculated above is the one corresponding to a second order phase transition. This is indeed the one in which we are interested, since at the compensation point we have only an orbital effect on the conduction electrons, which in type II superconductors always produces a second order phase transition. However, when we are far from the compensation point it might be that the effect on the spins is strong enough to produce a first order transition. This must be checked in each particular case, but since it is not essential to the present investigation we will not consider it here.

3. Discussion of the Critical Field

(a) *A few simple cases*

In absence of a magnetic field equation (33) gives

$$\ln \frac{1}{t_c} = \psi\left(\frac{1}{2} + \frac{\lambda_m}{2\,t_c}\right) - \psi\left(\frac{1}{2}\right), \quad t_c = \frac{T_c}{T_{c0}}, \tag{34}$$

which is the well-known result of Abrikosov and Gorkov [2] for T_c as a function of concentration of magnetic impurities. If we define a universal pair breaking function $\varrho(t)$ given by

$$\ln\left(\frac{1}{t}\right) = \psi\left(\frac{1}{2} + \frac{\varrho}{2\,t}\right) - \psi\left(\frac{1}{2}\right). \tag{35a}$$

Equation (34) becomes

$$\varrho(t_c) = \lambda_m \,. \tag{36}$$

It is useful to note that

$$\left(\frac{\partial\varrho}{\partial t}\right)_{t=1} = \frac{4}{\pi^2} \quad \varrho(t=0) = \frac{1}{2\,\gamma_E} \approx 0.281 \,, \tag{35b}$$

where $C = \ln\gamma_E$ and C = Eulers Constant. Thus all superconductivity is destroyed when

$$\lambda_m > \lambda_{m\,crit} = \frac{1}{2\,\gamma_E} \simeq 0.281 \,. \tag{36b}$$

In absence of magnetic impurities and neglecting the Clogston limit (e.g. $\alpha = 0$) we get from equation (33)

$$\ln\frac{1}{t} = \psi\left(\frac{1}{2} + \frac{h^\nu}{2\,t}\right) - \psi\left(\frac{1}{2}\right), \tag{37}$$

which may be written

Bulk samples: $h_{c_2}^0(t) = \varrho(t)$.

Thin films: $h_c^0(t) = \sqrt{\varrho(t)}$.   (38)

If we now include magnetic impurities, but still keep $\alpha = 0$ we get $\left(h = h_{c_2}^*(t)\right)$

$$\lambda_m = h_{c_2}^{*\nu}(t) = \varrho(t)$$

or

Bulk samples: $h_{c_2}^*(t) = h_{c_2}^0(t) - \lambda_m$.

Thin films: $h_c^*(t) = h_c^0(t) \sqrt{1 - \dfrac{\lambda_m}{\varrho(t)}}$.   (39)

The equations (39) give thus the temperature and concentration dependence of the *orbital* critical field $H_{c_2}^*(T, c)$ of a superconductor with magnetic impurities. This result was first derived by Fulde and Maki [11]. Figure 3 shows the different cases discussed here.
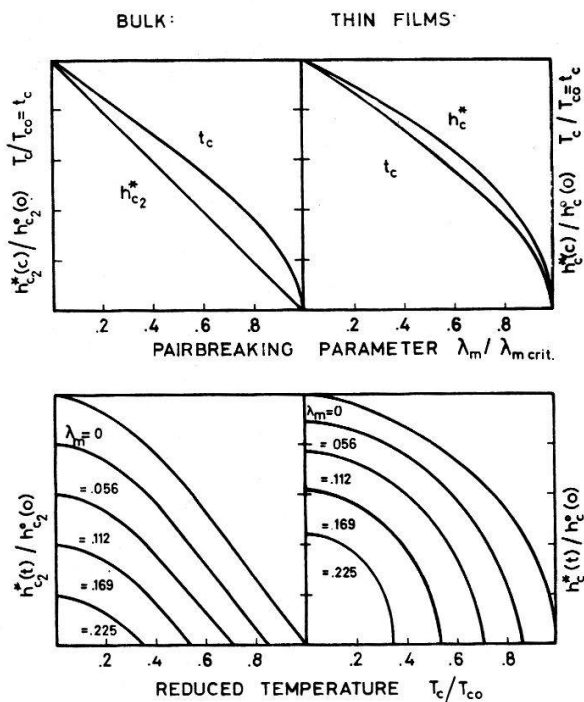
Figure 3
Orbital critical field as a function of temperature and of pairbreaking parameter λ_m ($\sim$ concentration) for bulk samples and thin films.

In the case of $\alpha \neq 0$, $\lambda_{s0} \neq 0$ it is only possible to give a simple expression for h if $\lambda_{s0} \gg \chi h$ (i.e. strong spin-orbit coupling). This will be discussed in the next section. However we will here look at the case of a high field superconductor *without* magnetic impurities. Putting $\lambda_m = 0$, $h_J = 0$ in equation (33) we get the WHH [17] result. In Figure 4 we show the computer solution of this equation for $\lambda_{s0} = 1.0$ and different α. The effect of an increasing α is to push down the high h-values. The effect of increasing λ_{s0} for fixed α is to push these curves upwards again, and in the limit $\lambda_{s0} \to \infty$ we find the curve for $\alpha = 0$. (When discussing h we have to keep in mind that h is mea-

sured with respect to $H_{c_2}^*(T = 0, c = 0)$ [see equation (40)] and since $\alpha \sim H_{c_2}^* (T = 0, c = 0)$ [equation (41)] (for T_{c0} fixed) the real critical field does of course increase when we increase α.)
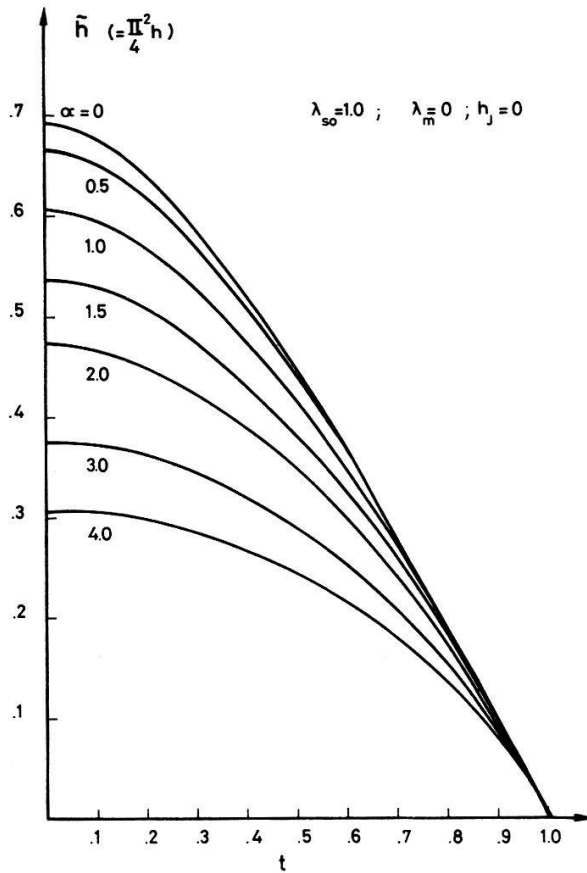
Figure 4
Critical field $\boldsymbol{h}_{c_2}$ ($= (\pi^2/4) \, h_{c2}$) as a function of temperature $t = T/T_{c0}$ for different values of the Maki parameter α assuming $\lambda_{s0} = 1$.

We now note that the case of a compensation we have $(h + h_J) = 0$ at a certain temperature i.e. it corresponds to the case of $\alpha = 0$ for a certain temperature. Therefore the maximum amount that can be gained in h by compensation is the difference $h(\alpha = 0, t = 0) - h(\alpha, t = 0)$.

Finally, we note that from equation (38) and equation (1) it follows by using the BCS relation between Δ and T that the definitions (29), (30), (31), (32) may be written:

Bulk:
$$h = \frac{1}{2 \, \gamma_E} \frac{H_{c_2}(c, T)}{H_{c_2}^*(c = 0, T = 0)} , \tag{40}$$

$$\alpha = \frac{\sqrt{2} \, H_{c_2}^*(c = 0, T = 0)}{H_{p0}} . \tag{41}$$

Thin films:
$$h = \frac{1}{\sqrt{2} \, \gamma_E} \frac{H_c(c, T)}{H_c^*(c = 0, T = 0)} , \tag{42}$$

$$\alpha = \frac{\sqrt{2} \, H_c^*(c = 0, T = 0)}{H_{p0}} , \tag{43}$$

where c is the concentration of magnetic impurities. Equation (41) is identical to Maki's definition [12].

In Appendix F we have collected a few useful formulas written in ordinary units, to permit comparison with experimental data.

(b) *Discussion of the compensation effect in the limit of strong spin-orbit scattering*

We suppose now that $\alpha(h + h_J) \ll 1/2 \, \lambda_{s0}$. Then we may write:

$$\gamma \approx \frac{i}{2} \left((\lambda_{s0} - \lambda_m) - \frac{2 \, \alpha^2 (h + h_J)^2}{\lambda_{s0} - \lambda_m} \right)$$

and equation (33) becomes

$$\ln \frac{1}{t} = \psi \left(\frac{1}{2} + \frac{h^\nu + \lambda_m + \dfrac{\alpha^2 (h + h_J)^2}{\lambda_{s0} - \lambda_m}}{2t} \right) - \psi \left(\frac{1}{2} \right). \tag{44}$$

The solution is

$$h^\nu + \lambda_m + \frac{\alpha^2 (h + h_J)^2}{\lambda_{s0} - \lambda_m} = \varrho(t) . \tag{45}$$

Making use of equation (39) this may be written:

For bulk samples: $\quad h_{c_2}(t) = h_{c_2}^*(t) - \dfrac{\alpha^2}{\lambda_{s0} - \lambda_m} \left(h_{c_2}(t) + h_J(t) \right)^2 . \tag{46}$

For thin films: $\quad h_c^2(t) = h_c^{*2}(t) - \dfrac{\alpha^2}{\lambda_{s0} - \lambda_m} \left(h_c(t) + h_J(t) \right)^2 .$

Finally we now define a reduced field h_{red} which is defined as

Bulk: $\qquad h_{red} = \dfrac{h_{c_2}(t)}{1 - \dfrac{\lambda_m}{\varrho(t)}} .$

Thin films: $\qquad h_{red} = \dfrac{h_c(t)}{\sqrt{1 - \dfrac{\lambda_m}{\varrho(t)}}} . \tag{47}$

Making use of equations (38)–(39) we get from equation (42)

Bulk: $\qquad h_{red} = h_{c_2}^0(t) - \dfrac{\alpha^2}{\lambda_{s0} - \lambda_m} \dfrac{\left(h_{c_2}(t) + h_J(t) \right)^2}{\left(1 - \dfrac{\lambda_m}{\varrho(t)} \right)} .$

Thin films: $\qquad h_{red}^2 = h_c^{02}(t) - \dfrac{\alpha^2}{\lambda_{s0} - \lambda_m} \dfrac{\left(h_c(t) + h_J(t) \right)^2}{\left(1 - \dfrac{\lambda_m}{\varrho(t)} \right)} . \tag{48}$

Note that our reduced field is essentially the quantity $H_{c_2}/H_{c_2}^*$ discussed in the introduction. Using equations (29)–(32) we may write equations (48) in terms of H:

Bulk:
$$H_{red} \equiv \frac{H_{c_2}(c, T)}{\left(1 - \dfrac{\lambda_m}{\varrho(t)}\right)} \equiv \frac{H_{c_2}(c, T)}{H_{c_2}^*(c, T)} H_{c_2}^*(c = 0, T) , \tag{49a}$$

$$= H_{c_2}^*(c = 0, T) - \frac{3\,e}{2\,m^2\,v_F^3}\left(\frac{\lambda}{\lambda_{s0} - \lambda_m}\right)\frac{1}{1 - \dfrac{\lambda_m}{\varrho(t)}}$$
$$\times \left(H_{c_2}(c, T) + H_J(c, T)\right)^2 . \tag{49b}$$

Thin films:
$$H_{red}^2 \equiv \frac{H_c^2(c, T)}{1 - \dfrac{\lambda_m}{\varrho(t)}} \equiv \frac{H_c^2(c, T)}{H_c^{*2}(c, T)} H_c^{*2}(c = 0, T) , \tag{50a}$$

$$= H_c^{*2}(c = 0, T) - \frac{3}{m\,v_F\,d}\left(\frac{\lambda}{\lambda_{s0} - \lambda_m}\right)\frac{1}{1 - \dfrac{\lambda_m}{\varrho(t)}}$$
$$\times \left(H_c(c, T) + H_J(c, T)\right)^2 . \tag{50b}$$

Here we have as in the previous section written c for the concentration of magnetic impurities. $H_{c_2}^*$ and H_c^* denotes as before the orbital critical field (i.e. by neglecting the Clogston limit). Note the difference in definition of H_{red} for a bulk sample and H_{red} for a thin film. Let us now suppose that we are at sufficiently low temperatures so that the magnetic ions are aligned in the magnetic field at $H = H_{c_2}$ (i.e. $\langle S_z \rangle = S$). It is then easy to see what happens to H_{red} if H_J points opposite to H. Let us look at H_{red} as a function of concentration c. For $c = 0$ we have $H_{red}(T) < H_{c_2}^*(T', c = 0)$, due to the second term. However at $H_{c_2} = |H_J|$ the second term vanishes and we have $H_{red} = H_{c_2}^*(T, c = 0)$. For higher c's H_{red} decreases again. Thus H_{red} shows a maximum which occurs precisely at the compensation point

$$H_{c_2}(c, T) = H_{c_2}^*(c, T) = |H_J| = \frac{c\,|J_0|\,S}{g\,\mu_B} . \tag{51}$$

On the other hand, if H and H_J has the same sign H_{red} will decrease monotonously. Finally if there is no effect on the spin H_{red} will remain constant.

Therefore H_{red} is in fact the characteristic quantity to plot to demonstrate the spin polarization effects on H_{c_2}. We note that H_{red} can be calculated from H_{c_2} (measured) and T_c/T_{c0} since λ_m is determined by the latter quantity (equation (36)).

The above statements hold always for h_{red} defined by equation (47), and it will hold for H_{red} if the conversion factors between h and H (equations (29), (31)) are independent of concentration of magnetic impurities c. Now τ will in general depend on c, since it contains all the different scattering times due to all the impurities. Thus τ can only be supposed constant if the concentration of non-magnetic impurities, dislocations and disorder, is much larger than the concentration of magnetic impurities (c).

This point however is not too difficult to check experimentally, since a compensation effect, as we shall see, essentially changes the form of $H_{c_2}(T)$, whereas a change in τ leaves the form unchanged and only change the value of $H_{c_2}(T)$ by a constant

factor. For a bulk sample for instance the initial slope will remain essentially constant at low concentrations c if τ does not change. If τ changes, the slope will increase at the rate $(1/\tau)$ increases. Furthermore, the variation of τ can be estimated by introducing non-magnetic impurities isoelectronic with the magnetic impurities. In the case of a thin film, the thickness d plays a similar role as τ^{-1}. Note finally that λ_{s0} depends also on the concentration c, both through the exchange scattering and the additional spin-orbit scattering. There is also a slight temperature dependence due to the temperature and field dependence of $\langle S_z^2 \rangle$.

From equation (51) it is seen that the position of the maximum in H_{red} allows one to determine J. Furthermore, as described above the maximum of H_{red} gives us $H_{c_2}^*(T, c = 0)$ $\big($or $H_c^*(T, c = 0)$ for a thin film$\big)$ i.e. the critical field that the 'pure' superconductor (i.e. without magnetic impurities) would have if we neglected the Clogston limit. From equations (41), (43) we than may calculate the Maki-parameter, and finally from the ratio $H_{c_2}(T, c = 0)/H_{c_2}^*(T, c = 0)$, we may determine λ_{s0} by using equation (33) in the limit $c = 0, t = 0$ or more direct by using the computer results of Hake [25] for $h(0)$ as a function of α and λ_{s0}. Note that this determination of J, α, λ_{s0} is *not* restricted to the limit of strong spin-orbit scattering.

To conclude this section we will discuss the form of the solutions of equation (46) i.e. the form of the curve critical field vs. Temperature. Since h_J depends on h (paramagnetic case) there exists the possibility of having more than one solution for h at a given temperature t. To illustrate this point we have plotted in Figure 5 and Figure 6 the functions.

$$\text{Bulk:} \qquad F_1(h) = \varrho)t) - \lambda_m - \frac{\alpha^2}{\lambda_{s0} - \lambda_m}(h + h_J)^2$$

and

$$\text{Thin films:} \quad F_J(h) = \sqrt{\varrho(t) - \lambda_m - \frac{\alpha^2}{\lambda_{s0} - \lambda_m}(h + h_J)^2}$$

and assuming in both cases $\alpha = 2$, $\lambda_{s0} - \lambda_m = 1$, $\lambda_m = 0.04$, and $h_J(t = 0) = -2\,h_{c_2}^*(t = 0)/3$. Furthermore we have assumed that h_J follows a Brillouin function:

$$h_J = h_{J0}\,B_s\left(2\,\tau\,\alpha\,S\,\frac{h}{t}\right).$$

We assume in the following $S = 5/2$. The solution of equation (46) are given by the intersections of F_1 or F_2 with the 45° line $(F_1 = h, F_2 = h)$. The second maximum in F_1 and F_2 occurs at the compensation point where $(h + h_J)^2 = 0$. However, in the bulk case (Fig. 5) the maximum is much less pronounced than in the thin film case (Fig. 6). This results in a single-valued function $h(t)$ for the bulk case but for the thin film the function $h(t)$ becomes triple-valued below a certain temperature t.

To see what happens physically in this last case, we look at the behaviour of the superconductor as we raise the external magnetic field. What happens is that h_J raises much faster than h and eventually $(h + h_J)^2$ becomes so large that the argument under the square root in F_2 vanishes. This means that the superconductivity is destroyed by the exchange field, and corresponds to the lowest solution. If we in-

crease the field more the exchange field will start to saturate and $(h + h_J)^2$ will decrease due to the compensation effect. The argument under the root in F_2 becomes again positive and at the second intersection with the 45° line in Figure 6 the system becomes superconducting again. As h continues to grow we pass the compensation point and $(h + h_J)$ starts to increase again. Finally at the third intersection the superconductivity is destroyed by the effect of the *external* field on the conduction electron spins.
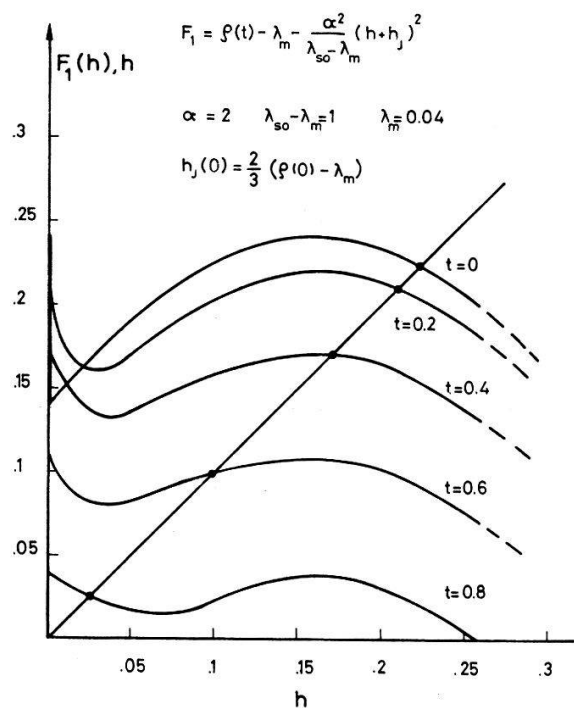

Figure 5
Graphical solution of the equation for the critical field in the case of a bulk superconductor with magnetic impurities in the limit of strong spin orbit scattering.
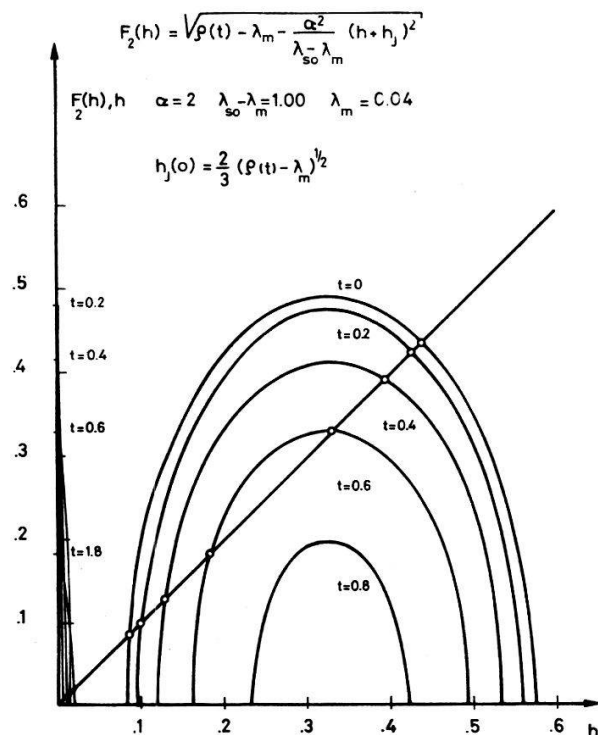

Figure 6
Graphical solution of the equation for the critical field in the case of a superconducting thin film with magnetic impurities in the limit of strong spin orbit scattering.

This second domain corresponds to the domain of ultra-high field superconductivity suggested by Jaccarino and Peter for a ferromagnet and by Schwartz and Gruenberg for a superconductor with magnetic impurities in the limit $H_p \gg H_{c_2}^*$. We find here that for a thin film this second domain may be realized even in the case $H_p \approx H_{c_2}^*(0, 0)$ whereas a bulk sample with the same parameters as the thin film does only show one domain, which includes the compensation domain. For this domain to split up in two domains one needs approximately $\alpha > 3$ and $\lambda_{so} < 1$. The reason for this difference between a thin film and a bulk sample is the following: In the case of a thin film the field h enters with the same power ($n = 2$) in the paramagnetic term as in the orbital term in the equation for H_{c_2}. This produces a strong paramagnetic effect. In the bulk case, on the contrary, the paramagnetic term enters with h^2 whereas the orbital term enters with h. For not too high α's this means that the paramagnetic effect is relatively weak.

The result of the graphical solution in Figure 5 and Figure 6 is shown in Figure 7. We note that for the bulk case the compensation effect will show itself in a more or less pronounced *upwards* curvature. For the thin film this may be replaced by a jump in the upper critical field from the uncompensated region to the compensated one. This jump will occur at a temperature t', slightly above the compensation point $(h(t) + h_J(t))^2 = 2$. (This can be easily seen from Figure 6. The jump will occur when F_2 just touches the 45° line. The compensation point corresponds to the temperature where the maximum of F_2 falls on the 45° line.) The temperature range for the compensation domain will therefore depend on the h_J chosen. For the most favourable compensation case $h_J(t = 0) = h_c^*(t = 0)$ this domain will only occur at very low temperatures.
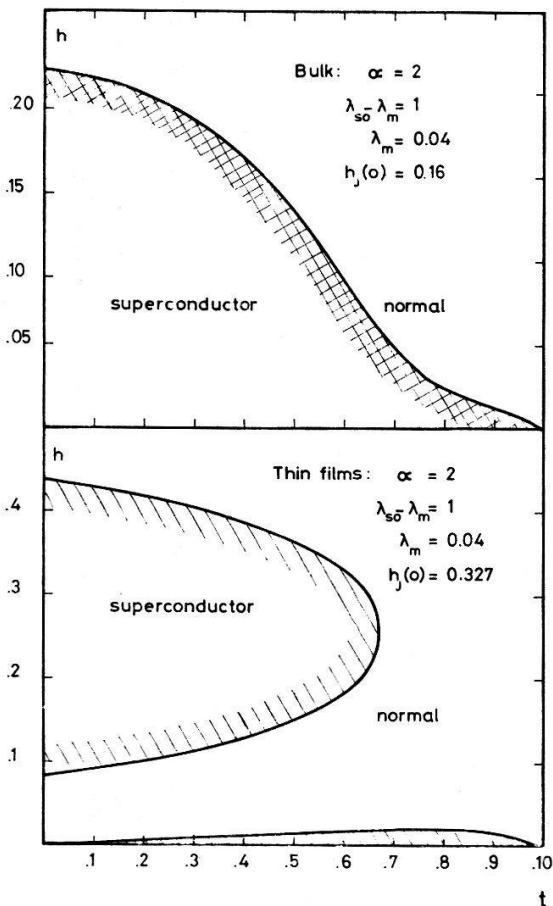

Figure 7
Critical field as a function of temperature as determined from the graphical solutions in Figures 5 and 6.

The above discussion is only qualitative, since the equation (46) are not strictly valid for the parameters chosen above.

Computer solutions of equation (33) show that the simplified equations (46) overestimate the paramagnetic effect slightly if we are not in the strong spin-orbit scattering limit (see chapter 3d).

(c) *Determination of the compensation point. Possibility if a real increase in H_{c_2}*

In the foregoing section we have described how to detect the compensation effect, and how this effect can be used to determine the parameters J_c, α, λ_{s0}. However, in the original paper by Jaccarino and Peter it was also suggested that one might actually increase the critical field by this effect. From equation (46) it is seen that if α is large this may actually be the case. However it depends also on how much T_c has been reduced before the compensation point is reached, i.e. the value of λ_m on the compensation point: λ_{mc}. To examine this point we make use of the explicit expression for λ_m given in Appendix F to rewrite H_J as

$$H_J = \lambda_m \frac{2\,k_B\,T_{c0}}{N(0)\,(S+1)\,J_0\,g\,\mu_B}.$$

We have here supposed thet $J(q)$ is independent of q so that the J occuring in λ_m is equal to the J_0 occuring in H_J. From equations (39) and (51) we now get for the bulk case and for $T = 0$:

$$\lambda_{mc} = \lambda_{mcrit} \frac{H_{c_2}^*(c=0, T=0)}{\dfrac{2\,\lambda_{mcrit}\,T_{c0}}{N(0)\,(S+1)\,J_0\,g\,\mu_B} + H_{c_2}^*(c=0, T=0)}, \tag{52}$$

where λ_{mcrit} is defined by equation (36b). To get a real H_{c_2}-increase it is obvious that we must have $\lambda_{mc} \ll \lambda_{mcrit}$, thus from (52) we must have:

$$\frac{0.57\,T_{c0}}{N(0)\,(S+1)\,J_0\,g\,\mu_B} \gg H_{c_2}^*(c=0, T=0). \tag{53}$$

On the other hand we must have a large α, say $\alpha > 1$. By making use of the definition (41) of α we now get

$$\frac{1.14}{N(0)\,(S+1)\,J_0} \gg \alpha > 1. \tag{54}$$

This can only be fulfilled if

$$(S+1)\,N(0)\,J_0 \ll 1. \tag{55}$$

Thus a real increase in the critical field can only occur if $N(0)\,J_0$ is relatively small, and it seems that the best chances to realize this increase in H_{c_2} is in high field superconductors where the high critical field is due to disorder and impurities rather than an anomalous high density of states.

Note however that we have assumed that the J in λ_m (Appendix F) and in H_J are the same. If $J(q)$ depends really on q the J in λ_m may be much smaller than the one in H_J in which case we may relax the condition (53). Finally we note that if for instance in the β-W structures ($A_3 B$) we may put the magnetic impurity on the B-sites the effective density of states in equation (52) may be much smaller than the density of states determined by electronic properties (χ, γ) since the superconducting electrons are believed to be localized on the A-sites.

(d) *Computer solutions. A few typical examples*

In most interesting cases the approximation $\alpha(h + h_J) \ll \lambda_{s0}/2$ does not hold, and the critical field cannot be calculated by the simple relations (46). However it follows from equation (33) that H_{red} defined by equations (49a) and (50a) will still show a maximum at the compensation point, but the form of $H_{red}(c)$ will not be given by the relations (49b) and (50b). To show what the critical field curves $H_{c_2}(T, c)$ will look like in the case of the compensation effect we will now give a few examples based on computer solutions of equation (33).

As a concrete example we take the system Nb$_3$Al. Hechler and Saur [26] found, by fitting the experimental H_{c_2} vs. T curve to the theoretical curve calculated from equation (33) with $\lambda_m = 0$, $h_J = 0$, that $\alpha = 2.08$, $\lambda_{s0} = 1$. The critical temperature is $18.0°$K and the critical field extrapolated to zero temperature 252 kGauss. The density of states has been given by Spitzli [27], who finds $N(0) = 1.7$ states/eV. We now assume that we may introduce magnetic impurities with a spin $S = 5/2$ and with an exchange constant J into Nb$_3$Al. For the case where the sign of J is such that we may compensate, the compensation point (λ_{mc}) is given by the absolute value of J by equation (52). Assuming $J = -0.005$ eV we get $\lambda_{mc} = 0.035$, for $J = -0.015$ eV we get $\lambda_{mc} = 0.085$ and finally for $J = -0.025$ eV, $\lambda_{mc} = 0.117$. These three cases are shown in Figures 8, 9, 10. For the first (two) cases there is a substantial increase in the critical field. We note that the form of the critical field curves are strongly different from the cases of non-magnetic systems. The uwpards curvature should be a characteristic feature of a strong compensation effect. In these figures are also shown the case where H_J has the same sign as H. The part of the curves that shows a $dH_{c_2}/dT > 0$ might not be real since it is possible that the transition might be first order in this region. However, Crow et al. [28], observed in La$_{3-x}$Gd$_x$In a behaviour qualitatively similar to the curves given by the dotted lines, indicating a positive exchange constant in that case. Crow et al. found that all the transitions measured were second order. In Figure 11 is shown $T_c(c)$, $T_c(c)/T_{c_0}$, $H_{c_2}(c, T = 0)/H_{c_2}(0, T = 0)$, $H_{red}(c\ T = 0)/H_{c_2}(0, T = 0)$ for two cases.

In the case of a thin film, α is defined with the orbital critical field of the thin film (equation (43)). By using the Gennes-Tinkham [24] formula (see Appendix F) one finds that a thin film of about 40 Å thick may have an α of about 3. Assuming $\lambda_{s0} = 1$ and $\lambda_{mc} = 0.07$ we get the results shown in Figure 12. To allow a comparison with the bulk case for Nb$_3$Al we show in Figure 13 the case of $\alpha = 2$, $\lambda_{s0} = 1.04$, $\lambda_{mc} = 0.057$. As demonstrated in chapter 3b) there is a net difference between the behaviour of a thin film and a bulk superconductor.

Figure 8
Critical field as a function of temperature for different pairbreaking parameters assuming a negative exchange field and $\alpha = 2.08$, $\lambda_{s0} = 1$, $\lambda_{mc} = 0.035$. The dotted lines correspond to a positive exchange field.
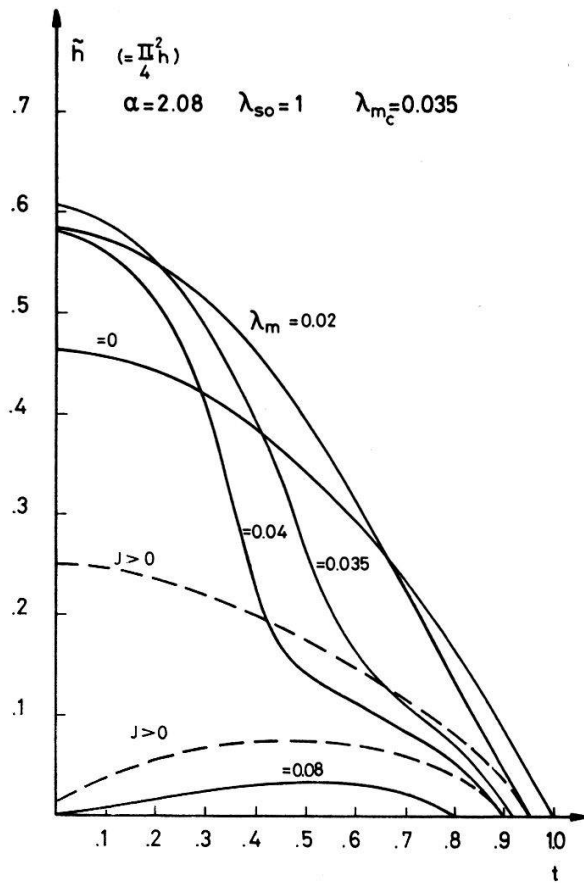

Figure 9
Critical field as a function of temperature for different pairbreaking parameters, assuming a negative exchange field and $\lambda_{mc} = 0.085$, $\alpha = 2.08$, $\lambda_{s0} = 1$. The dotted lines correspond to a positive exchange field.

Figure 10
Critical field as a function of temperature for different pairbreaking parameters λ_m assuming a negative exchange field $\lambda_{mc} = 0.117, \alpha = 2.08, \lambda_{s0} = 1.00$. The dotted lines correspond to a positive exchange field.
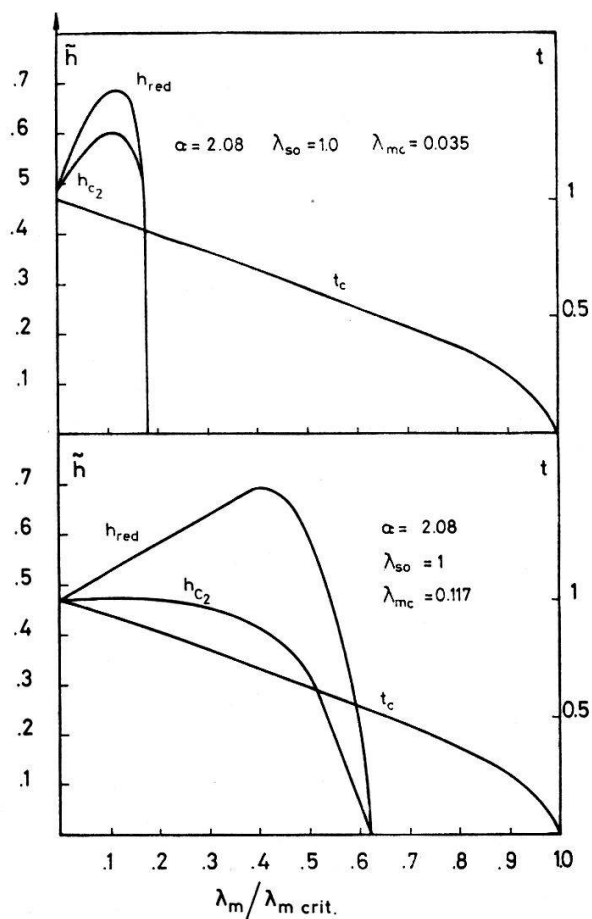
Figure 11
h_{c_2}, h_{red} and t_c as a function of λ_m ($\sim$ concentration of magnetic impurities for $\alpha = 2.08$, $\lambda_{s0} = 1$, and the two cases $\lambda_{mc} = 0.035$ and 0.117.
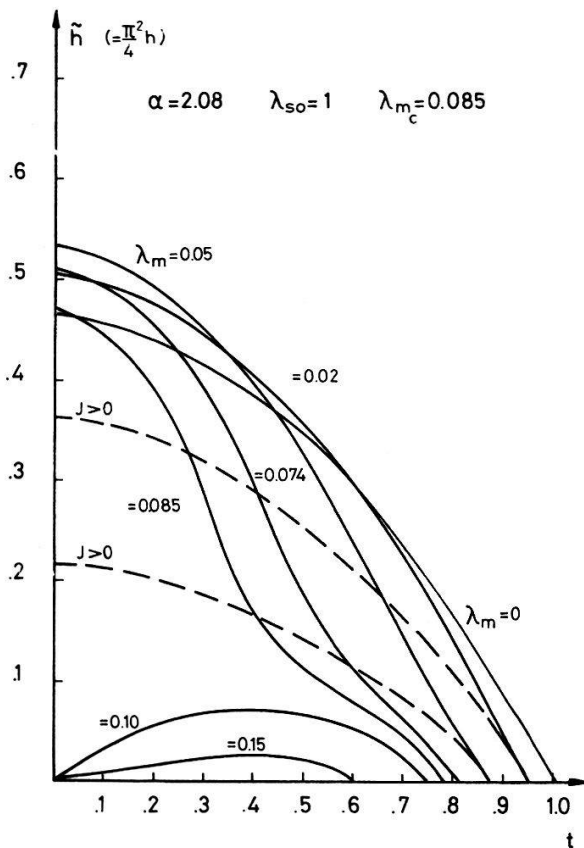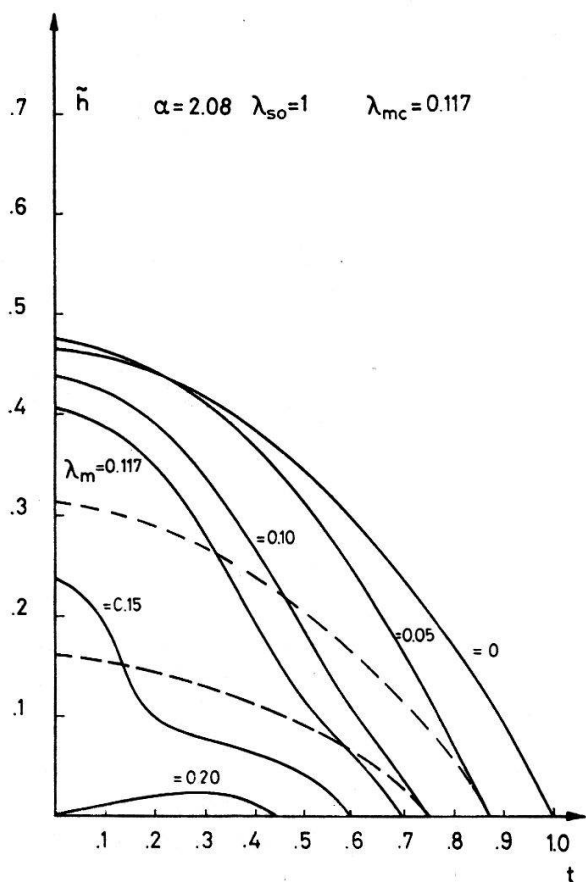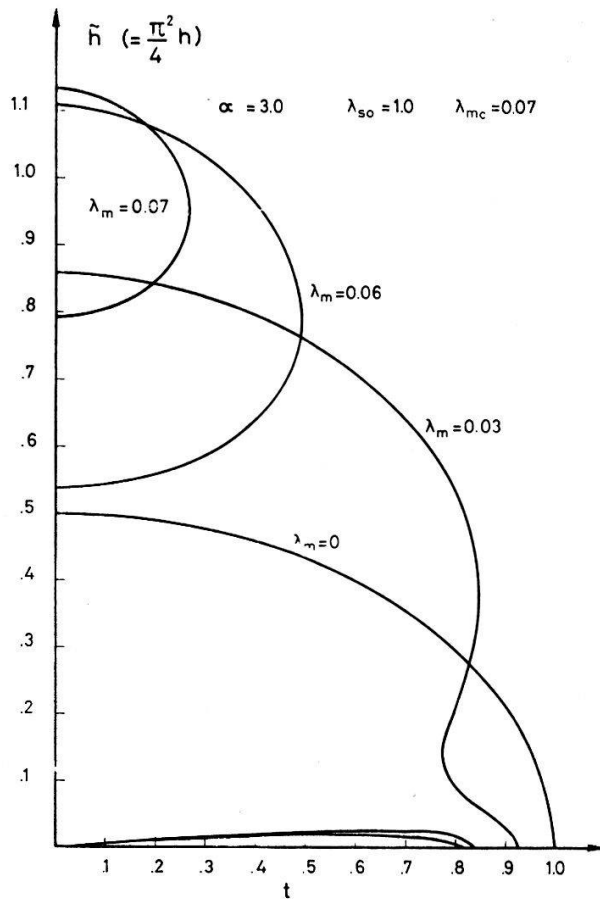
Figure 12
Critical field as a function of temperature
for a thin film for different pairbreaking
parameters, assuming a negative exchange
field and $\alpha = 3.0$, $\lambda_{s0} = 1.0$, $\lambda_{mc} = 0.07$.
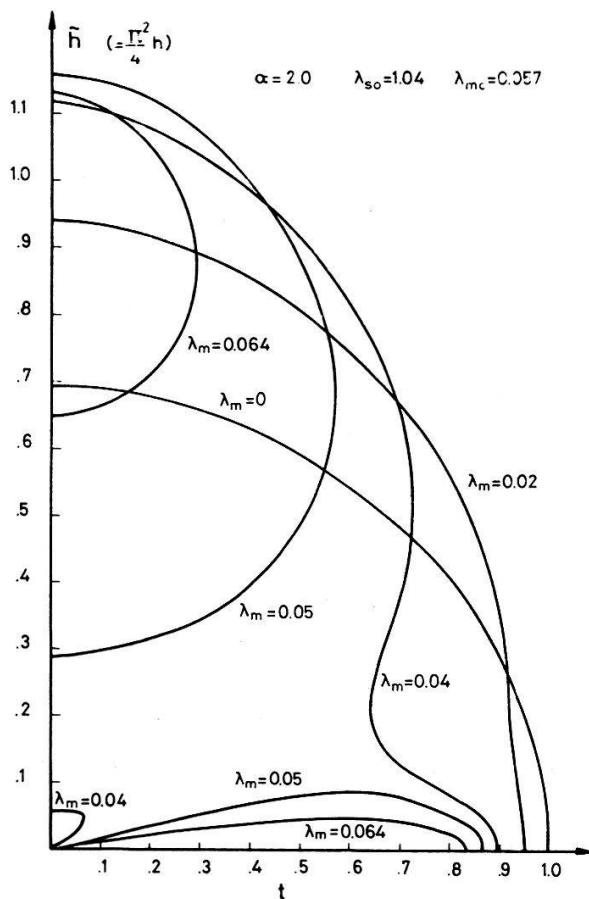
Figure 13
Critical field as a function of temperature
for a thin film for different pairbreaking
parameters λ_m, assuming a negative ex-
change field and $\alpha = 2.0$, $\lambda_{s0} = 1.04$, λ_{mc}
$= 0.057$.

4. Description of the Pulsed Field Apparatus

(a) *The principle of pulsed magnetic fields*

To observe the effect described in the preceeding chapter we need substances with a large Maki-parameter α. In practice this means that we need high magnetic fields, say 100 kGauss [29]. On the other hand, there exist superconductors with critical fields above 400 kG [30] and the range of interesting field may reach 500 kG. Since the highest static magnetic fields that can be obtained in our laboratory is about 60 kGauss we were forced to use pulsed magnetic fields.

The basic idea of the pulsed field method is to store a certain amount of energy in an energy bank and then, during a short time transform this energy into magnetic field energy, created by a current through a solenoid.

In his early work, Kapitza [31], [32] used batteries or an electromecanic generator (the energy being stored in a heavy flywheel) as energy-banks. However as first noted by Wall [33] it is most convenient to store the energy in a bank of condensors. To get a rough estimate of the energies needed to give a certain field one may assume that the magnetic field H is constant over a volume V and zero outside this volume. If all the electrostatic energy is transformed into magnetic energy we have

$$\frac{1}{2} C U^2 = \frac{1}{2} \mu_0 H^2 \cdot V , \tag{56}$$

where C is the capacity of the condensors and U their voltage. Thus for a given condenser bank, the maximum H depends on the volume needed. In principle there is no limit on H_{max} if one can make the volume small enough. However there are practical limits due to losses. There are two types of losses:

(1) Ohmic losses due to the resistance of the coil.
(2) Losses due to the distribution of the magnetic field in space. This becomes especially important when one approaches the region of Megagauss. In this region one has to use coils with very few turns, to avoid ohmic losses. However then the self-induction of the coil becomes easily comparable with the self-induction of the condenser bank and the connections, and one is not able to concentrate the energy of the bank in the coil.

Detailed calculations, taking into account these effects have been given by Champion [34].

Further complications are introduced by the forces acting on the windings of the coil, tending to make the coil explode. In fact, an ordinary coil, wound with ordinary commercial copper wire will generally explode when the field goes above 200 kGauss. Thus coils operating above, say 150 kGauss, should be reinforced.

The above discussion shows that the main difficulty in the pulsed field technique is the construction of the coils. Many different techniques have been described in the literature [35]–[42]. One may conclude that for fields below 500 kG the best results are obtained with ordinary reinforced many layer coils wound with copper wire [42]. However for fields above 500 kG one has to go to single layer helical type coils [36].

Note that one important condition imposed by the experiment in our case is that the discharge should be as slow as possible to reproduce static conditions. This is

especially important for measuring H_{c_2} since the typical 'relaxation time' connected with flux line mouvements may be relatively long.

(b) *Description of the discharge circuit*

The circuit used to produce the pulsed fields is shown in Figure 14. C is the condenser-bank, L is the high field coil. I_1 and I_2 are tow ignitrons used as switches. D is a high tension, high current diode. The discharge is started when I_1 is fired. I_2 is fired when the field is maximum (i.e. when C changes polarity). Thus if A is closed the current in L will decrease slowly exponentially according to the value of L/R where R is the resistance of the coil. This allows us to have a slow decrease of the magnetic field. In this way we also avoid to charge the condenser-bank with inverse polarity. In some cases, for instance by measuring magnetization curves, it is of interest to get the full hysteresis curve. Opening A and closing B allows one to get a full cycle discharge.

POWER SUPPLY
V= 2500 V.

C= 6mF

PRINCIPLE OF THE PULSED FIELD CIRCUIT
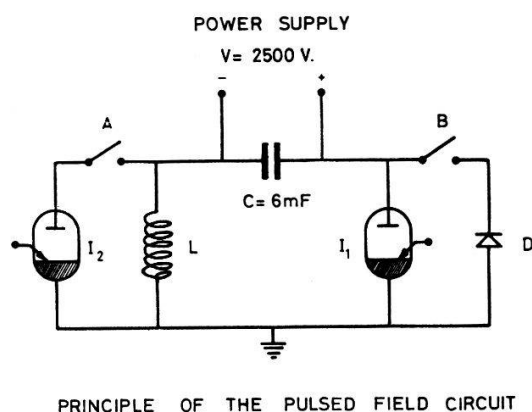
Figure 14
Principle of the discharge circuit for pulsed magnetic fields.

The condenser-bank is composed of 150 40 μF metallic paper condensers mounted in parallel. The maximum voltage is 2.5 kV. This gives a total capacity of 6 mF and a maximum stored energy of 18.75 kJoule.

The coil construction is shown in Figure 15. The coils are wound with commercial rectangular copper wire on a resocel body. The coils are then reinforced with a 5 to 10 mm thick layer of fiberglass and epoxy. The surface if this layer is machined so that its diameter is 0.03 mm larger than the inner diameter of a 10 mm thick hollow stainless steel cylinder. Heating the stainless steel cylinder to about 150°C and cooling

brass
plexiglass
stainless steel
araldite
copper
resocel
stainless steel

Figure 15
Pulsed field coil construction.

the coil and fiberglass with liquid nitrogen allows one to push the coil into the stainless steel cylinder. This procedure assures one that there is a good mechanical contact between the copper windings and the stainless steel. It provides also a negative bias stress to compensate the Maywell stress from the magnetic field.
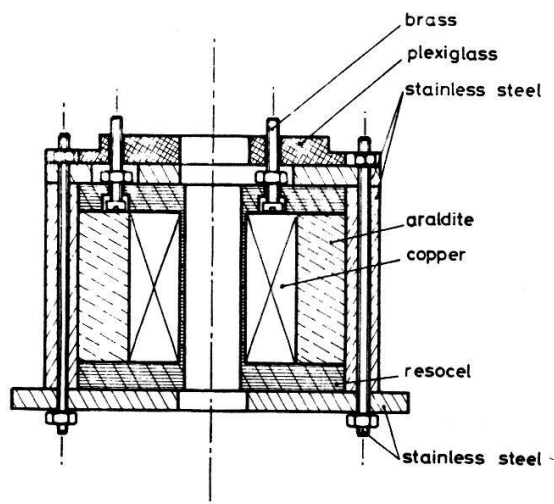
To reduce the ohmic losses in the coil, it is cooled by liquid nitrogen. It is fixed in a stainless steel nitrogen dewar to avoid that the coil moves during the pulse. The Helium dewar in which the measurements are made is of glass and has a tail which is introduced into the coil. The coil and the He-dewar are mounted on a lift, to make the interchange of coils and dewars easy. This mounting is shown in Figure 16.
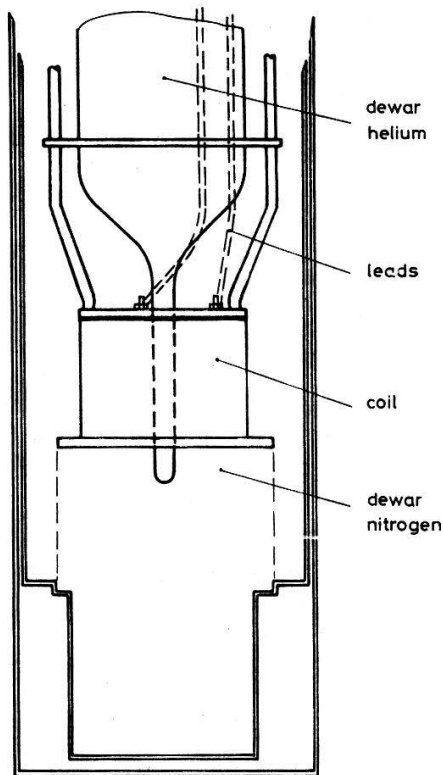

Figure 16
Mounting of the coil and the dewars for nitrogen and helium.

The number of turns and the dimensions of the coil are essentially determined by the maximum field wanted and the desire to have as slow discharge as possible. The rise time of the field τ_c (i.e. the time it takes the field to reach its maximum value) is approximately given by $(\pi/2)\sqrt{LC}$ thus a large number of turns gives a large τ_c. However a large number of turns means large ohmic losses which reduces the maximum field. Thus one has to choose a compromise between high field and slow pulse. The parameters for a few coils are given in Table 1. For the present investigation we only needed fields up to 80 kG. All measurements were thus made with coil No 10 where we dropped the stainless steel reinforcements.

coil n.	turns	inner diameter (mm)	length (m m)	self ind. (m Henry)	rise time (m sec)	max.field (kGauss)	reinforcements	remarks
1	210	16	45	0.50	2.7	310	thin layer of fiberglass + araldite	Exploded at 300 kGauss
2	192	16	45	0.48	2.6	300		
5	445	18	60	2.5	6.0	300	fiberglass + araldite + stainless steel	
6	173	16	35	0.35	2.3	410		extra turns at the end to increase homogeneity
9	2845	22	100	60.0	30.0	150	fiberglass + araldite	
10	4980	20	100	300.0	55.0	110		

PULSED FIELD COIL CHARACTERISTICS

Table 1
Pulsed field coil characteristics

To increase the homogeneity of the field, some of the coils were wound with additional turns at each end. The estimated homogeneity for coil No 9 is about $3 \cdot 10^{-3}$ at a distance of ± 2 cm from the center along the axis of the coil. For No 10 this value is 10^{-2} and for No 5 it is about $3 \cdot 10^{-2}$.

(c) *Magnetization measurements*

To determine the critical field H_{c_2}, we measured the magnetization curves of the superconductors. This was done in the standard way [43] using two balanced pick-up coils. One measures H, and the other one, which contains the sample, measures B. The two signals are integrated and the difference of the integrated signals gives M. M and H are displayed on the Y and X axis, respectively, of a storage oscilloscope. The principle of the circuit is shown in Figure 17. This method is particularly suited for the pulsed field technique since it allows one to draw the whole magnetization curve in a short time. This fact, that the measurement is performed during a very short time, makes the errors due to drift in offset voltage and input current of the amplifiers negligible.

PRINCIPLE OF CIRCUIT FOR MAGNETIZATION MEASUREMENTS
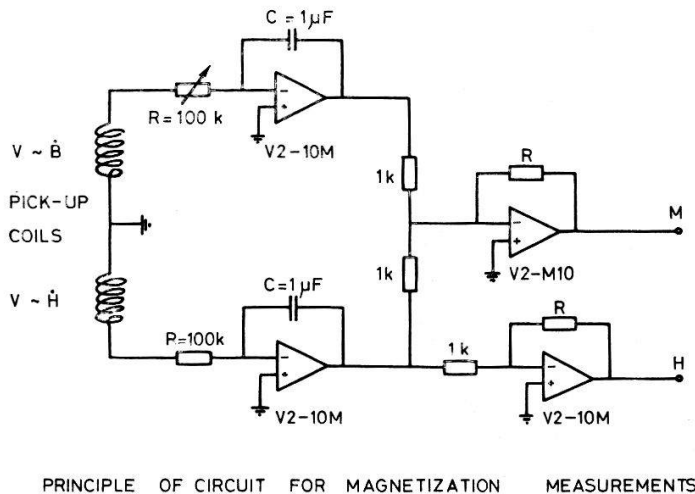
Figure 17
Principle of the circuit for magnetization measurements.

If we look at the integrator for B in Figure 17 and assume that the drift in offset voltage and input current are V_d and J_d, respectively, we may write for the output voltage as a function of time t

$$U(t) = \frac{1}{R_0 C} \left(B F - \int_0^t V_d\, dt - R_c \int_c^t I_d\, dt \right),$$

where B is the magnetic induction, F the total surface of the pick-up coil, R_0 the integration resistance and C the integration capacity.

The condition to have a good measure is that the second and the third term in the parenthesis are small compared to $B F$. This can be achieved in two ways, by making F very large i.e. by using a large number of turns in the pick-up coil and (or) choosing the time t, during which the measurement is performed, very short. Since the last term is proportional to R_0, the integration resistance should not be chosen too large. A reasonable value is given by $V_d = R I_d$. Apart of this influence of R_0, the

only effect of R_0 and C is to determine the amplitude of the final signal. $R\,C$ has therefore to be chosen such that U always is smaller than the saturation voltage of the amplifiers (which in our case was ~ 10 V). Another practical detail important to note is that if the pulse is very fast the voltage across the pick-up coil, $B\,F$, may become very large (> 1000 V) and one has to be careful with the isolation of the leads.

In our case the time of one measurement is typically 10^{-2}–10^{-1} sec. Therefore the above conditions were easy to fulfill, and we could use a set of cheap amplifiers. The amplifiers used were the type V2–10M, developed at the Institute for applied Physics, University of Basle. Typical drift values were $V_d = 10\ \mu$V, $I_d = 100$ pA. The pick-up coils contained about 3000 turns, and $R_0\,C$ was chosen to be 10^{-1} ($R_0 = 100$ k, $C = 1\ \mu$F). This gave $U \approx 3$–5 Volt for $B \approx 100$ kG.

A typical example of the magnetization curves obtained for a superconductor is shown in Figure 18a. The upper curve is displaced with a sensitivity which is 5 times larger than the lower one. H_{c_2} is taken as the point where the hysterisis disappears. To increase the precision of H_{c_2} determined in that way, each measurement was repeated several times and the mean value taken. An example of such a measurement is shown in Figure 18b. (Mo.995Mn.005Ga4 at $T = 1.9°$K.)
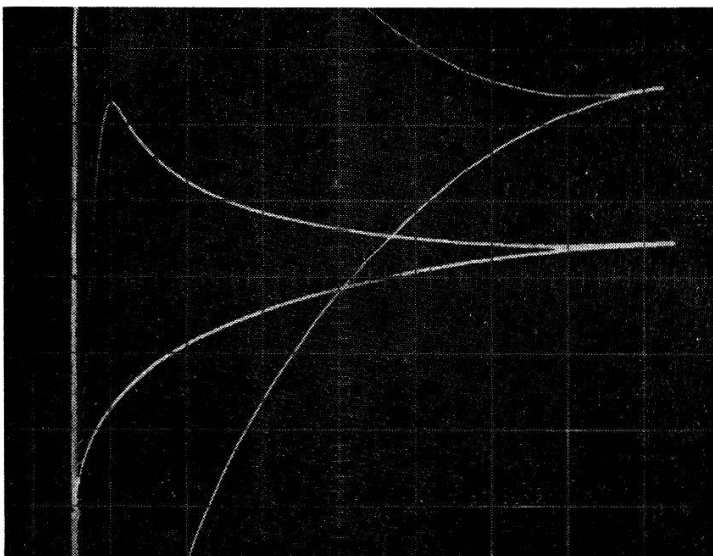

Figure 18a
Magnetization curve for Mo.98Nb.02Ga4 at $T = 4.2°$. In the upper curve the magnetization was amplified 5 times with respect to the lower one.
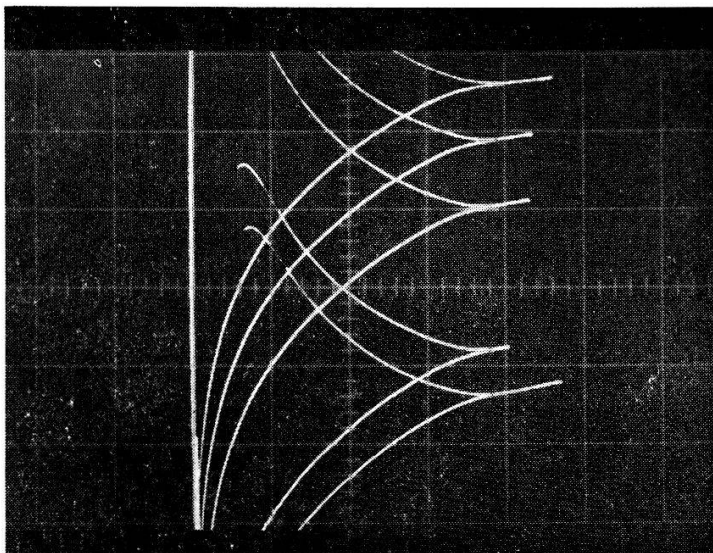

Figure 18b
Magnetization curves for Mo.995Mn.005Ga4 at $T = 1.9°$K.

5. Experimental Investigation of the $Mo_{1-x}M_xGa_4$ System (M = Nb, Ru, Mn, Fe, Co)

(a) *Introductory remarks*

To observe the effect described in chapters 1 to 3 the superconductor (without magnetic impurities) has to fulfill two conditions. The Maki-parameter α should be large, i.e. we should have a large ratio $H_{c_2}(0)/T_{c0}$ and the spin-orbit parameter λ_{so} should be not too large, i.e. we should use light elements. Furthermore the superconductor must accept magnetic impurities and the exchange interaction J must be negative (in the case of the light rare earth ions where S points opposite to the total angular momentum J should be positive).

To fulfil all these conditions we chose a system of which very little is known until now, the Mo-Ga system. Two intermetallic phases have been found in this system, Mo_3Ga with the A-15 structure and $MoGa_4$ (assumed stochiometric composition) with unknown structure. Both compounds were found by Matthias et al. [44], [45], [46]. They determined the superconducting transition temperatures to be $0.76°K$ for Mo_3Ga and $9.8°K$ for $MoGa_4$. We have reinvestigated the $MoGa_4$ compound, including ternary alloys of the type $Mo_{1-x}M_xGa_4$ where M = Nb, Ru, Mn, Fe, Co. For the pure compound ($x = 0$) we found $T_{c0} = 8.0°$ and $H_{c_2}(0) = 73.7$ kGauss. Among the impurities, only Mn showed a well-developed magnetic moment. Ru, Fe, Co, showed resonant state type behaviour and Nb acted as an ordinary non-magnetic impurity.

Although only Mn is interesting in connection with the Jaccarino-Peter compensation effect, we also discuss the cases of resonant non-magnetic states. These resonant non-magnetic states produces a decrease in T_c with concentration of impurities, which is similar, but weaker, to the one produced by magnetic impurities. The resonant state may also produce an anomalous behaviour of H_{c_2}, not connected in an evident way with the effect we are looking for. Since the condition $J < 0$ means a strong s-d mixing, and since the s-d mixing produces the resonant states [47], [48] we must be careful to distinguish between true magnetic moments and non-magnetic resonant states. The samples with Mn-impurities show, as we shall see, an anomalous sharp drop in T_c at a certain impurity concentration. In section 4c we suggest a mechanism, based on spin correlations, to explain that behaviour.

(b) *Preparation of the samples*

The samples were prepared by melting the constituents in a Al_2O_3 crucibel under a pressure of 2 atmospheres of Argon. The maximum temperature was $1300°C$. Samples prepared at $1700°C$ showed no essential difference from the ones prepared at $1300°C$, apart from more important losses, probably due to evaporated Gallium. The losses of the samples melted at $1300°C$ were about 0.5%. The furnace used was a resistance furnace [49] which allowed a slow decrease of the temperature. The superconducting phase was formed at about $730°C$, which was also determined to be the melting point. Samples quenched from above that temperature did not contain the superconducting phase.

The compound did not form a bulk sample, but falled into a fine powder at $730°C$. This powder was pressed into pellets and annealed in sealed quarz tubes for 1 week at $700°C$ and then quenched. The samples produced in this way showed reproducible

values for T_c and H_{c_2}. X-ray measurements made on powder samples and on small single crystals [50] showed that the samples were single phase except for a small amount (~ 5 at%) of Mo_3Ga. This was confirmed by T_c measurements which showed a small second transition at $T = 1.2°K$. The disagreement with the value reported by Matthias et al. is probably due to non-stochiometric composition of the A-15 compound. The single crystals were isolated from powderous samples, which were prepared by reacting Mo with Ga at $700°C$ for about one week in sealed quartz tubes. The structure of $MoGa_4$ has not yet been determined.

The samples used for T_c and H_{c_2} measurements were cylindrical with diameter 3.8 mm and length 10–12 mm.

(c) *Susceptibility and critical temperature measurements*

The critical temperature measurements were made using a standard AC Bridge [51] to measure the initial susceptibility of the samples. The width of the transitions were typically $0.2°K$ except the ones with the highest Mn and Fe concentrations where the width increased to about $0.5°K$.

The susceptibility was measured using the Faraday method in fields up to 17 kGauss [52]. $MoGa_4$ without impurities, turned out to be diamagnetic $\chi = -4.7 \times 10^{-8}$ emu/gram. To get a rough estimate for the density of states $N(0)$ we assume the orbital diamagnetism to be identical to the maximum one for the free atoms. We find, using the values given by Selwood [53] $\chi_{dia} = -13.9 \cdot 10^{-8}$ emu/gram. Assuming that $\chi_{Landau} = 1/3\, \chi_{para}$ we find $\chi_{para} = +9.2 \cdot 10^{-8}$ emu/gram. Using further that $\chi_{para} = 2\,\mu_B^2\, N(0)$ we get $N(0) = 0.11$ states/eV.

The critical temperature as a function of concentration x of impurities is shown in Figure 19. Nb has no influence on T_c, Ru produces an initial decrease in T_c and after that T_c stays constant. The effect of Co on T_c is stronger, but the tendency for T_c to flatten out is still there. Fe impurities decreases T_c strictly linearly to very low temperatures, and finally Mn gives the type of curve that one expects for a magnetic impurity. This is consistent with the susceptibility measurements, which show a very weak tendency of magnetism for Co, a small magnetic moment of $0.3\ \mu_B$ per atom for Fe and a well-developed magnetic moment for Mn.
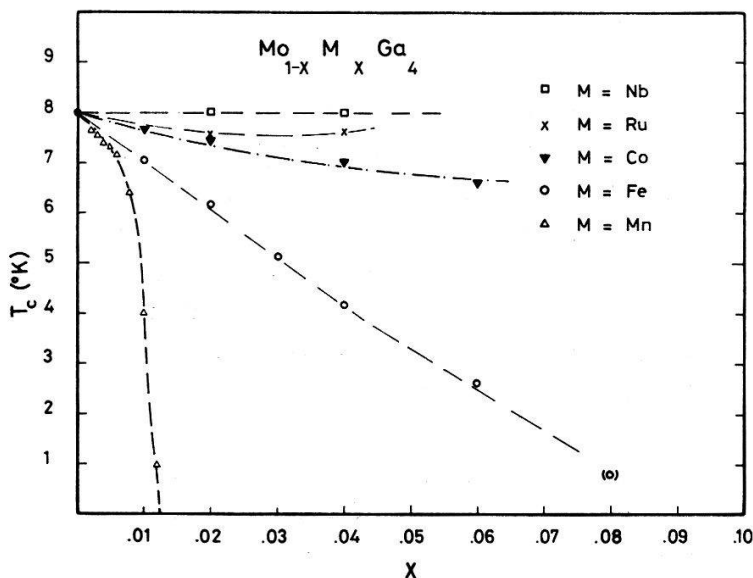

Figure 19
T_c as a function of x in $Mo_{1-x}M_xGa_4$ where M = Nb, Ru, Co, Fe, Mn.

We start with discussing the behaviour of Co and Fe. The susceptibility of these impurities behaves like

$$\chi_{imp} = \chi_0 + \frac{C}{T},\tag{57}$$

where χ_0 is relatively large and C small. This is a typical behaviour of a non-magnetic resonant state near the magnetic threshold [54]. For Fe we get $\chi_0 = 0.167$ emu/gram % Fe and for Co $\chi_0 = 0.042$ emu/gram % Co.

The magnetic moment corresponding to C is 0.3 μ_B/atom for Fe. For Co it is too small to allow an appropriate determination of the magnetic moment. Using the Anderson formula for χ_0 for the case of a resonant state at the fermi surface

$$\chi_0 = \frac{2\,\mu_B^2}{\pi\,\Delta - U},\tag{58}$$

we get from the above values

Fe $\pi\,\Delta - U = 0.05$ eV ,

Co $\pi\,\Delta - U = 0.20$ eV .   (59)

Δ is the width of the resonant state and U is the Coulomb interaction among the localized electrons.

The influence of a non-magnetic resonant bound state on superconductivity was first investigated by Zuckermann [55]. His calculation was later generalized by Ratto and Blandin [56] to include the Coulomb interaction U. Near the magnetic threshold ($\pi\,\Delta \approx U$) and for a resonant state at the Fermi surface, their formula for the initial decrease in T_c with concentratino of impurities (C) may be written:

$$\frac{T}{T_{c0}}\frac{dT_c}{dc} = \frac{5\,\alpha^2\,U}{N(0)\,(\pi\,\Delta)^2},\tag{60}$$

where $N(0)$ is the density of states of the electron gas and is defined as

$$\alpha = \ln\left(\frac{2\,\gamma_E\,\hbar\,\omega_D}{\pi\,k_B\,T_{c0}}\right),\tag{61}$$

ω_D is the frequency and γ_E Eulers constant as defined in chapter 2. The coupling parameter is typically 4 or larger for weak coupling superconductors and smaller than 4 for strong coupling superconductors. The factor 5 comes from the orbital degeneracy $(2\,l + 1)$. Of one knows α and $N(0)$ (for instance from specific heat measurements) equations (58) and (60) allow one to determine Δ and U. Unfortunately the specific heat for $MoGa_4$ is not known. Using the above estimated value of $N(0) = 0.11$ states/ eV and assuming $\alpha = 4$ as a typical value we get from the measured initial slopes in Figure 17.

Fe $\Delta = 2.2$ eV $U = 6.9$ eV ,

Co $\Delta = 8.4$ eV $U = 26.5$ eV .

These values, especially the ones for Co, are probably much to high. This may indicate that α is smaller than 4 and that our system has a tendency to strong coupling superconductivity.

We note now that there is a good correlation between the measured values of χ_0 and the initial slopes of T_c vs. concentration. We find to a good approximation

$$\frac{\left(\dfrac{dT_c}{dc}\right)_{\text{Fe}}}{\left(\dfrac{dT_c}{dc}\right)_{\text{Co}}} = \frac{\chi_0^{\text{Fe}}}{\chi_0^{\text{Co}}}. \tag{62}$$

Such a relationship does not follow from equations (58) and (60). Actually there is no anomaly in equation (60) at the magnetic transition point $U = \pi \Delta$. Zuckermann has carried the calculation one step further and included localized spin fluctuations. He finds essentially that U has to be replaced by U^s:

$$U^s \sim \frac{U}{\pi \Delta - \dfrac{U}{Z_1}},$$

where Z_1 is a normalization factor which depends on U/Δ in such a way that U^s never diverges. (This means that we have a smooth transition from the non-magnetic to the magnetic state). Introducing U^s in equation (60) we get an expression for dT_c/dc which may account for the relation (62). Unfortunately we have not enough experimental data to analyze the equations properly.

It is interesting to note that the tendancy to an upwards curvature in the T_c vs. concentration curves found for Fe, Co and Ru has also been found in other systems with nearly magnetic impurities [54], [58]. Bennemann [59] showed that interactions among the impurities will wash out the localized spin fluctuations and this produce such an effect. However it would not be surprising if this effect takes place also for non-interacting impurities, since Rivier and Zuckermann [60], and Suhl and coworkers [61], [62], [63] have shown that such impurities will become completely non-magnetic at low enough temperature.

We now turn to the case of Mn. The susceptibility shows some anomalous features. In Figure 20 is shown the susceptibility of $Mo_{.98}Mn_{.02}Ga_4$ as a function of temperature. At high temperature it shows a Curie-Weiss behaviour with a negative θ of about $- 156\,^\circ K$. The slope corresponds to a moment of $4.81\ \mu_B$. The susceptibility of the other samples shows similar behaviour, however, at low concentrations the effective moment raises to the anomalous high value of $7.5\ \mu_B$. This is correlated with a decrease in θ to $- 212\,^\circ K$. The effective moment and the paramagnetic Curie temperature θ is shown in Figure 21 as a function of concentration.

The behaviour of the superconducting transition temperature does not reflect this variation of the moment. In fact, in the region ($x = 0$, $x = 0.006$) where the moment varies strongly, the critical temperature decreases linearly with concentration. An anomaly is seen however at higher concentrations, where T_c decreases very rapidly to zero. This is contrary to what one might expect from the variation of the magnetic moment.

This, at first sight anomalous, behaviour is probably due to correlations among the impurities. In fact, the concentration dependence of μ_{eff} and θ show that there are interactions between the impurities. We now give a simple qualitative argument to show how even weak correlations between the ions may produce strong deviations

from the AG behaviuor [2]. According to de Gennes and Friedel [64] the spin scattering time may be written, in the case of correlations between the ions.

$$\frac{1}{\tau_s} = \frac{\pi \, N(0)}{4 \, q_F^2} \int_0^{2q_F} q \, dq \, J^2(q) \, \langle S^2(q) \rangle \,, \tag{63}$$

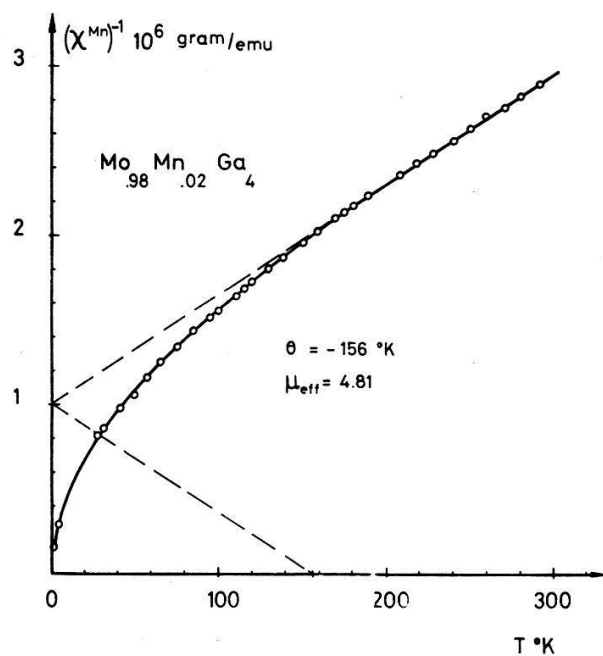
Figure 20
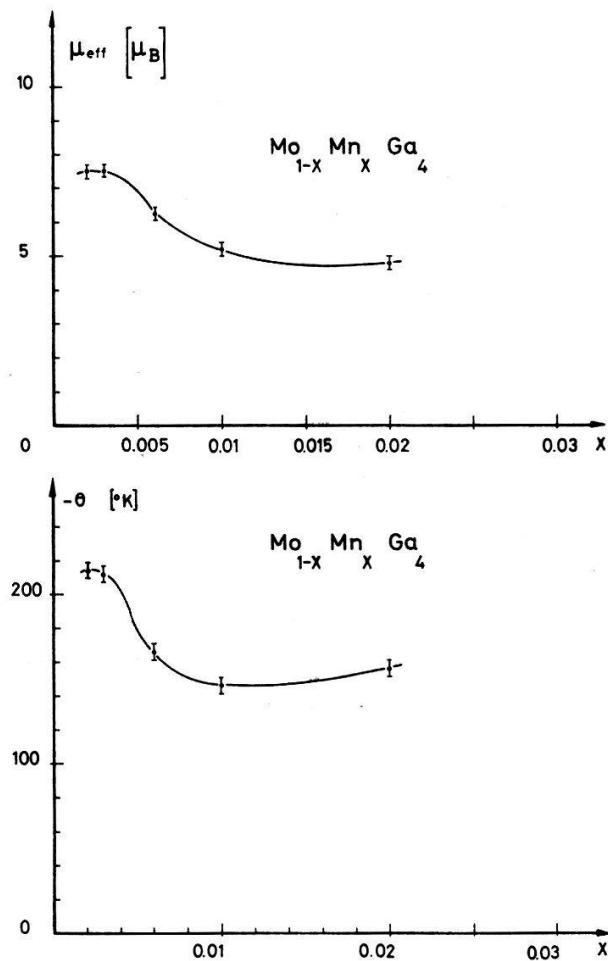$(\chi \, \text{Mn})^{-1}$ as a function of temperature for $\text{Mo}_{.98}\text{Mn}_{.02}\text{Ga}_4$.

Figure 21
μ_{eff} and θ as functions of x in $\text{Mo}_{1-x}\text{Mn}_x\text{Ga}_4$.

where $\langle S^2(q) \rangle$ is defined as

$$\langle S^2(q) \rangle = \left\langle \sum \frac{1}{N} \exp[i\, \boldsymbol{q}(\boldsymbol{R}_i - \boldsymbol{R}_j]\, (\boldsymbol{S}_i\, \boldsymbol{S}_j) \right\rangle . \tag{64}$$

Since the Mn ions do not order ferromagnetically in the concentration range we are interested in, we have assumed $\langle S_z \rangle = 0$ in equation (63). This equation follows also from the work of Abrikosov and Gorkov [2] if one includes chain diagrams correlating two different impurities but still keeps the other approximations. The explicit formula (63) is only valid if the spins are not too strongly correlated $\big($i.e. if $(h\, q_0)^2/2\, m > \hbar/\tau_s$ where q_0 is defined below$\big)$.

The spin correlation function $\langle S^2(q) \rangle$ must satisfy a sum rule:

$$\frac{1}{N} \sum_q \langle S^2(q) \rangle = \frac{1}{N} \sum \langle S_i^2 \rangle = c\, S(S+1) , \tag{65}$$

where c is the concentration of magnetic impurities. From equations (64) and (65) it now follows that for uncorrelated spins we have

$$\langle S^2(q) \rangle = c\, S(S+1) . \tag{66}$$

For ferromagnetically aligned spins in an ordered lattice we get

$$\langle S^2(q) \rangle = c\, S(S+1)\, \delta(q) . \tag{67}$$

In the intermediate range with spin correlations $\langle S^2(q) \rangle$ will be a function more or less peaked at $q = 0$. In the case of long-range correlations one may write [65]

$$\langle S^2(q) \rangle = \frac{A}{q^2 + q_0^2} , \tag{68}$$

where q_0^{-1} gives the range of correlation. The constant A is determined from the sum rule (65). What happens physically is the following: q in equation (63) is the change in momentum in the intermediate state in one scattering process. Only those q's can occur for which $J(q)$, the Fourier transform of the potential, is non zero and they occur with the weight $J^2(q)$.

However, if the impurities are correlated at a distance $\sim 1/q_0$ the largest change in momentum possible in the intermediate state is roughly q_0. Thus as the spins start to order the small q's get more and more weight in the integral in equation (63). Now if $J(q) = $ const., $1/\tau$ is rather insensitive to the ordering process, since $\langle S^2(q) \rangle$ obeys the sum rule (65). If, on the contrary, $J(q)$ depends strongly on q it is evident that $1/\tau$ will be very sensitive to the ordering process.

To get a more quantitative estimate for this effect we have to assume a form for $J^2(q)$. If $J(q)$ is a gaussian with half-width q_J, $J^2(q)$ will also be a gaussian, but with half-width $q_J/\sqrt{2}$. To simplify the calculation we represent $J^2(q)$ by a step function.

$$J^2(q) = \begin{cases} J_0^2 & q \leqslant \dfrac{q_J}{\sqrt{2}} , \\[2ex] 0 & q > \dfrac{q_J}{\sqrt{2}} . \end{cases}$$

The situation that arises if $q_J < 2^{3/2} q_F$ is illustrated in Figure 22. At very low concentrations the spins will be uncorrelated and the initial slope of T_c versus concentration will be small and determined by (see Fig. 22a)

$$\left(\frac{1}{\tau_s}\right)_{uncorr} = \pi N(0) \, c \, S(S+1) \frac{J_0^2}{4 \, q_F^2} \int_0^{q_J\sqrt{2}} q \, dq$$

$$= \pi N(0) \, c \, S(S+1) \, J_0^2 \frac{1}{16} \left(\frac{q_J}{q_F}\right)^2 . \tag{69}$$

When the spins start to get correlated the correlation distance $r_0 \sim 1/q_0$ must be at least the mean distance between the magnetic impurities. Since we are concerned with concentrations of the order 10^{-3} the mean distance between the Mn-ions is 30–40 Å. This corresponds to a small q_0 (i.e. $q_0 \ll q_F$). The spin scattering time for this situation is large and is given by (see Fig. 22b)

$$\left(\frac{1}{\tau_s}\right)_{corr} = \pi N(0) \frac{J_0^2}{4 \, q_F^2} \int_0^{q_J\sqrt{2}} dq \, q \, \frac{A}{q^2 + q_0^2}$$

$$\approx \pi N(0) \frac{J_0^2}{4 \, q_F^2} A \log\left(\frac{q_J \sqrt{2}}{q_0}\right) . \tag{70}$$

From the sum rule (65) it follows approximately

$$A = \frac{1}{3} c \, S(S+1) \, q_B^2 , \tag{71}$$

where q_B is a reciprocal lattice vector (the sum in (65) goes over the first Brillouin zone).
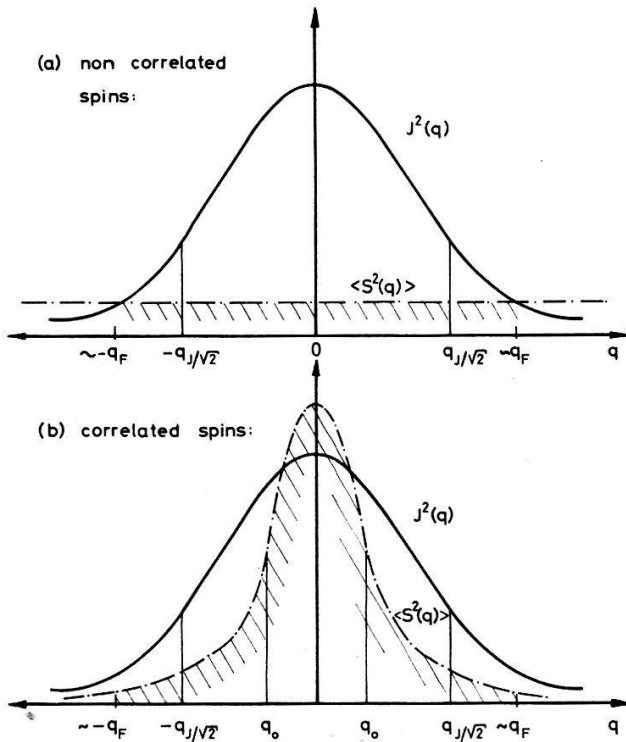

Figure 22
Illustration to the effect of spin correlations on the spin scattering time.

Introducing this into equation (70) we get

$$\left(\frac{1}{\tau_s}\right)_{corr} = \pi\, N(0)\, c\, S(S+1)\, J_0^2 \frac{1}{12} \log\left(\frac{\sqrt{2}\, q_J}{q_0}\right)\left(\frac{q_B}{q_F}\right)^2. \tag{72}$$

We note that this result is only weakly dependent on q_J and q_0. If we suppose $q_B \approx 2\, q_F\; q_J \approx 10\, q_0$ we get

$$\left(\frac{1}{\tau_s}\right)_{corr} \approx 0.88\, \pi\, N(0)\, c\, S\, (S+1)\, J_0^2. \tag{73}$$

The ratio of $1/\tau_s$ for the two cases give

$$\frac{\dfrac{1}{c}\left(\dfrac{1}{\tau_s}\right)_{uncorr}}{\dfrac{1}{c}\left(\dfrac{1}{\tau_s}\right)_{corr}} \approx 0.07 \left(\frac{q_J}{q_F}\right)^2. \tag{74}$$

If we now suppose that in the case of $Mo_{1-x}Mn_xGa_4$ the spins are correlated around the critical concentration, we have to compare 74 with the spin scattering times determined experimentally from the initial slope (equation (36)) and the one determined from the critical concentration (equation (36)).

We find:

$$\frac{\left(\dfrac{1}{c\,\tau_s}\right)_{initial}}{\left(\dfrac{1}{c\,\tau_s}\right)_{crit}} = 0.32\,.$$

From (74) we then get for Mn in $MoGa_4$

$$\frac{q_J}{q_F} \approx 2.1\,. \tag{75}$$

This is a quite reasonable value for $3\,d$ electrons, as in the case of Mn. According to calculations by Watson, Freeman and Koide [66] this may even be a reasonable value for rare earth impurities. It is therefore not surprising that one gets strong deviations from the Abrikosov-Gorkov curve [2] when the spins start to correlate. If $J(q)$ is a more complicated function than assumed above, $(1/\tau_s)$ as a function of concentration may show a more complicated behaviour. This effect might therefore offer an alternative explanation to the peak effect observed in T_c versus concentration curve in several cases [67]–[70]. The explanation given by Benneman [71] has recently been criticized by Keller and Benda who showed that the Bennemann effect is too small to account for the anomalies observed.

The idea to use the q-dependence of $\langle S^2(q)\rangle$ to describe anomalous dependences of T_c on impurity concentration was first used by Toxen et al. [72]. However they did not respect the sum rule 65 and they got therefore quite unrealistic results.

We now return to our calculation for $Mo_{1-x}Mn_xGa_4$. As already noted as $q_0 < q_J$, $1/\tau_s$ changes very little. On the other hand for $q_0 > q_J$ the spins are uncorrelated since it corresponds to a case where the correlation distance is much smaller than the mean distance between the ions. We therefore expect a sudden change in the spin scattering amplitude at a certain concentration, where the spin correlations start to build up.

This is acually what is observed in the $Mo_{1-x}Mn_xGa_4$ system.

In the next section we will determine the mean exchange field $J_0 = J(q = 0)$. From equation (69) we may then determine the density of states $N(0)$ from the initial slope of T_c vs. concentration. Using the experimental values of $(dT_c/dc_{initial}) = 7.25\,°K$ at % Mn, $J_0 = -0.3$ eV and the result (75) we get $N(0) = 0.12$ states(eV, a value in good agreement with the value estimated from susceptibility measurements.

(d) Critical field measurements

The critical field of the samples was measured with the method described in chapter 4. The magnetization curves were irreversible and allowed therefore a relatively easy determination of H_{c_2}. in Figure 18 is shown a typical example of a magnetization curve in the system $Mo_{1-x}M_xGa_4$. The critical field was determined with a relative accuracy of ± 1.5 kGauss.

All measurements were made in a pulsed magnetic field using the coil with 55 msec. rise time. To check that the measured values corresponded to static values, a few samples were measured in a static magnetic field below 50 kGauss. These measurements gave results identical with the pulsed field measurements. However, when decreasing the rise time to below 10 msec we observed a dependence of the measured critical field on the rise time. The measured critical field tended to increase as the rise time decreased.

In Figure 23 we show the critical field versus temperature for a few samples in the system $Mo_{1-x}Mn_xGa_4$. The characteristic of these curves is the marked upwards curvature occuring in a certain temperature interval for all samples with relatively high impurity concentration.
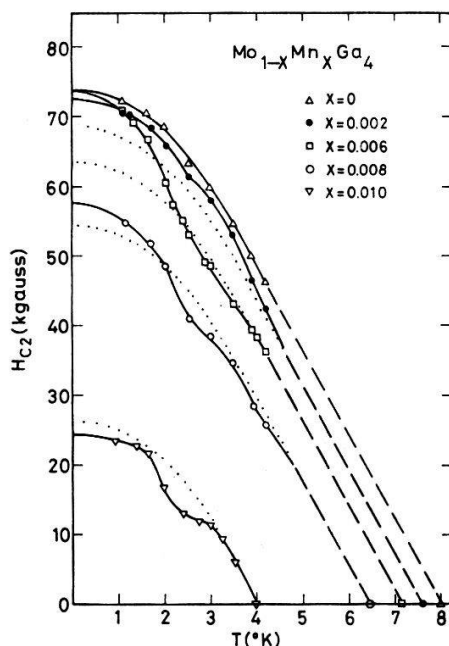

Figure 23
Critical field as a function of temperature in the sys tem $Mo_{1-x}Mn_xGa_4$. The dotted lines indicate what we would expect if there were no effects on the conduction electron spins.

This is actually what we predicted in chapter 3 for the case of a compensation of the paramagnetic effect on H_{c_2}. To demonstrate more clearly this effect we have also plotted in Figure 23 the critical field that would result for the Mn doped samples if there were no effect on the conduction electron spins, i.e. if:

$$H_{c_2}(c, T) = H_{c_2}(0, T) - H_{c_2}(0, 0) \frac{\lambda_m}{\lambda_{mcrit}}, \tag{76}$$

where as before

$$\lambda_m = \frac{\hbar}{\pi k_B T_{c0} \tau_s} \quad \lambda_{mcrit} \approx 0.281 \, .$$

For $x = 0.003$ and $x = 0.006$ the measured critical field lies clearly above the critical field determined by equation (76). For $x = 0.008$ the measured critical field approximately corresponds to the field predicted by equation (76) and finally by $x = 0.01$ it lies clearly below. In Figure 24 we have plotted the critical temperature together with the critical field, extrapolated to zero temperature, as well as $H_{red}(0)$ defined by equation (49a). The extrapolation was done by fitting the experimental values between 1 and $2°K$ to a parabola. For the case of $x = 0.010$ where H_{c_2} tends to become temperature independent at low temperatures we used the value at $T = 0.92°K$. The highest value of the zero temperature critical field ($H_{c_2} = 76$ kGauss) was found for $x = 0.005$. The critical field for the pure system was determined to 73.7 kGauss. The highest measured critical field (for $x = 0.005$) was only slightly higher than the one measured for the pure system. The critical field for $x = 0.005$ is shown separately in Figure 25.
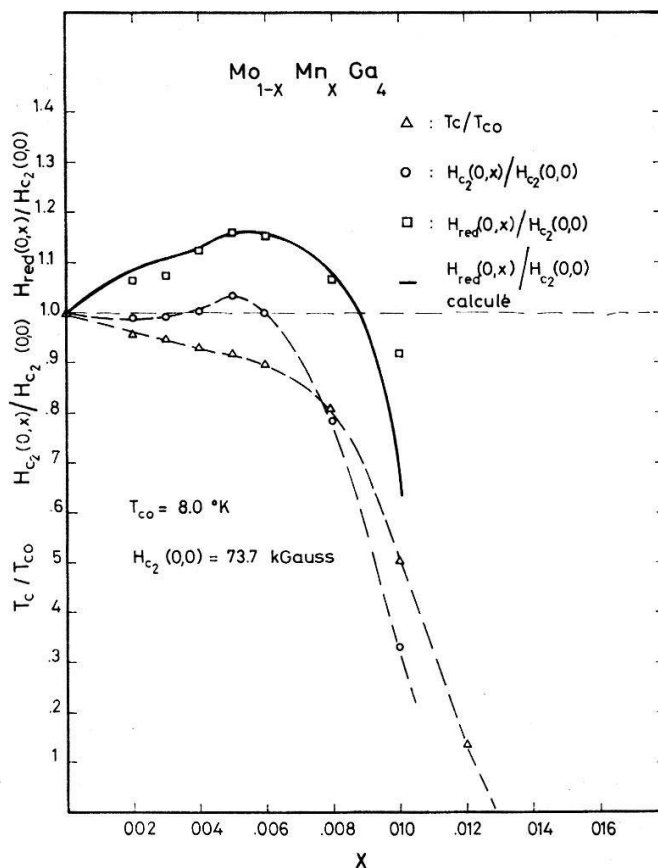

Figure 24
Critical temperature T_c, critical field $H_{c_2}(T = 0)$ and reduced critical field $H_{red}(T = 0)$ plotted as a function of concentration x. The solid line shows the calculated reduced critical field.
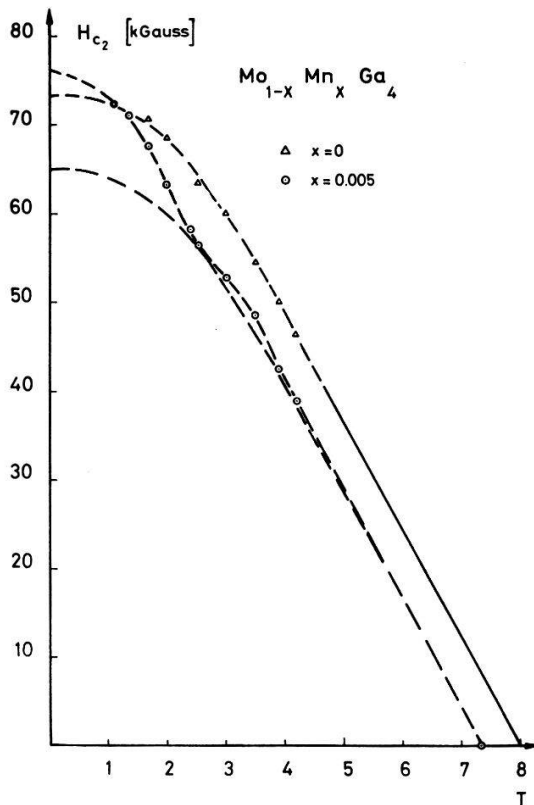
Figure 25
Critical field as a function of temperature for
$MoGa_4$ and $Mo_{.995}$-$Mn_{.005}Ga_4$.

The reduced critical field H_{red} shown in Figure 24 shows the expected maximum. From the experimental points alone the maximum is determined to occur somewhere between $x = 0.005$ and $x = 0.006$, however the strong asymmetry in H_{red} versus c shows that the maximum occur near $x = 0.006$. As described in chapter 3 b we may now determine different parameters of the system. We get assuming $S = 5/2$:

$$J_0 = -0.3 \text{ eV} ,$$

$$H_{c_2}^*(0, 0) = 86.0 \text{ kGauss} ,$$

$$\alpha = 0.83 , \quad \lambda_{s0} = 0.5 .$$

These values are slightly different from the values reported in a preliminary version of this work [73]. The difference comes from the fact that we there analyzed the result with an expression for H_{red} that did not take into account the magnetic scattering and that therefore neglected the strong asymmetry of H_{red}.

Using the values determined above, and assuming that the mean exchange field varies proportionally to the magnetic moment determined from susceptibility measurements, we have calculated the critical field from equation (33). The corresponding value for H_{red} $(T = 0)$ is also shown in Figure 24, and is in reasonable agreement with the experiments. One might argue here that there will be a reduction in the spin scattering amplitude [71] when the spins are aligned. From the work of Keller and Benda [19] it follows that this reduction is very weak. But even if it would be $S/S + 1$ as for the case of fixed aligned spins, it could not account for the anomalies observed.

The critical field calculated as a function of temperature, does only show qualitative agreement with the measurements (Fig. 26). The reason for this may be seen by looking at the pure system. In Figure 27 we have plotted the measured critical field

together with the critical field calculated for three cases: $\alpha = 0$; $\alpha = 0.83$, $\lambda_{s0} = 0$; $\alpha = 0.83$, $\lambda_{s0} = 0.5$. All the theoretical curves lie below the experimental curve, which is linear between $T_{c0} = 8°$K and $T = 2.5°$K. This linearity cannot be reproduced by the WHH formula (equation (33) for $h_J = \lambda_m = 0$) by any choice of the parameters α λ_{s0}. From the work of Helfand and Werthamer [16] this is also found to be true
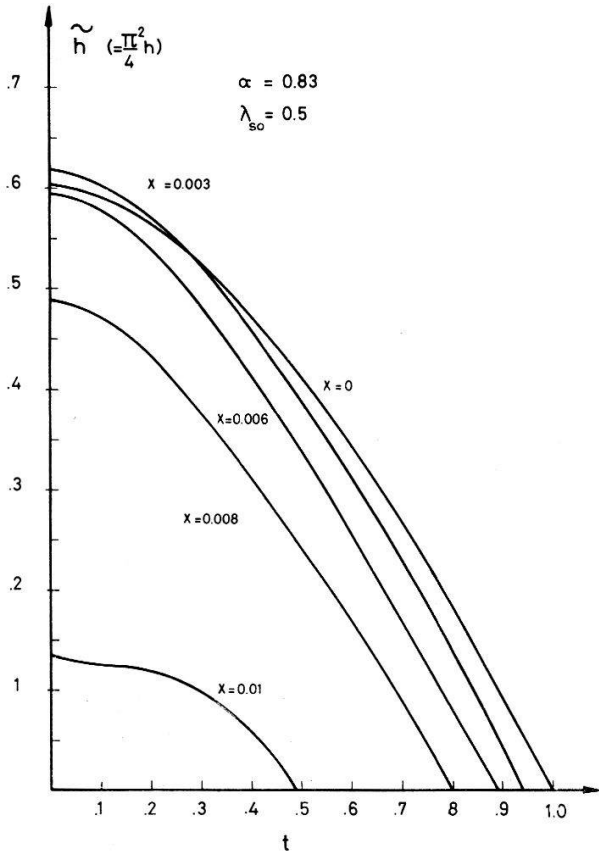
Figure 26
Calculated critical field $\boldsymbol{h}_{c_2}$ $(= (\pi^2/4) \, h_{c_2})$ for $\alpha = 0.83$ $\lambda_{s0} = 0.5$, corresponding to $x = 0$, $x = 0.003$, $x = 0.006$, $x = 0.008$ and $x = 0.01$ in the system $Mo_{1-x}Mn_xGa_4$ assuming that h_J follows a Brillouin function without molecular field.
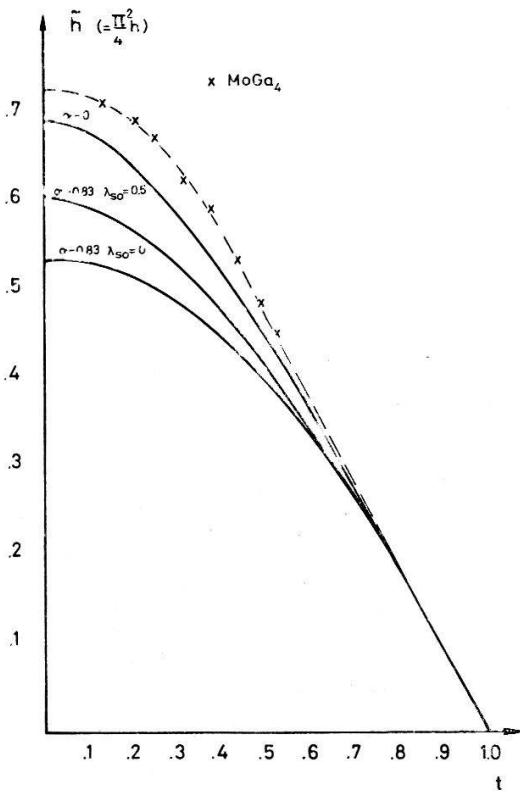

Figure 27
Measured critical field for $MoGa_4$ plotted together with the calculated ones for $\alpha = 0.83$ and $\lambda_{s0} = 0$, 0.5, ∞.

in the pure limit. Thus we must conclude that the critical field curves cannot be satisfactorily explained by the WHH weak coupling theory [17]. This is, however, not the first time such deviations are observed. McConville and Serin [74] found that the upper critical field of Nb deviates in the same way from the predictions of Helfand and Werthamer [16]. (The critical field is linear in temperature between $T_{c0} = 9.2°$K and $T = 2.5°$K. The same result was found by Finnemore et al. [75] who also found that Nb is an intermediate coupling superconductor. Farrell et al. [76] measured the anisotropy in H_{c_2} on Nb monocrystals. They found that the anisotropy fits well a theory by Hohenberg and Werthamer [77]. This anisotropy comes from non-local corrections to the gap equation (12). Such corrections might perhaps also account for the deviations from the Helfand-Werthamer theory. Another example of such deviations is the La$_3$In compound. The results of Crow et al. [28] show that H_{c_2} versus T is linear between $T_{c0} = 9.6°$K and $T = 2°$K.

Although the work of Hohenberg and Werthamer may show the way how to explain these deviations from the WHH theory, there exists up to now no theory that reproduces these deviations. We are therefore obliged to discuss the results, concerning the $Mo_{1-x}Mn_xGa_4$ system, only qualitatively.

We note first two features:

(1) The upwards curvature in the samples with Mn occurs between 2 and 3°K. This is also the temperature where H_{c_2} versus T for the pure sample starts to deviate from a straight line.

(2) The initial slopes of the H_{c_2} versus T curves, determined from T_c and the H_{c_2} measurements at $T = 4.2°$ are all equal.

Now, since for all samples (except $x = 0.01$) the critical field at 4.2° is high enough to partly of fully align the impurity spins, we should in fact expect the above defined slopes to vary strongly due to the mean exchange field. That this is not the case suggests that the paramagnetic effect is quite weak in this region. This suggests further that as long as the H_{c_2} versus T curve is linear there is only very weak paramagnetic effect in H_{c_2} and that when the latter one becomes important the H_{c_2} versus T curve starts to deviate from a straight line. This assumption is consistent with the fact that the anomalies produced by the magnetic impurities occur just in that region. Note also that the H_{c_2} curve never passes higher than the extrapolated straight line of the initial slope. The two samples nearest the compensation point ($x = 0.005$, $x = 0.006$) just touch this line.

The only sample where there is a large discrepancy between the measured and the calculated $H_{red}(0)$ is the one with $x = 0.01$.

The calculated curve in Figure 26 does not show an intermediate plateau. Actually, the plateau in the calculated curve corresponds very well to the first plateau in the measured curve. An analysis similar to the one presented in chapter 3b (Fig. 5, 6, 7) shows that the calculated value (Fig. 26) corresponds to the lowest solution i.e. the solution where the superconductivity is destroyed by the exchange field before the external field can compensate it. But one finds also that the compensation domaine is nearly realized. This explains why the calculated curve starts to bend upwards at the lowest temperatures. A small change in the parameters may make the compensation domain appear, and produce a curve similar to the measured one. These changes may

be given by the modifications necessary to the theory to reproduce the H_{c_2} versus T curve for the pure sample. Note, however that the calculated curves assume that h_J follows a Brillouin curve without molecular field. This is certainly not correct a this concentration. Correlations between the ions change certainly $h_J(T)$ and therefore $h(T)$.

In the above discussion we have left out the possibility of a change in τ with impurity concentration. To check this point we measured H_{c_2} in the system $Mo_{1-x}Nb_xGa_4$ (Fig. 28). These measurements showed a linear increase in $H_{c_2}(0)$ with x at a rate of 6 kGauss/% Nb. This effect is much smaller than the effects found with Mn. When we calculated the experimental values of $H_{red}(0, c)$ (Fig. 24) we did suppose that the change in τ for Mn is the same as for Nb, and the H_{red} plotted is for a constant τ.
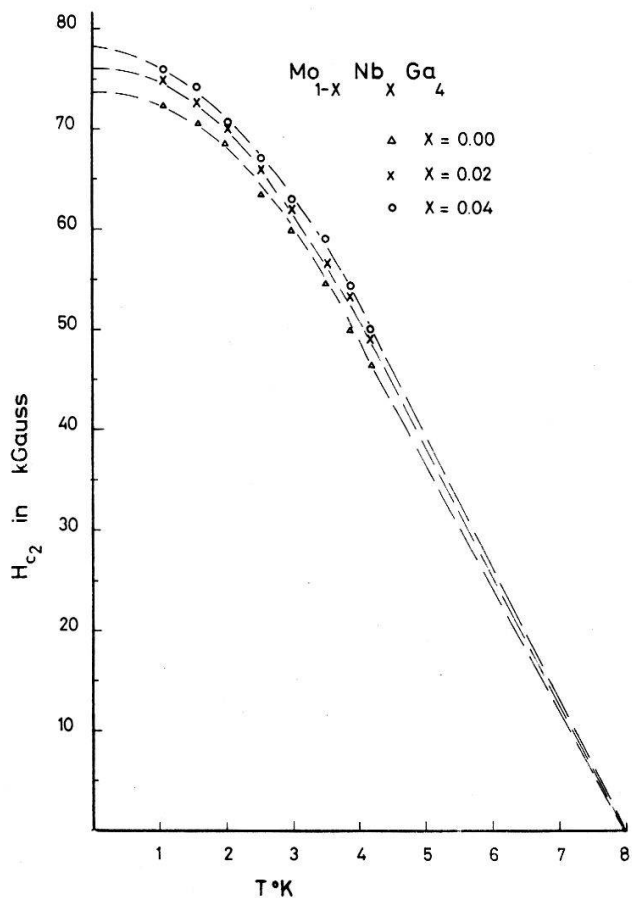
Figure 28
Critical field as a function of temperature for $Mo_{1-x}Nb_xGa_4$.

The critical field curves for the impurities which show resonant state behaviour, are much more difficult to interpret. The non-magnetic scatterings are probably strong due to the resonant character of the localized state. This should show itself in an increase in the initial slope at low concentration. On the other hand, since the ions are slightly magnetic we also expect a polarisation of the conduction electrons and thus a similar behaviour as in the case of Mn. Finally we are working with higher concentrations which means that we might introduce changes in the energy spectra and the density of states. In Figure 29 we show as an example the case of Fe. The variation of the initial slope and the tendency to a compensation effect is clearly seen.

4
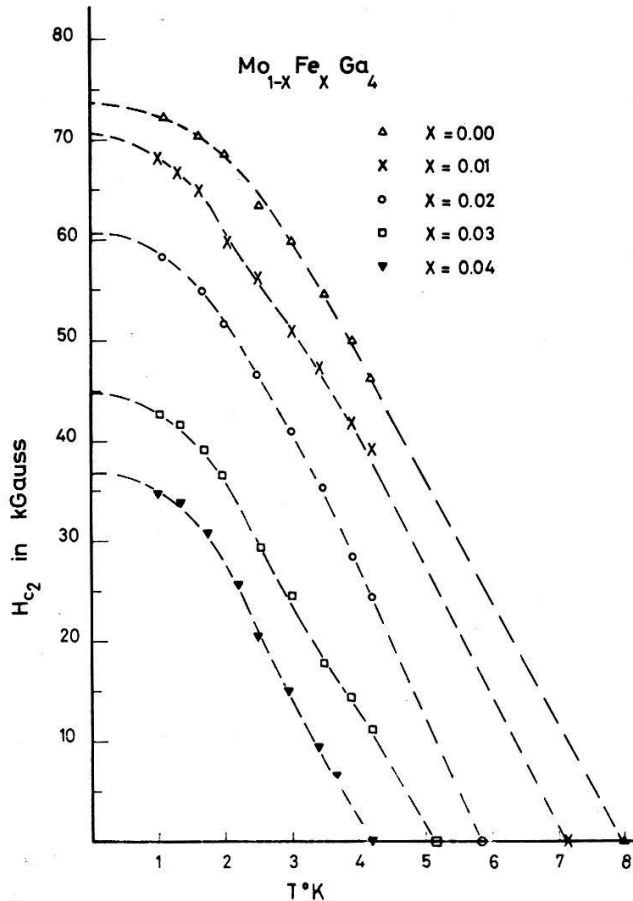
Figure 29
Critical field as a function of temperature
for $Mo_{1-x}Fe_xGa_4$.

(e) *Kondo effect in* $Mo_{1-x}Mn_xGa_4$?

We have found in the preceding section that the exchange interaction between the conduction electrons and the Mn-ions is antiferromagnetic (i.e. $J < 0$). In such a case one expects a Kondo effect with a Kondo temperature T_K [80]

$$k_B T_K = D\, e^{-[1/N(0)J_0]} \,, \tag{77}$$

where D is the conduction electron band width. Assuming D to be a few electron volts and using the above determined values of J and $N(0)$ one gets $T_K \ll 1\,°K$. However the density of states in equation (77) should be the local density around the impurity and this might be somewhat higher than the mean value of the density of states. It is therefore difficult to predict anything from equation (77).

However the susceptibility shown in Figure 20 behaves as a typical Kondo system. Scalapino [81] has calculated the susceptibility in the high temperature limit $(T > T_K)$. As shown by Heeger his expression might be written to a very good approximation

$$\chi = \frac{\dfrac{\mu^2}{1.22}}{T + 4.5\,T_K} \,,$$

where μ is the magnetic moment. From Figure 20 this yields $T_K = 32°K$ and $\mu = 5.3\ \mu_B$ for $x = 0.02$. At lower concentrations T_K and U increase to $47°K$ and $8.3\ \mu_B$. Preliminary measurements on EPR [78] show that there is a Kondo type anomaly between $30°K$ and $40°K$ in the line-width. The g-shift, however, which from the superconductivity and susceptibility measurements is determined to be -0.03 ($\Delta g = J\ N(0)$ [79]), seems to be slightly positive. A more detailed investigation on $Mo_{1-x}Mn_xGa_4$ with respect to the Kondo effect is in preparation.

Müller-Hartmann and Zitterartz [83], [84], [85] have calculated the effect of magnetic impurities on T_c in the Kondo case. They find that the initial slope of T_c versus concentration depends on the ratio T_K/T_{c0}. The decrease of T_c is strongest for $T_K/T_{c0} = 1$. In a recent letter [86] they have extended their calculations to finite concentrations. For $T_K/T_{c0} > 1$ they predict that T_c should decrease linearly with c and then at about $T_c = 0.5\ T_{c0}$ begin to flatten out and finally approach $T_c \to 0$ asymptotically. This is due to the fact that the spin flip scattering decreases when T_K/T increases. However, in our case with $T_K/T_{c0} \approx 4$ and experimental domain $8° > T > 1°$ the predicted effect is not very large and may easily be masked by the correlation effect described above (chapter 5c). We note also that the predictions of Müller-Hartmann and Zitterartz for $T_K/T_{c0} > 1$ are quite similar to the predictions of Bennemann, for the case of resonant scattering and the predictions of Fulde and Hoenig [87] for magnetic impurities in a singlet ground state. Thus one must be careful when interpreting such experimental results.

Unfortunately the critical field of a superconductor with magnetic impurities which show a Kondo effect has not yet been calculated. However, from the calculations of Müller-Hartmann and Zitterartz one might expect that as $T \to 0$, $H_{c_2} \to H_{c_2}$ ($c = 0, T = 0$) since the spin flip scattering decreases to zero. At first sight this could offer an alternative explanation for the anomalies in H_{c_2} versus T. However in that case we should see a tendency of saturation in χ between $2°$ and $3°K$, which is not the case (Fig. 20). Furthermore, the H_{c_2} curves for $x = 0.008$ and $x = 0.01$ should not become horizontal at low temperatures, but continue to increase until $H_{c_2} = H_{c_2}$ ($c = 0, T = 0$). Finally according to the theory of Müller-Hartmann and Zitterartz one does not expect a great change in the spin flip scattering for $8° > T > 1°$ in the case of $T_K/T_{c0} \approx 4$, and certainly not a sudden change as would be required to explain the results in Figure 23. We therefore conclude that although the Kondo effect may exist in our system, it changes very little the behaviour of the system in comparison to the case without Kondo effect, and is not able to account for the anomalies observed in H_{c_2}.

6. On the Possibility to Observe the Jaccarino-Peter Effect in Dense Ferromagnetic Systems

(a) *Introduction*

In the preceding chapters we have only discussed dilute systems. However, in the original paper by Jaccarino and Peter, it was suggested that this compensation effect could be seen in a dense ferromagnet, which in zero external field would be a normal metal due to the mean exchange field. For this to be possible one has to admit that the ferromagnet, without the mean exchange field would be superconducting. That

this is possible is made highly probable through the paper by Baltensperger and Strässler, where they demonstrated the possibility of a coexistence between superconductivity and antiferromagnetism. Although the arguments used by them cannot be used directly in the ferromagnetic case, it is clear that the essential condition is that all electrons in a distance ω_0 from the Fermi surface should see the same exchange field. In that case it is possible to compensate the mean exchange field of all superconducting electrons by one external field. Furthermore it has been shown by Klose et al. [98] that the indirect electron-electron interaction via virtual spin waves for the ferromagnetic case is weak as soon as one applies an external field to produce a gap in the spin wave energy spectrum. In what follows we will assume that this is the case and that the ferromagnet without a mean exchange field would be superconducting with a critical temperature T_{c0}.

From the previous chapters it is clear that the maximum field that can be compensated is $H_{c_2}^*(T = 0)$, the orbital critical field. On the other hand, the mean exchange fields may reach very high values in dense ferromagnets. Our discussion of the compensation effect will therefore be a discussion of $H_{c_2}^*$ in magnetic superconductors. The calculation of Baltensperger and Strässler was done for a well-ordered system. The periodicity of the magnetic lattice was used in an essential way when they constructed the BCS-wave function. Now it is well known that the critical field of a pure and well-ordered superconductor is rather low. The critical field can be increased in two ways: (a) By introducing impurities and disorder in the bulk system in order to decrease τ, the electron life time, (b) By using a very thin film.

However, both these methods will generally introduce magnetic scatterings as well as non-magnetic scatterings. This can be seen as follows: an ordered ferromagnetic superconductor can for our purposes be described by the Hamiltonian [5] with $V_a = 0$, $H = 0$, plus an interaction term, and where the magnetic ions occupy a regular lattice. The interaction term is taken to be $-\sum (\boldsymbol{H}_M, \boldsymbol{S}_j)$ where H_M is the molecular field acting on the spins. If we now remove one magnetic ion and replace it by a non-magnetic one, our new Hamiltonian may be written as the unperturbed Hamiltonian plus a non-magnetic impurity, minus a magnetic one. Since the unperturbed Hamiltonian describes our unperturbed superconductor with singlet pairing, we have the same situation as for a non-magnetic superconductor with a magnetic impurity. The same argument holds for the case of disorder in the lattice. For a thin film these impurities are replaced by the surface of the thin film. When discussing $H_{c_2}^*$ we have to take into account these scatterings since they cannot be compensated as the mean exchange field. We have therefore two competing mechanisms determining $H_{c_2}^*$.

Since we are interested in the case where the paramagnetic effect is compensated, we shall in the following consider a hypothetical system where the mean exchange fields is exactly compensated by the external field. We then discuss the critical field $H_{c_2}^*$ of this system. In cases where H_J, the exchange field, turns out to be smaller than $H_{c_2}^*$, the compensation is possible, and our hypothetical system may describe a real system in a narrow range of magnetic field around $H = -H_J$.

(b) *Bulk systems*

It follows from the discussion above that our system is equivalent to a pure and well-ordered superconductor with magnetic impurities. As shown in chapter 2 the

critical field is given by equation (27). Since we are interested in the orbital critical field, we put $(H \cdot \sigma) = 0$ in α_ω and equation (17) reduces to

$$\ln\left(\frac{T_{c0}}{T}\right) = \sum_{-\infty}^{+\infty} \left[\frac{1}{|2n+1|} - \frac{1}{\dfrac{1}{s_\omega^0} - \lambda + \lambda_m} \right],$$ (78)

$$s_\omega^0 = \frac{2\pi k_B T}{v_F \left(\dfrac{2e\hbar H}{c}\right)^{1/2}} J(\alpha_\omega),$$ (79)

$$\alpha_\omega = \frac{v_F \left(\dfrac{2e\hbar H}{c}\right)^{1/2}}{2|\omega|\hbar + \dfrac{\hbar}{\tau}},$$ (80)

$$J(\alpha) = 2\int_0^\infty dq \, \tan^{-1}(\alpha q)\, e^{-q^2}.$$ (81)

We have here restored ordinary units. In the dirty case one finds $H_{c_2} \sim \lambda$ and therefore we defined in chapter 2 a reduced field $h \sim H_{c_2}/\lambda$ so that h is independent of λ. In the pure limit, however, the proportionality between H_{c_2} and λ does not hold. Following Ref. [16] we now introduce a new reduced field, $h_p = \lambda h/3$ or

$$h_p = \frac{2e\hbar}{c} H_{c_2} \left(\frac{v_F}{2\pi k_B T_{c0}}\right)^2.$$ (82)

With this definition we may write equation 78 as

$$\ln\frac{1}{t} = \sum_{-\infty}^{+\infty} \left(\frac{1}{|2n+1|} - \frac{\left(\dfrac{t}{h_p^{1/2}}\right) J(\alpha_\omega)}{1 - \left[\dfrac{\lambda - \lambda_m}{h_p^{1/2}}\right] J(\alpha_\omega)} \right),$$ (83)

$$\alpha_\omega = \frac{h^{\cdot 2}}{|2n+1|t + \lambda} \qquad t = \frac{T}{T_{c0}}.$$ (84)

As stated above we suppose that λ and λ_m are created by the same impurities. If we look at the behaviour of the system as a function of concentration of impurities we may assume $\lambda = \delta\lambda_m/2$ where δ is a proportionality constant. Using the expression for the different scattering times given in Appendix C we may write

$$\delta = \frac{2\lambda}{\lambda_m} = \frac{\tau_s}{\tau} = \frac{4|U_{b1}|^2 + \left(\dfrac{J}{N}\right)^2 \langle s^2 \rangle}{\left(\dfrac{J}{N}\right)^2 \langle s^2 \rangle},$$

δ measures the strength of the non-magnetic scattering with respect to the magnetic one, produced by the same ion.

To calculate the maximum critical field $H^*_{c_2 max}$ we have to calculate h as a function of concentration (i.e. as a function of λ_m) in the limit $t \to 0$ for different values of δ. However since we are only interested in an estimate of $H^*_{c_2 max}$ we will solve equation (83) only approximately. As shown in Ref. [16], in the case of non-magnetic impurities the reduced field h_p defined by

$$h_p = - \frac{h_p(t = 0)}{\left(\dfrac{dh_p}{dt}\right)_{t=1}},$$

is nearly independent of λ. On the other hand it follows from a calculation by Gorkov [88] that

$$\left(\frac{dh_p}{dt}\right)_{t=1} = - \frac{3\,\lambda^2}{\dfrac{\pi^2}{4} - \psi\left(\dfrac{1}{2} + \dfrac{\lambda}{2}\right) + \psi\left(\dfrac{1}{2}\right)}. \tag{85}$$

Using the values for h_p given in Ref. [16] we may calculate $h_p(\lambda)$ for non-magnetic impurities ($\delta \to \infty$) from equation (85) [89]. The result is shown in Figure 30. The value for the pure limit has been given by Gorkov [90], $h_p(\lambda = 0) = 1.04$ (see also Ref. [16]). The dirty limit approximation is given by the dashed line through the origin.
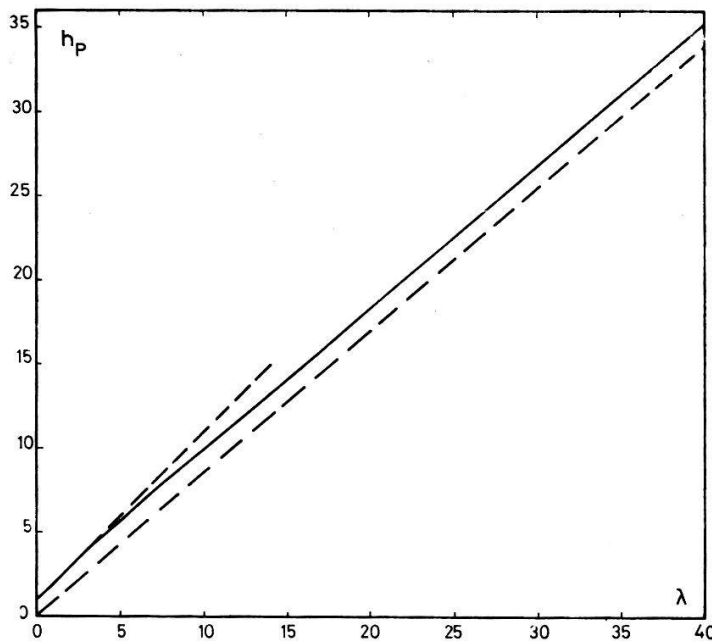
Figure 30
Orbital critical field h_p as a function of the non-magnetic scattering parameter λ. The dotted line through the origine shows the dirty limit.

In the case of magnetic impurities it is physically clear that h_p must decrease approximately as T_c when λ_m increases, if we keep λ constant for a moment (in the dirty limit we have seen that h decreases somewhat faster than T_c (see Fig. 3). We therefore take into account the exchange scattering in an approximate way by using equation (83) for $\lambda_m = 0$, but replacing T_{c0} by T_c determined by equation (34). We can now easily calculate the ratio of the critical field for a certain concentration of impurities to the critical field for the pure sample (h_r).

We introduce the reduced concentration

$$\Gamma = \frac{\lambda_m}{\lambda_{m\,crit}} \cong \frac{\lambda_m}{0.281} \,. \tag{86}$$

In terms of Γ we get from equation (82)

$$h_r \equiv \frac{H_{c_2}^*(\Gamma)}{H_{c_2}^*(0)} = \frac{1}{h_p(0)} \, t^2(\Gamma) \, h_p\big(\lambda(\Gamma)\big) \,, \tag{87}$$

where $t(\Gamma)$ and $\lambda(\Gamma)$ are given by

$$\Gamma = \frac{1}{0.281} \, \varrho(t) \,, \tag{88}$$

$$\lambda(\Gamma) = 0.140 \, \delta \cdot \Gamma \,. \tag{89}$$

The only parameter in these equations is δ. Its value can be estimated from experiments on magnetic impurities in pure and ordered superconductors. Using equations (26b), (36b) and assuming that the resistivity in the normal state can be written $\varrho = (m/n) \, e^2 \, \tau$ we get

$$\delta = \frac{2 \, \gamma_E \, \hbar \, n \, e^2 \, \varrho_{crit}}{\pi \, k_B \, T_{c0} \, m} \,, \tag{90}$$

where ϱ_{crit} is the normal state resistivity at the critical concentration ($\Gamma = 1$) minus the resistivity of the pure metal. With this formula one finds that δ is typically of the order 100. For the system $Th_{1-x}Gd_x$ we find, using the resistivity measurements of Peterson et al. [91] and the T_c measurements of Decker and Finnemore [92], $\delta = 170$. A particularly favourable case is the one of $Th_{1-x}Er_x$. Using the results of Andres and Bucher [93] and of Ref. [91] we find $\delta = 1900$.

In Figure 31 we plotted h for $\delta = 100$ and $\delta = 1000$. One finds:

$$h_{\Gamma max} = 4.2 \quad (\delta = 100) \,,$$

$$h_{\Gamma max} = 37.0 \quad (\delta = 1000) \,.$$

To find $H_{c_2 max}^*$ we now need to know $H_{c_2}^*(\Gamma = 0)$. With $h_p(\lambda = 0) = 1.04$ we get from equation (82)

$$H_{c_2}^* \, (\Gamma = 0) = 0.22 \, \frac{\phi_0}{\xi_0^2} \,, \tag{91}$$

where

$$\xi_0 = 0.18 \, \frac{\hbar \, v_F}{k_B \, T_{c0}} \,,$$

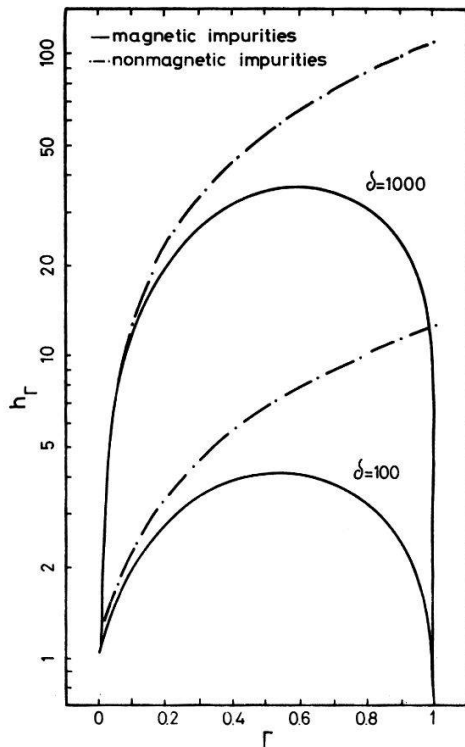$$\phi_0 = \frac{h \, c}{2 \, e} = 2 \cdot 10^{-7} \, \text{Gauss} \cdot \text{cm}^2 \,.$$

Figure 31

Amplification $h_\Gamma = [H_{c_2}^*(\Gamma)]/[H_{c_2}^*(\Gamma = 0)]$ of the orbital critical field produced by magnetic and non-magnetic impurities in a pure superconductor. The first case corresponds to the case of non-magnetic impurities in an ordered ferromagnetic superconductor.

It is easily seen that for most superconductors where $\xi_0 > 500$ Å there is actually no possibility to reach high enough values for $H_{c_2max}^*$ so that a compensation can be possible ($H_{c_2max}^*$ will then generally be lower than the Clogston limit, thus the real ferromagnet should be superconducting in zero external field if H_J is small enough to make a compensation possible). However, for substances with a large density of states, ξ_0 will be small and $H_{c_2}^*$ ($\lambda = 0$) will become large. The situation is different from the one encountered in the case of a dilute system. There we concluded that $N(0)$ should not be too large in order to observe an increase in H_{c_2}. The reason is that in that case the two competing effects were the exchange scattering and the exchange field whereas here the two competing mechanisms are the non-magnetic- and exchange-scattering. Since both λ_m and λ are proportional to the density of states the latter one drops in the ratio δ.

Using Hake's [25] estimations for ξ_0 we find as an example:

Nb$_3$Sn $H_{c_2}^*(\Gamma = 0) = 70$ kGauss ,

V_3Ga $H_{c_2}^*(\Gamma = 0) = 175$ kGauss .

To estimate the upper limit of the compensation effect, we calculated $H_{c_2}^*$ as a function of δ for a constant amount of discorder (i.e. for a constant λ), assuming $H_{c_2}^*(\Gamma = 0) = 175$ kGauss. Two cases are shown in Figure 32. The upper curve show the case where $H_{c_2}^* = 2.5$ MGauss in the nonmagnetic case (Hake's limit for V_3Ga). In the lower curve we show a more reasonable case where $H_{c_2}^*$ is 1 MGauss in the non-magnetic case. Since δ is typically of the order 100 we may therefore expect that it is possible to reach $H_{c_2}^*$ values of 600–800 kGauss for the ferromagnetic case. The corresponding J values calculated from the condition $H_J < H_{c_2}^*$ are also given in Figure 32. It was assumed that only the B atoms in A_3B were magnetic.
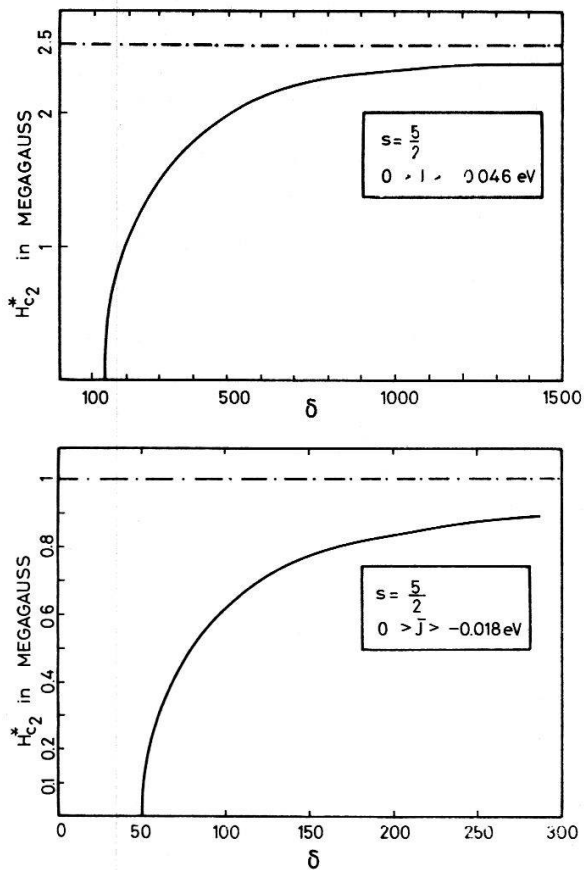
Figure 32
Orbital critical field for a ferromagnetic superconductor as a function of $\delta = \tau_s/\tau$ assuming $\tau = $ const. and $H_{c_2}^*(\tau_s = \infty)$ = 2.5 MGauss (Hake's limit) and $H_{c_2}^*(\tau_s = \infty) = 1$ MGauss.

The above estimates give an idea of what one can expect to reach with the compensation effect. However to reach the limits discussed above one has to be able to control the amount of disorder in the system, This is a very difficult problem even for the non-magnetic superconductors and there is no reason to believe that it will be easier in the magnetic case. Furthermore it has been shown that impurities in a superconductor with a high density of states has a tendency to decrease T_c due to a broadening of the peaks in the density of states [94]. This effect may of course reduce the maximum value of $H_{c_2}^*$.

(c) *Thin films*

In a pure and ordered thin film the electrons scatter at the surface. Using a similar picture that we used in the previous section, we may say that the electrons scatter on the atoms that are missing. Since these atoms are supposed to be magnetic the scattering amplitude will have a magnetic part. Following the arguments above we replace our ferromagnetic thin film by a superconducting film between two layers of a ferromagnetic oxide. As de Gennes [95] we now assume that the electrons are scattered by the first atomic layer in the oxide, and that this is equivalent to a concentration $2 a_0/d$ of magnetic impurities. a_0 is the interatomic distance and d the thickness of the film. To calculate the critical field as a function of thickness d we now use the result of Tinkham and de Gennes [24] that for a thin film a long mean free path the dirty limit result is still valid if we replace l by $16 d/q$.

The critical field is therefore determined by

$$\ln \frac{T_{c0}}{T} = \psi \left(\frac{1}{2} + \frac{\hbar}{4 \pi k_B T_c} \left(\frac{1}{\tau_H} + \frac{2}{\tau_s} \right) \right) - \psi \left(\frac{1}{2} \right), \tag{92}$$

where

$$\frac{1}{\tau_H} = 0.34 \frac{k_B T_{c0}}{\hbar \phi_0^2} \xi_0 H_c^2 d^3, \tag{93}$$

$$\frac{1}{\tau_s} = \frac{2 \pi}{\hbar} N(0) S(S+1) J^2 \frac{a_0}{d}. \tag{94}$$

For $T_c = 0$ we then get the following equations for H_c:

$$H_c^* = \sqrt{\frac{c_1}{d^3} - \frac{c_2}{d^4}}, \tag{96}$$

$$c_1 = 2.19 \cdot 10^{-14} \frac{1}{\xi_0} \, (\text{cm}^3), \tag{97}$$

$$c_2 = 5.9 \cdot 10^{-45} \frac{a_0 N(0) S(S+1) J^2}{\xi_0 T_{c0}} \, (\text{cm}^4)$$

$$= 0.95 \cdot 10^{-13} \frac{a_0 \gamma S(S+1) J^2}{\xi_0 T_{c0}} \, (\text{cm}^4). \tag{98}$$

γ is the specific heat coefficient. All parameters are measured in cgs units.

A typical case for H_c^* as a function of d is shown in Figure 33. H_c has a maximum H_{c_m} at a certain thickness d_m. From equations (96), (97) and (98) we find:

$$d_m = \frac{4}{3} \frac{c_2}{c_1} = 5.8 \frac{\gamma S(S+1) J^2 a_0}{T_{c0}},$$

$$H_{cm}^* = \sqrt{\frac{9}{64} \frac{c_1^4}{c_2^3}} = 6.16 \cdot 10^{-18} \frac{1}{\xi_0 J^3} \left(\frac{T_{c0}}{\gamma S(S+1) a_0} \right)^{3/2}.$$
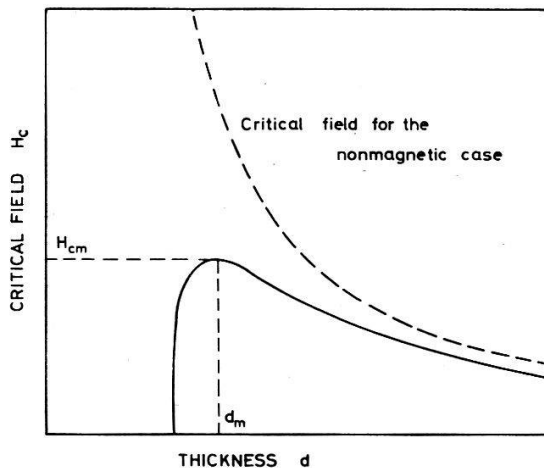

Figure 33
Orbital critical field for a thin ferromagnetic and superconducting film as a function of thickness.

It is seen from this formula that to get a high $H_{c_m}^*$ we should *not* take a substance with a very high density of states. The best substances are those which show a high ratio (T_{c0}/γ) (as for instance Nb₃Al). Assuming that the electronic properties of our hypothetical system correspond to those of Nb₃Sn we have plotted in Figure 34 $H_{c_m}^*$, H_J and d_m as a function of the exchange interaction J. The compensation is possible when $H_{c_m}^* > H_J$. This is the case when d_m is smaller than 34 Å and H_J smaller than 400 kGauss.
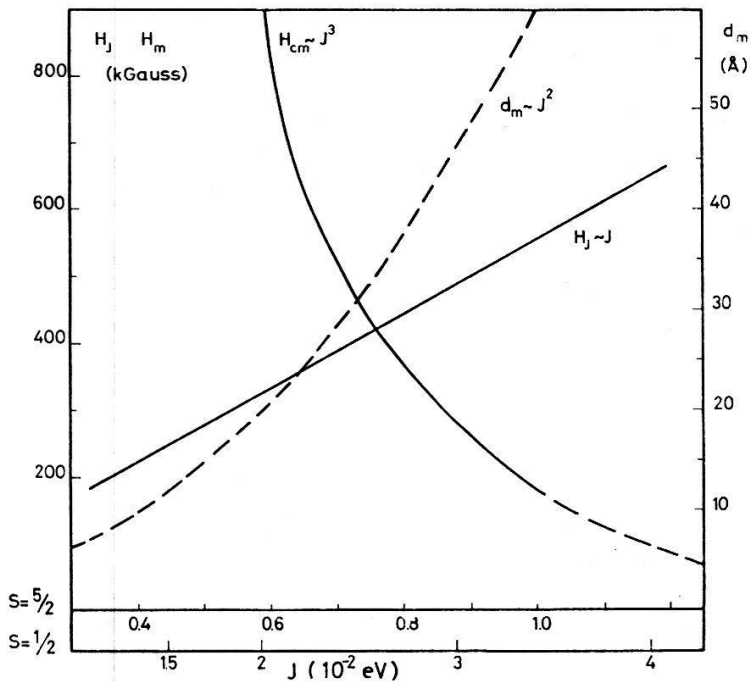

Figure 34

Exchange field H_j, Maximum orbital critical field H_{cm} and the corresponding thickness d_m as a function of exchange interaction J for $S = 5/2$ and $S = 1/2$.

It is of course a serious question if one still has the bulk electronic properties in such thin films. Zeller and Giaever [96] studied the superdonductivity in small particles with diameter down to 25 Å. They found that the critical field increased faster than predicted by equation (96) with $C_2 = 0$. Since we are actually only interested in the critical field, this experiment may indicate that the thin films may be more favourable for the compensation effect than estimated above.

7. Conclusion

We have studied the effect of magnetic ions on superconductivity, with emphasis on the compensation effect suggested by Jaccarino and Peter.

In the main part of this work we have studied the influence of magnetic impurities on the properties of high field superconductors, and how the compensation effect will show up in the H_{c_2} vs. T_c-curve. This compensation effect has two interesting aspects: (1) It allows one to determine several of the important parameters of the system. (2) It may in certain cases produce a net increase in the critical field. Experimentally we were able to demonstrate the compensation effect in the system $Mo_{1-x}Mn_xGa_4$ where Mn behaved as a magnetic impurity. From the behaviour of the reduced critical field H_{red}, defined in chapter 3, we could determine the orbital critical field $H_{c_2}^*(T = 0)$

and the exchange constant $J(q = 0)$. The behaviour of H_{c_2} in the limit $T = 0$ were good agreement with the theory presented in chapter 2, and it allowed us to determine the Maki parameter α and the spin-orbit parameter λ_{s0}. However, the curves H_{c_2} vs. T did only agree qualitatively with the calculated curves. This correlated with the fact that even for the sample without magnetic impurities the theory did not reproduce the measured curve. This discrepancy which has also been observed in other systems, show that it might be quite misleading to determine the parameters α, λ_{s0}, by fitting the measured critical field curves to the WHH-formula. Especially the conclusions that $\lambda_{s0} = \infty$ for some systems [30] may be quite wrong. The above discussed compensation effect may provide a good tool to check more directly the paramagnetic effect on H_{c_2} in these substances and thus check the validity of the WHH-model.

In the last chapter we have studied the possibility to realize the compensation effect in a dense ferromagnet. The compensation effect has been shown to be possible. However it may be difficult to realize experimentally due to the many conditions that must be fulfilled.

We therefore conclude that at the present time it seems most reasonable to investigate superconductors with magnetic impurities. Since there is a great number of interesting substances for such an investigation, one may hope to get much new information of the high field properties of superconductors.

Appendix A

Inversion of the Gorkov equations

To invert the Gorkov equations (7a) and (7b), we define:

$$\hat{D}_{\pm} = \left(\frac{1}{2\,m} \, (\nabla \pm i\,e\,\boldsymbol{A})^2 + g\,\mu_B(\boldsymbol{H} + \boldsymbol{H}_J)\,\boldsymbol{\sigma} + \mu \right), \tag{A1}$$

$$\hat{V}(r_1, r_2) = \hat{V}_a(r_1, r_2) + \hat{V}_b(r_1, r_2) . \tag{A2}$$

We then write the Gorkov equations as

$$\left(i\,\omega_n + \hat{D}_-(r_1)\right)\hat{G}_\omega(r_1, r') - \int \hat{V}(r_1, r_2)\,\hat{G}_\omega(r_2, r')\,d^3r_2$$

$$+ \hat{\Delta}(r_1)\,\hat{F}_\omega^+(r_1, r') = \delta(r_1 - r')\,, \tag{A3}$$

$$\left(i\,\omega_n - \hat{D}_+(r_1)\right)\hat{F}_\omega^+(r_1, r') + \int \hat{V}^t(r_2, r_1)\,\hat{F}_\omega^+(r_2, r')\,d^3r_2$$

$$+ \hat{\Delta}^*(r_1)\,\hat{G}_\omega(r_1, r') = 0\,. \tag{A4}$$

Multiplying (A3) from left by $G_\omega^n(r, r_1)$ and (A4) by $G_{-\omega}^{nt}(r_1, r)$ ($G_\omega^n(r, r')$ is the normal state Green function defined by equation (A3) with $\Delta = 0$ and integrating by parts over r_1 we get

$$\int d^3r_2 \left[\left(i\,\omega_n + \hat{D}_+(r_2)\right)\hat{G}_\omega^n(r, r_2) - \int \hat{G}_\omega^n(r, r_1)\,\hat{V}(r_1, r_2)\,d^3r_1\right]\hat{G}_\omega(r_2, r')$$

$$+ \int \hat{G}_\omega(r, r_1)\,\hat{\Delta}(r_1)\,\hat{F}_\omega^+(r_1, r')\,d^3r_1 = \hat{G}_\omega^n(r, r')\,, \tag{A5}$$

$$- \int d^3r_2 \left[\left(-i\,\omega_n + \hat{D}_-(r_2)\right)\hat{G}_{-\omega}^{nt}(r_2, r) - \int \left(\hat{V}(r_2\,r_1)\,\hat{G}_\omega^n(r_1\,r)\right)^t d^3r_1\right]\hat{F}^+(r_2, r')$$

$$+ \int \hat{G}_{-\omega}^{nt}(r_1, r)\,\hat{\Delta}(r_1)\,\hat{G}_\omega(r_1, r')\,d^3r_1 = 0\,. \tag{A6}$$

To transform equation (A7) we note that (see Ref. [20])

$$\left(i\,\omega_n + \hat{D}_+(r_2)\right)\hat{G}_\omega^n(r, r_2) - \int \hat{G}_\omega^n(r, r_1)\,\hat{V}(r_1, r_2)\,d^3r_1 = \delta(r - r_2)\,. \tag{A7}$$

To transform equation (A8) we use equation (A3) with $\Delta = 0$. We find

$$\hat{G}_\omega(r, r') = \hat{G}_\omega^n(r, r') - \int \hat{G}_\omega^n(r, s)\,\hat{\Delta}(s)\,\hat{F}_\omega^+(s, r')\,d^3s\,, \tag{A8}$$

$$\hat{F}_\omega^+(r, r') = \int \hat{G}_{-\omega}^{nt}(s, r)\,\hat{\Delta}^\ast(s)\,\hat{G}_\omega(s, r')\,d^3s\,. \tag{A9}$$

To calculate G_ω and F_ω^+ in terms of G_ω and Δ we simply iterate equations (A8) and (A9). To the lowest order in Δ we get

$$\hat{G}_\omega(r, r') = \hat{G}_\omega^n(r, r')\,,$$

$$\hat{F}_\omega^+(r, r') = \int \hat{G}_{-\omega}^n(s, r)\,\hat{\Delta}^*(s)\,\hat{G}_\omega^n(s, r')\,d^3s\,. \tag{A10}$$

This is the result used in chapter 2. (Note that $G_\omega^t = G_\omega$).

If one writes the equations analogous to equations (A8) and (A9) for $\hat{G}^t_\omega(r', r)$ and $\hat{F}_\omega(r, r')$ the four equations obtained may be written in matrix form

$$\mathscr{G}_\omega(r, r') = \mathscr{G}^n_\omega(r, r') + \int \mathscr{G}^n_\omega(r, s) \sum (s) \, \mathscr{G}_\omega(s, r') \, d^3s \, , \tag{A11}$$

where

$$\mathscr{G}_\omega = \begin{pmatrix} G_\omega & -F_\omega \\ F^+_\omega & G^t_\omega \end{pmatrix} \quad \mathscr{G}^n_\omega = \begin{pmatrix} G^n_\omega & 0 \\ 0 & G^{nt}_\omega \end{pmatrix} \quad \sum = \begin{pmatrix} 0 & \Delta \\ \Delta* & 0 \end{pmatrix}$$

and

$$G^t_{\omega\alpha\beta}(r_1, r_2) = G_{-\omega\beta\alpha}(r_2, r_1) \quad \alpha, \beta = \text{spinindices} \, .$$

Thus the equations for G_ω and F^+_ω may be combined to an equation analogous to the Dyson equation for the normal state Green function. This matrix form was first introduced by Nambu [99] and by Gorkov and Rusinov [100].

In the WHH paper this matrix formalism is adopted. However, their normal state Green function $\mathscr{G}^n$ is defined without the scattering potentials. From equations (A5) and (A6) it is seen that in this case we have to add a potential dependent term in equation (A11) of the form

$$\int \mathscr{G}^n_\omega(r, s) \, V(s, t) \, \mathscr{G}_\omega(t, r') \, d^3s \, d^3t \, ,$$

equation (A11) then turns into equation (1) of WHH.

Appendix B

Transformation of the Gap equation

The sum over ω in equation (11) diverges. This is the same divergence as found in ordinary BCS-theory. If we neglect all interactions, Δ might be taken as constant and using that the Fourier transform of $G_\omega(r, s)$ is given by

$$G_\omega(p) = \frac{1}{\xi(p) + i \omega} \, .$$

Equation (11) may be written

$$1 = N(0) \, | \, g \, | \, T_{c0} \sum_\omega \int \frac{d\xi}{\xi^2 + \omega^2} \, . \tag{B1}$$

If the integral is taken between $-\infty$ and $+\infty$ the sum over ω diverges. One therefore generally introduces the BCS cutoff: (ω_D = Debye frequency).

$$1 = N(0) \, | \, g \, | \, T_{c0} \sum_\omega \int_{-\omega_D}^{+\omega_D} \frac{d\xi}{\omega^2 + \xi^2} = N(0) \, | \, g \, | \, \log \left(\frac{1.14 \, \omega_D}{T_{c0}} \right) . \tag{B2}$$

The divergence in equation (11) in the more general case is of the same type as above. It is therefore generally removed in the following way. We subtract from both sides in equation (11) the term

$$| g | \, N(0) \, T \sum_\omega \int \frac{d\xi}{\omega^2 + \xi^2} \, \Delta(r) \tag{B3}$$

and get

$$- \Delta(r) \left(1 - | g | \, T \, N(0) \sum_\omega \int \frac{d\xi}{\omega^2 + \xi^2} \right)$$

$$= | g | \, T \, N(0) \sum_\omega \int d^3s \left(\int \frac{\delta(s - r) \, d\xi}{\xi^2 + \omega^2} - \frac{1}{2} \operatorname{tr} \langle G^n_{-\omega}(s, r) \, G^n_\omega(s, r) \rangle_{ij} \right) \Delta(s) \, .$$

In the term to the right the divergence in the two terms just compensates each other. In the term to the left we now introduce the BCS cutoff. Using equation (B2) and carrying out the integral over ξ to the right, we may write

$$N(0) \, | g | \ln \left(\frac{T_{c0}}{T} \right) \Delta(r)$$

$$= N(0) \, | g | \, T \sum_\omega \int d^3s \left(\frac{\delta(s - r) \, \pi}{| \omega |} - \frac{1}{2 \, N(0)} \operatorname{tr} \langle G^n_{-\omega}(s, r) \, G^n_\omega(s, r) \rangle_{ij} \right) \Delta(s) \, ,$$

with $\omega = \pi \, T (2 \, n + 1)$ we get:

$$\ln \left(\frac{T_{c0}}{T_c} \right) \Delta(r) = \sum_\omega \int d^3s \left(\frac{\delta(s - r)}{| 2 \, n + 1 |} - \frac{T}{2 \, N(0)} \operatorname{tr} \langle G^n_{-\omega}(s, r) \, G^n_\omega(s, r) \rangle_{ij} \right) \Delta(s) \, ,$$

from which equation (12) follows immediately.

Appendix C

Calculation of the eigenvalue s_ω

If we introduce equation (16) in the integral equation (15) the latter one turns into an equation for the eigenvalue s_ω of $S_\omega(r, r')$. We find:

$$S_\omega = S^0_\omega + S^0_\omega$$

$$\times \frac{N(0)}{T (\delta^3(0))^2} \int d^3r'' \left[\langle V_a(r, r'') \, S_\omega \, \tilde{V}_a(r'', r) \rangle + \langle V_b(r, r'') \, S_\omega \, \tilde{V}_b(r'' \, r) \rangle \right] . \tag{C1}$$

To Fourier transform the integral in equation (C1) we now introduce the Fourier transforms of the potentials defined in equations (6a) and (6b)*

$$V_a(r, r') = \sum_i \int d^3p \, d^3q \; e^{ip[(r + r'/2) - Ri] + iq(r - r')} \times \left(u_{a1}(p) + u_{a2}(p, q) \, (\hat{p} \times \hat{q} \, \hat{\sigma}) \right) ,$$

$$V_b(r, r') = \sum_j \int d^3p \, d^3q \; e^{ip[(r + r'/2) - Ri] + iq(r - r')}$$

$$\times \left(u_{b1}(p) + u_{b2}(p, q) \, (\hat{p} \times \hat{q} \, \hat{\sigma}) + \frac{1}{N} \, J(p) \, (s \cdot \boldsymbol{\sigma}) \right) . \tag{C2}$$

Introducing equation (C2) into equation (C1) and averaging over the impurity positions R_i and R_j we get:

$$s_\omega = s_\omega^0 + s_\omega^0 \frac{N(0)}{T}$$

$$\times \left[n_a\, u_{a1}^2\, s_\omega + n_a\, u_{a2}^2 \int d\hat{p}\, d\hat{q}\, (\hat{p} \times \hat{q}\,\hat{\sigma})\, s_\omega (\hat{p} \times \hat{q}\,\hat{\sigma}) + n_b\, u_{b1}^2\, s_\omega \right.$$

$$\left. + n_b\, u_{b2}^2 \int d\hat{p}\, d\hat{q}\, (\hat{p} \times \hat{q}\,\hat{\sigma})\, s_\omega (\hat{p} \times \hat{q}\,\hat{\sigma}) - \frac{n_b}{N} J^2\, (s, \sigma)\, s_\omega (s, \sigma) \right]. \qquad (C3)$$

Here we have assumed that the potentials $U(p)$ are constants. We have also used the relation:

$$\frac{V}{(2\,\pi)^2\, \delta^3(0)} \int d^3p\, f(\hat{p}) = \int d\hat{p}\, f(\hat{p}), \qquad (C4)$$

where the integral $\int d\hat{p}$ is over the directions of p:

$$\int d\hat{p} = 1.$$

As discussed in chapter 5c the p dependence of the potentials may be important in some cases. This is especially the case for the exchange interactions. Expressions for the scattering times which include the p dependence are given in Appendix F and in chapter 5c n_e and n_a are the number of non-magnetic and magnetic impurities respectively.

Since s_ω^0 depends on σ, s_ω must also depend on σ. However, they only depend on the component of σ parallel to the external field. We therefore decompose s_ω and s_ω^0 in two terms[1]):

$$s_\omega = s_\omega^1 + s_\omega^2 (\hat{H} \cdot \hat{\sigma}),$$

$$s_\omega^0 = s_{\omega 1}^0 + s_{\omega 2}^0 (\hat{H} \cdot \hat{\sigma}), \qquad (C5)$$

where $s_\omega^1\, s_\omega^2\, s_{\omega 1}^0\, s_{\omega 2}^0$ are independent of spin.

To evaluate equation (C3) we must calculate the expressions

$$L_1 = \int (\hat{p} \times \hat{q}\,\hat{\sigma})\, (\hat{H}\,\hat{\sigma})\, (\hat{p} \times \hat{q}\,\hat{\sigma})\, d\hat{p}\, d\hat{q},$$

$$L_2 = \langle (s\,\hat{\sigma})\, (\hat{H}\,\hat{\sigma})\, (s\,\hat{\sigma}) \rangle. \qquad (C6)$$

Using the identity

$$(a\,\hat{\sigma})\, (b\,\hat{\sigma}) = a\, b) + i(\hat{\sigma} \cdot a \times b), \qquad (C7)$$

---

[1]) $\hat{p}$, $\hat{q}$, and $\hat{H}$ are unit vectors in the direction of p, q, and H, respectively. $\hat{\sigma}$ is the Pauli matrix: $\hat{\sigma} = 2\,\sigma$.

we get

$$L_1 = \int d\hat{q}\, d\hat{p}\, [2(\hat{p} \times \hat{q}\, \hat{\sigma})\, (\hat{H}\, \hat{p} \times \hat{q})\, |\, p \times q\, |^2]\, (\hat{H}\, \hat{\sigma})$$

$$= \int d\hat{p}\, d\hat{q}\, [2(\hat{p} \times \hat{q}\, H)^2 - |\, \hat{p} \times \hat{q}\, |^2]\, (\hat{H}\, \hat{\sigma}) = \frac{4}{q} - \frac{2}{3} = -\frac{2}{q}\,, \qquad (C8)$$

$$L_2 = \langle 2(\hat{H}\, S)\, (S\, \hat{\sigma}) - S^2(\hat{H}\, \hat{\sigma})\rangle = (\langle S_z^2\rangle - \langle S_x^2\rangle - \langle S_y^2\rangle)\, (\hat{H}\, \hat{\sigma})\,. \qquad (C9)$$

Introducing these results together with equation (C5) into equation (3C) we find:

$$S_\omega^1 + S_\omega^2(\boldsymbol{H}\, \boldsymbol{\sigma}) = \left(S_{\omega 1}^0 + S_{\omega 2}^0(\hat{H}\, \hat{\sigma})\right)$$

$$\times \left\{ 1 + \frac{N(0)}{T}\left[n_a\, u_{a1}^2 + \frac{2}{3}\, n_a\, u_{a2}^2 + n_b\, u_{b1}^2 + \frac{2}{3}\, n_b\, u_{b2}^2 - \frac{n_b}{N}\left(\frac{J}{2}\right)^2 \langle S^2\rangle\right] S_\omega^1 \right.$$

$$+ \frac{N(0)}{T}\left[n_a\, u_{a1}^2 - \frac{2}{q}\, n_a\, u_{a2}^2 + n_b\, u_{b1}^2 - \frac{2}{q}\, n_b\, u_{b2}^2\right.$$

$$\left. \left. - \frac{n_b}{N}\left(\frac{J}{2}\right)^2 \langle S_z^2\rangle - \langle S_x^2\rangle - \langle S_y^2\rangle\right] S_\omega^2 \cdot (\hat{H} \cdot \hat{\sigma})\right\}. \qquad (C1)$$

We now introduce the life times

$$\frac{1}{\tau_{a1}} = 2\,\pi\, n_a\, N(0)\, u_{a1}^2 \qquad \frac{1}{\tau_{a2}} = \frac{2}{3}\cdot 2\,\pi\, n_a\, N(0)\, u_{a2}^2\,,$$

$$\frac{1}{\tau_{b1}} = 2\,\pi\, n_b\, N(0)\, u_{b1}^2 \qquad \frac{1}{\tau_{b2}} = \frac{2}{3}\, 2\,\pi\, n_b\, N(0)\, u_{b2}^2\,,$$

$$\frac{1}{\tau_s} = 2\,\pi\, \frac{n_b}{N}\, N(0)\left(\frac{J}{2}\right)^2 \langle S^2\rangle = \frac{\pi}{2}\, c\, N(0)\, J^2\, \langle S^2\rangle\,. \qquad (C11)$$

We also introduce the total life time τ of the electrons, and τ_{s0}, the generalized spin-orbit scattering time:

$$\frac{1}{\tau_{s0}} = \frac{1}{\tau_{a2}} + \frac{1}{\tau_{b2}} + \frac{3}{2\,\tau_s}\frac{\langle S_z^2\rangle}{\langle S^2\rangle}\,,$$

$$\frac{1}{\tau} = \frac{1}{\tau_{a1}} + \frac{1}{\tau_{a2}} + \frac{1}{\tau_{b1}} + \frac{1}{\tau_{b2}} + \frac{1}{\tau_s}\,. \qquad (C12)$$

Equation (C10) can now be written:

$$S_\omega^1 + S_\omega^2(\hat{H} \cdot \hat{\sigma}) = \left(S_{\omega 1}^0 + S_{\omega 2}^0(\hat{H}\, \hat{\sigma})\right)$$

$$\times \left\{ 1 + \frac{S_\omega^1}{2\,\pi\, T}\left[\frac{1}{\tau} - \frac{2}{\tau_s}\right] + \frac{S_\omega^2}{2\,\pi\, T}\left[\frac{1}{\tau} - \frac{4}{3}\frac{1}{\tau_{s0}}\right](\hat{H} \cdot \hat{\sigma})\right\}. \qquad (C13)$$

5

We separate the terms in $(\hat{\sigma} \cdot \hat{H})$

$$S_\omega^1 = S_{\omega 1}^0 \left(1 + \frac{S_\omega^1}{2\pi T}\left(\frac{1}{\tau} - \frac{2}{\tau_s}\right)\right) + \frac{S_{\omega 2}^0 S_\omega^2}{2\pi T}\left(\frac{1}{\tau} - \frac{4}{3\tau_{s0}}\right),$$

$$S_\omega^2 = S_{\omega 2}^0 \left(1 + \frac{S_\omega^1}{2\pi T}\left(\frac{1}{\tau} - \frac{2}{\tau_s}\right)\right) + \frac{S_\omega^0 S_\omega^2}{2\pi T}\left(\frac{1}{\tau} - \frac{4}{3\tau_{s0}}\right). \tag{C14}$$

To solve for s_ω^1 and s_ω^2 in terms of $s_{\omega 1}^0$, $s_{\omega 2}^0$ we introduce the abbreviations

$$Q = \frac{1}{2\pi T}\left(\frac{1}{\tau} - \frac{4}{3\tau_{s0}}\right),$$

$$P = \frac{1}{2\pi T}\left(\frac{4}{3\tau_{s0}} - \frac{2}{\tau_s}\right). \tag{C15}$$

The equation (C14) now read

$$s_\omega^1 = s_{\omega 1}^0\left(1 + s_\omega^1(Q + P)\right) + s_{\omega 2}^0 s_\omega^2 Q,$$

$$s_\omega^2 = s_{\omega 2}^0\left(1 + s_\omega^1(Q + P)\right) + s_{\omega 1}^0 s_\omega^2 Q.$$

Solving the second equation for s_ω^2 and introducing this into the first equation yields

$$s_\omega^1 = s_{\omega 1}^0\left(1 + s_\omega^1(Q + P)\right) + s_{\omega 2}^0 Q\, \frac{1 + s_\omega^1(Q + P)}{(1 - s_\omega^0 Q)}.$$

This may also be written:

$$\frac{1}{s_\omega^1} = \frac{1 - s_{\omega 1}^0 Q}{s_{\omega 1}^0(1 - s_{\omega 1}^0 Q) + (s_{\omega 2}^0)^2 Q} - Q - P.$$

If we now use the fact that $s_{\omega 1}^0$ is real and that $s_{\omega 2}^0$ is imaginary we may write:

$$\frac{1}{s_\omega^1} = \left(\mathrm{Re}\, \frac{1}{\frac{1}{s_{\omega 1}^0 + s_{\omega 2}^0} - Q}\right)^{-1} - P. \tag{C16}$$

Since $\mathrm{tr}\, s_\omega/2 = s_\omega^1$ we do not need to know s_ω^2. Introducing (C16) with the definitions (C15) into the gap equation (12) and using the fact that s_ω is an eigenvalue of $S_\omega(r, r')$ we get the final equation (26).

Appendix D

The dirty limit

In chapter 2 we found

$$s_\omega^0 = A\, J(\alpha_\omega), \tag{D1}$$

where A and α_ω are defined by equations (19), (22), (23) and (25). In the dirty limit we can assume $\alpha_\omega \ll 1$. Using the asymptotic series for J given by Helfand and Werthamer

$$J(\alpha) = \sum (-1)^n \frac{\alpha^{2n+1} \, n!}{(2\,n+1)} + R_{2N+1} \,,$$

we get

$$J(\alpha) \cong \alpha - \frac{1}{3}\,\alpha^3 + \cdots . \tag{D2}$$

If we write $(\hat{H}\,\hat{\sigma}) = 1$ in α_ω we may write for s_ω^1 $\left(\text{equation (C16)}\right)$

$$\frac{1}{s_\omega^1} = \left(\mathrm{Re}\,\frac{1}{\dfrac{1}{s_\omega^0} - Q}\right)^{-1} - P \,, \tag{D3}$$

$\left(\text{for definitions of } Q \text{ and } P \text{ see Appendix C, equation (C15)}\right)$.
    From equations (D1) and (D2) we find

$$\frac{1}{s_\omega^0} \approx \frac{1}{A\,\alpha_\omega}\left(1 + \frac{1}{3}\,\alpha_\omega^2\right). \tag{D4}$$

We now put

$$\frac{1}{s_\omega^0} - Q = x + i\,y \,. \tag{D5}$$

Then

$$\left(\mathrm{Re}\,\frac{1}{x + i\,y}\right)^{-1} = x + \frac{y^2}{x} \,. \tag{D6}$$

Introducing equation (D4) into equation (D5) and using

$$\alpha_\omega = \frac{2\,\pi\,T}{A}\,\frac{1}{2\,|\omega| + \dfrac{1}{\tau} + 2\,i\,\mu_B(H + H_J)\,sgn\,\omega} \,, \tag{D7}$$

we find

$$x = \frac{1}{2\,\pi\,T}\left(2.|\omega| + \frac{4}{3\,\tau_{s0}}\right) + \frac{2\,\pi\,T}{3\,A^2}\,\frac{\left(2\,|\omega| + \dfrac{1}{\tau}\right)}{\left(2\,|\omega| + \dfrac{1}{\tau}\right)^2 + 4\,\mu_B^2(H + H_J)^2} \,, \tag{D8}$$

$$y = \frac{1}{2\,\pi\,T}\left(2\,\mu_B(H + H_J)\,sgn\,\omega\right) - \frac{2\,\pi\,T}{3\,A^2}\,\frac{2\,\mu_B(H + H_J)\,sgn\,\omega}{\left(2\,|\omega| + \dfrac{1}{\tau}\right)^2 + 4\,\mu_B^2(H + H_J)^2} \,. \tag{D9}$$

The second term in x and in y is only important for small ω. We therefore replace $2\,\omega + 1/\tau$ by $1/\tau$. We suppose furthermore that

$$\frac{1}{\tau} \gg 2\,\mu_B(H + H_J)\,.$$

Then we may write:

$$x = \frac{1}{2\,\pi\,T}\left(2\,|\,\omega\,| + \frac{4}{3\,\tau_{s0}}\right) + \frac{2\,\pi\,T\,\tau}{3\,A^2}\,, \tag{D10}$$

$$y = \frac{\mu_B}{\pi\,T}\,(H + H_J)\,. \tag{D11}$$

Introducing these results into equation (D3) we get $\left(\text{with } \omega = 2\,\pi\,T(n + 1/2)\right)$

$$\frac{1}{s_\omega^1} = |\,2\,n + 1\,| + \frac{2\,\pi\,T\,\tau}{3\,A^2} + \frac{1}{\pi\,T\,\tau_s} + \frac{\dfrac{\mu_B^2}{(\pi\,T)^2}\,(H + H_J)^2}{|\,2\,n + 1\,| + \dfrac{2}{3\,\pi\,T\,\tau_{s0}} + \dfrac{2\,\pi\,T\,\tau}{3\,A^2}}\,.$$

Using the definition (26b), (29), (30), (31), (32) the above equation may be written:

$$\frac{1}{s_\omega^1} = |\,2\,n + 1\,| + \frac{h^\nu + \lambda_m}{t} + \frac{\alpha^2(h + h_J)^2}{|\,2\,n + 1\,| + \dfrac{h^\nu + \lambda_{s0}}{t}}\,, \tag{D12}$$

where $\nu = 1$ for bulk samples and $\nu = 2$ for thin films. Introducing this result into the gap equation (12) yields the equation (28).

Appendix E

The ψ-function

The digamma function ψ is defined as the logarithmic derivative of the Gamma-function

$$\psi(z) = \frac{d}{dz}\log \Gamma(z)\,. \tag{E1}$$

The most convenient form to represent $\psi(z)$ is in form of a series

$$\psi(z) = -\,c - \sum_{k=0}^{\infty}\left(\frac{1}{z + k} - \frac{1}{1 + k}\right)\,. \tag{E2}$$

This may also be written

$$\psi\left(\frac{1 + z}{2}\right) - \psi\left(\frac{1}{2}\right) = \sum_{-\infty}^{+\infty}\left(\frac{1}{|\,2\,n + 1\,|} - \frac{1}{|\,2\,n + 1\,| + z}\right)\,, \tag{E3}$$

a form which is very often met in theory of superconductivity.

From equation (E3) follows in particular:

$$\mathrm{Re}\left(\psi\left(\frac{1+z}{2}\right)-\psi\left(\frac{1}{2}\right)\right)=\sum_{-\infty}^{+\infty}\left(\frac{1}{|2n+1|}-\frac{|2n+1|+x}{(|2n+1|+x)^2+y^2}\right),\ (E4)$$

$$\mathrm{Im}\left(\psi\left(\frac{1+z}{2}\right)-\psi\left(\frac{1}{2}\right)\right)=\mathrm{Im}\,\psi\left(\frac{1+z}{2}\right)=\sum_{-\infty}^{+\infty}\frac{y}{(|2n+1|+x)^2+y^2}\,,\ (E5)$$

where $z=x+iy$.

For numerical calculations it is useful to note the functional relationship

$$\psi(z+1)=\psi(z)+\frac{1}{z}\,. \tag{E6}$$

Other formulas and relationships can be found in Ref. [97].

To transform equation (28) we multiply the second term at the right hand side with $(|2n+1|+\lambda_{s0}/t+h^v/t)$.

We then get:

$$\ln\left(\frac{1}{t}\right)=\sum_{-\infty}^{+\infty}\left\{\frac{1}{|2n+1|}-\frac{|2n+1|+\dfrac{h^v+\lambda_{s0}}{t}}{\left(|2n+1|+\dfrac{h^v+\dfrac{1}{2}(\lambda_m+\lambda_{s0})}{t}\right)^2+\left(\dfrac{\gamma}{t}\right)^2}\right\},\ (E7)$$

where

$$\gamma=\left(\alpha^2(h+h_J)^2-\frac{1}{4}(\lambda_{s0}-\lambda_m)^2\right)^{1/2}.$$

Identifying

$$x=\frac{h^v+\dfrac{1}{2}(\lambda_{s0}+\lambda_m)}{t}\qquad y=\frac{\gamma}{t}\,,$$

we may write using equations (E4) and (E5)

$$\ln\left(\frac{1}{t}\right)=\left(\frac{1}{2}+\frac{i(\lambda_{s0}-\lambda_m)}{4\gamma}\right)\psi\left(\frac{1}{2}+\frac{h^v+\lambda_m+\dfrac{1}{2}(\lambda_{s0}-\lambda_m)+i\gamma}{2t}\right)$$

$$+\left(\frac{1}{2}-\frac{i(\lambda_{s0}-\lambda_m)}{4\gamma}\right)\psi\left(\frac{1}{2}+\frac{h^v+\lambda_m+\dfrac{1}{2}(\lambda_{s0}-\lambda_m)-i\gamma}{2t}\right)$$

$$-\psi\left(\frac{1}{2}\right).$$

The above derivation does not hold for $\gamma^2 < 0$. The equation (E8) is, however, still correct. To show this we put $y^1 = i\,y$ and write equation (E7) in the form

$$\ln\frac{1}{t} = \Sigma\left(\frac{1}{|\,2\,n+1\,|} - \frac{|\,2\,n+1\,| + x + \dfrac{\lambda_{s0}}{t}}{(|\,2\,n+1\,| + x - y')\,(|\,2\,n+1\,| + x + y')}\right),$$

this may also be written:

$$\ln\frac{1}{t} = \frac{1}{2}\sum_{-\infty}^{+\infty}\left(\frac{1}{|\,2\,n+1\,|} - \frac{1}{|\,2\,n+1\,| + x + y'}\right)$$

$$+ \frac{1}{2}\sum_{-\infty}^{+\infty}\left(\frac{1}{|\,2\,n+1\,|} - \frac{1}{|\,2\,n+1\,| + x - y'}\right)$$

$$- \sum_{-\infty}^{+\infty}\frac{\lambda_{s0}}{4\,t\,y'}\left(\frac{1}{|\,2\,n+1\,| + x - y'} - \frac{1}{|\,2\,n+1\,| + x + y'}\right).$$

Using equation (E3) for real argument we get equation (E8) for $\gamma^2 < 0$.

Appendix F

A few useful formulas

(a) *Superconductor without magnetic impurities*

The critical field of the pure superconductor ($\lambda = 0$) (type II) can be written:

$$H_{c_2}^*(T = 0) = 0.22\,\frac{\phi_0}{\xi_0^2}\,,$$

where

$$\xi_0 = 0.18\,\frac{\hbar\,v_F}{k_B\,T_{c0}}$$

and $\phi_0 = 2 \cdot 10^{-7}$ Gauss cm².

In the dirty limit the orbital critical field may be written:

$$H_{c_2}^*(T = 0) = 3.06 \cdot 10^4\,\varrho\,\gamma\,T_{c0}\,.$$

where ϱ is the resistivity, γ the coefficient of the electronic specific heat, and T_{c0} the transition temperature. (All units in c.g.s.)

The Maki-parameter α may be written

$$\alpha = 2.35\,\varrho\,\gamma$$

or

$$\alpha = -2.58 \cdot 10^{-5}\left(\frac{dH_{c_2}}{dT}\right)_{T = T_{c0}}.$$

For a pure film

$$\left(d < 1 < \left(d\xi_0 \frac{T_{c0}}{T_{c0} - T}\right)^{1/2}\right),$$

one finds

$$H_c^*(T = 0) = \frac{4}{\pi^{4/3}} \frac{\phi_0}{(\xi_0\, d)^{1/2}\, d}\ .$$

For a dirty film

$$d^2 < l\, \xi_0 < d\xi_0\ ,$$

one finds

$$H_c^*(T = 0) = \frac{3}{\pi^{3/2}} \frac{\phi_0}{(\xi_0\, l)^{1/2}\, d}\ .$$

(b) *Superconductor with noninteracting magnetic impurities*

The initial decrease in T_c is given by

$$k_B \frac{dT_c}{dc} = -\frac{\pi^2}{8} N(0)\, S(S + 1) \frac{1}{2\, q_F^2} \int_0^{2q_F} dq \cdot q \cdot J^2(q) = -\frac{\pi^2}{8} N(0)\, S(S + 1)\, \overline{J^2}\ .$$

The critical concentration c_{crit} is

$$c_{crit} = \frac{0.562\, k_B\, T_{c0}}{N(0)\, S(S + 1)\, J^{-2}}\ .$$

$N(0)$ is the density of states at the Fermi surface per atom for one spin.

λ_m is given by

$$\lambda_m = \frac{1}{4\, k_B\, T_{c0}} N(0)\, S(S + 1) \frac{1}{2\, q_F^2} \int_0^{2q_F} dq \cdot q \cdot J^2(q) = \frac{1}{4\, k_B\, T_{c0}} N(0)\, S(S + 1)\, \overline{J^2}\ .$$

REFERENCES

[1] B. T. Matthias, H. Suhl and E. Corenzwit, Phys. Rev. Lett. *1*, 92, 449 (1958); H. Suhl, B. T. Matthias and E. Corenzwit, J. Phys. Chem. Solids *19*, 346 (1959).
[2] A. A. Abrikosov and L. P. Gorkov, Soviet Phys. JETP *12*, 1243 (1961).
[3] A. M. Clogston, Phys. Rev. Lett. *9*, 266 (1962).
[4] B. S. Chandrasekhar, Appl. Phys. Lett. *1*, 7 (1962).
[5] W. Baltensperger and S. Strässler, Phys. Condens Mat. *1*, 20 (1963).
[6] V. Jaccarino and M. Peter, Phys. Rev. Lett. *9*, 290 (1962).
[7] R. Avenhaus, Ø. Fischer, B. Giovannini and M. Peter, Helv. phys. Acta *42*, 649 (1969).
[8] C. Kittel, Phys. Rev. Lett. *10*, 339 (1963).
[9] B. B. Schwartz and L. W. Gruenberg, Phys. Rev. *177*, 747 (1969).
[10] R. D. Parks, in: *Superconductivity*, edited by P. R. Wallace, Vol. 2, page 625 (Gordon and Breach, New York 1969).
[11] P. Fulde and K. Maki, Phys. Rev. *141*, 275 (1966).
[12] K. Maki, Physics *1*, 21, 127 (1964).

[13] P. G. DE GENNES, Phys. Condens Mat. *3*, 79 (1964).

[14] W. A. B. EVANS and G. RICKAYZEN, Proc. Phys. Soc. *83, 311* (1964).

[15] G. RICKAYZEN, Phys. Rev. *138 A*, 73 (1965).

[16] E. HELFAND and N. R. WERTHAMER, Phys. Rev. *147*, 288 (1966).

[17] N. R. WERTHAMER, E. HELFAND and P. C. HOHENBERG, Phys. Rev. *147*, 295 (1966).

[18] K. H. BENNEMANN, J. W. GARLAND and F. M. MUELLER, Phys. Rev. Lett. *23*, 169 (1969).

[19] J. KELLER and R. BENDA, J. Low. Temp. Phys. *2, 141* (1970).

[20] L. P. GORKOV, Soviet Phys. JETP *36*, 1364 (1959).

[21] See for instance A. A. ABRIKOSOV, L. P. GORKOV and I. Y. DZYALOSSHINSKII, *Quantum Field Theoretical Methods in Statistical Physics* (Pergamon Press, Oxford 1965).

[22] It is important to notice that the condition Δ = constant fixes our choice of gauge for A.

[23] For a discussion of this point see for instance Ref. [13] or, P. G. DE GENNES, *Superconductivity of Metals and Alloys* (W. A. Benjamin Inc., New York 1966), p. 270.

[24] P. G. DE GENNES and M. TINKHAM, Physics *1*, 107 (1964).

[25] R. R. HAKE, Appl. Phys. Lett. *10*, 186 (1967).

[26] K. HECHLER and E. SAUR, Proc. of LT 11, St. Andrews (1968).

[27] P. SPITZLI, Thesis, University of Geneva 1970. To be published.

[28] J. E. CROW, R. P. GUERTIN and R. D. PARKS, Phys. Rev. Lett. *19*, 77 (1967).

[29] Note that a large α only means that H_c^*/T_{c0} is large. However if T_{c0} becomes small the domain accessible: for experiments may becomes too small, so that f. inst. extrapolations to $T = 0$ are impossible.

[30] S. FONER, E. J. McNIFF Jr., B. T. MATTHIAS, T. H. GEBALLE, R. H. WILLENS and E. CORENZWIT, Phys. Lett. *31 A*, 349 (1970). The results reported here on Nb₃Al are in disagreement with those reported in Ref. [26].

[31] P. KAPITZA, Proc. Roy. Soc. *A 105*, 691 (1924).

[32] P. KAPITZA, Proc. Roy. *A 115*, 658 (1927).

[33] T. F. WALL, J. Inst. Elec. Engrs. *64*, 409 (1926).

[34] K. S. W. CHAMPION, Proc. Phys. Soc. *B 63*, 795 (1950).

[35] H. P. FURTH and R. W. WANIEK, Rev. Sci. Inst. *27*, 195 (1956); H. P. FURTH, M. A. LEVINE and R. W. WANIEK, Rev. Sci. Inst. *28*, 949i (1957).

[36] S. FONER and H. H. KOLM, Rev. Sci. Instr. *28*, 799 (1957).

[37] P. COTTI, Z. angew. Math. Phys. *11*, 17 (1960).

[38] R. B. FLIPPEN, J. appl. Phys. *34*, 2026 (1963).

[39] N. PERRIN and B. PERRIN, J. Phys. *25*, 168 [A] (1964).

[40] Y. GROS and M. GUILLOT, Compt. Rend. *265*, 1283 (1967).

[41] A. VAN ITTERBEEK, W. VAN DRIESSCHE and I. DE GRAVE, Appl. Sci. Res. *18*, 105 (1967).

[42] S. ASKENAZI, A. SANTOUIL and J. CICHOSZ, Compl. Rend. *264 B*, 807 (1967).

[43] M. SUENAGA and K. M. RALLS, J. appl. Phys. *37*, 4, 197 (1966).

[44] B. T. MATTHIAS, E. A. WOOD, E. CORENZWIT and V. B. BALA, J. Phys. Chem. Solids *1*, 188 (1956).

[45] B. T. MATTHIAS, V. B. COMPTON and E. CORENZWIT, J. Phys. Chem. Solids *19*, 130 (1961)

[46] B. T. MATTHIAS, T. H. GABALLE and V. B. COMPTON, Rev. Mod. Phys. *35*, 1 (1963).

[47] P. W. ANDERSON, Phys. Rev. *124*, 41 (1961).

[48] P. A. WOLFF, Phys. Rev. *124*, 1030 (1961).

[49] E. WALKER, Thesis, University of Geneva (1971).

[50] K. YVON et al., to be published.

[51] J. D. G. LINDSAY, R. W. WHITE and R. D. FOWLER, Cryogenics *8*, 213 (1966).

[52] P. DONZE, Thesis, University of Geneva (1969); Arch. Sci. Genève *22*, 667 (1969).

[53] P. W. SELWOOD, *Magnetochemistry* (Interscience, New York 1964).

[54] A. D. CHAPLIN and C. RIZZUTO, Phys. Rev. Lett. *21*, 746 (1968).

[55] M. J. ZUCKERMANN, Phys. Rev. *140 A*, 899 (1965).

[56] C. F. RATTO and A. BLANDIN, Phys. Rev. *156*, 513 (1967).

[57] M. J. ZUCKERMANN, J. phys. C. Solid State Phys. *3*, 2130 (1970).

[58] G. BOATO, G. GALLINARO and C. RIZZUTO, Phys. Rev. *148*, 353 (1966).

[59] K. H. BENNEMANN, Phys. Rev. *183*, 492 (1969).

[60] N. RIVIER and M. J. ZUCKERMANN, Phys. Rev. Lett. *21*, 904 (1968).

[61] H. SUHL, Phys. Rev. Lett. *19*, 519 (1967).

[62] M. Levine and H. Suhl, Phys. Rev. *171*, 567 (1968).

[63] M. J. Levine, T. V. Ramakrishnan and R. A. Weiner, Phys. Rev. Lett. *20*, 1370 (1968).

[64] P. G. de Gennes and J. Friedel, J. Phys. Chem. Solids *4*, 71 (1958).

[65] See f. instance L. Landau and E. Lifshitz, *Statistical Physics* (Pergamon Press, London 1959).

[66] R. E. Watson and A. J. Freeman, Phys. Rev. *152*, 566 (1966); R. E. Watson and A. J. Freeman, Phys. Rev. *178*, 752 (1969); R. E. Watson, A. J. Freeman and S. Koide, Phys. Rev. *186*, 625 (1969).

[67] R. A. Hein, R. L. Falge, B. T. Matthias and E. Corenzwit, Phys. Rev. Lett. *2*, 500 (1959).

[68] J. E. Crow and R. D. Parks, Phys. Lett. *21*, 378 (1966).

[69] K. Yasukochi, Y. Kuwasawa and K. Sekizawa, Phys. Lett. *28 A*, 12 (1968).

[70] R. P. Guertin and R. D. Parks, Sol. State Comm. *7*, 59 (1969).

[71] K. H. Bennemann, Phys. Rev. Lett. *17*, 438 (1966).

[72] A. M. Toxen, P. C. Kwok and R. J. Gambino, Phys. Rev. Lett. *21*, 792 (1968).

[73] Ø. Fischer, H. Jones, G. Bongi, C. Frei and A. Treyvaud, Phys. Rev. Lett. *26*, 305 (1971).

[74] T. McConville and B. Sevin, Phys. Rev. *140*, AII 69 (1965).

[75] D. K. Finnemore, T. F. Stromberg and C. A. Swenson, Phys. Rev. *149*, 231 (1966).

[76] D. E. Farrel, B. S. Chandrasekhar and S. Huang, Phys. Rev. *176*, 562 (1968).

[77] P. C. Hohenberg and N. R. Werthamer, Phys. Rev. *153*, 493 (1967).

[78] R. Devine et al., to be published.

[79] M. Peter, J. Dupraz and H. Cottet, Helv. phys. Acta *40*, 301 (1967).

[80] J. Kondo, Progr. theor. Phys. *32*, 37 (1964).

[81] D. J. Scalapino, Phys. Rev. Lett. *16*, 937 (1966).

[82] A. H. Heeger, in: *Solid State Physics*, edited by H. Ehrenreich, F. Seitz and D. Turnbull (Academic Press, New York 1969), Vol. 23, p. 283.

[83] J. Zitterartz and E. Müller-Hartmann, Z. Phys. *232*, II (1970).

[84] E. Müller-Hartmann and J. Zitterartz, Z. Phys. *234*, 58 (1970).

[85] J. Zitterartz, Z. Phys. *237*, 419 (1970).

[86] E. Müller-Hartmann and J. Zitterartz, Phys. Rev. Lett. *26*, 428 (1971).

[87] P. Fulde and H. E. Hoenig, to be published.

[88] L. P. Gorkov, Sov. Phys., JETP *10*, 998 (1960).

[89] Ø. Fischer and M. Peter, to be published in Physica.

[90] L. P. Gorkov, Sov. Phys., JETP *10*, 593 (1960).

[91] D. T. Peterson, D. F. Page, R. B. Rump and D. K. Finnemore, Phys. Rev. *153*, 701 (1967).

[92] W. R. Decker and D. K. Finnemore, Phys. Rev. *172*, 430 (1968).

[93] K. Andres and E. Bucher, Helv. phys. Acta *42*, 590 (1969).

[94] P. Spitzli, R. Fluckiger, F. Heiniger, A. Junod, J. Muller and J. L. Staudenmann, J. Phys. Chem. Solids *31*, 1531 (1970).

[95] P. G. de Gennes, Phys. Lett. *23*, 10 (1966).

[96] H. R. Zeller and I. Giaever, Conf. on the science of superconductivity, Stanford, USA, 1969 (to be published).

[97] I. S. Gradshteyn and I. M. Ryzhik, *Table of Integrals, Series and Products* (Academic Press, New York 1965).

[98] W. Klose et al., to be published.

[99] Y. Nambu, Phys. Rev. *117*, 648 (1960).

[100] L. P. Gorkov and A. I. Rusinov, Sov. Phys. JETP *19*, 922 (1964).